



universität
wien

DISSERTATION / DOCTORAL THESIS

Titel der Dissertation / Title of the Doctoral Thesis

„Analysis of a spontaneous collapse in neutral meson systems“

verfasst von / submitted by

Kyrylo Simonov

angestrebter akademischer Grad / in partial fulfilment of the requirements for the degree of

Doktor der Naturwissenschaften (Dr.rer.nat)

Wien, 2017 / Vienna, 2017

Studienkennzahl lt. Studienblatt /
degree programme code as it appears on
the student record sheet:

A 796 605 411

Studienrichtung lt. Studienblatt /
degree programme as it appears on
the student record sheet:

Physik

Betreut von / Supervisor:

Univ. Doz. Dr. Beatrix C. Hiesmayr

TABLE OF CONTENTS

	Page
1 Introduction	11
2 Spontaneous collapse models	15
2.1 The measurement problem and the basic concepts of collapse models . . .	15
2.2 The GRW model	17
2.3 Spontaneous collapse models with a dynamical equation	19
2.3.1 Quantum Mechanics with Universal Position Localization (QMUPL)	22
2.3.2 Continuous Spontaneous Localization (CSL)	23
3 Neutral meson systems	25
3.1 Basic formalism of neutral mesons physics	25
3.2 \mathcal{CP} violation	28
4 Hidden variable models	31
4.1 Local realism and Bell inequalities	31
4.2 Bell inequalities for neutral kaons	34
5 Spontaneous collapse in flavor oscillations	37
5.1 Perturbative calculation of the probabilities	37
5.1.1 The neutral meson dynamics predicted by the QMUPL model . . .	38
5.1.2 The neutral meson dynamics predicted by the CSL model	40
5.2 Including the \mathcal{CP} violation effects to the predictions of the CSL model . .	41
5.3 Interpretation of the results via the CSL model	42
5.4 The mathematical and physical meanings of $\vartheta(0)$	48
6 Comparison of the predictions of the mass-proportional CSL model with another approaches	51
6.1 Semi-classical gravity	51

TABLE OF CONTENTS

6.2	Decoherence models	52
7	Spontaneous collapse and Bell inequalities	57
7.1	Calculation of the 2-particle probabilities including spontaneous collapse	57
7.2	Bell inequalities including spontaneous collapse	59
8	Conclusions and outlook	61
9	Acknowledgements	65
A	Computations for the QMUPL model	67
A.1	Transition probabilities for the mass eigenstates	67
A.2	d -dimensional case	70
A.3	Transition probabilities for the flavor states	72
B	Computations for the CSL model	75
B.1	Transition probabilities for mass eigenstates	75
B.2	Transition probabilities for the flavor states	81
B.3	Transition probabilities with included effect of \mathcal{CP} violation	82
C	Correlation functions of the noise field	87
C.1	Calculations with a 2-point correlation function	87
C.2	Calculations with a 4-point correlation function	88
D	Computations of the decay rates	93
	Bibliography	95

ABSTRACT

Dynamical reduction models propose a solution to the measurement problem in quantum mechanics by introducing an ontologically objective mechanism for the collapse of a wave function. By this mechanism the unobserved macroscopic superpositions are avoided. Neutral mesons are particle-antiparticle oscillating and decaying systems. In this thesis we provide an analysis of the two most promising collapse models, the QMUPL (Quantum Mechanics with Universal Position Localization) model and the mass-proportional CSL (Continuous Spontaneous Localization) model by computing the effects of a spontaneous collapse to neutral meson systems. We investigate the effects of a spontaneous collapse for a single neutral meson including the tiny violation of \mathcal{CP} symmetry, which is a symmetry between matter and antimatter. Our results show a strong sensitivity to the assumptions of the noise field underlying the dynamical reduction models. We find that the decay dynamics in a neutral meson system can be recovered by the spontaneous collapse dynamics, which allows us to predict the effective collapse rates solely based on the measured frequency of the flavor oscillation and decay constants. Proceeding to a system of two neutral kaons we explore the role played by the violation of the \mathcal{CP} symmetry in the spontaneous collapse scenario and tests of the local realism. By these means, neutral mesons are shown to be very sensitive to possible modifications of the standard quantum theory, which make them a powerful system to study physical scenarios which could solve the measurement problem in quantum mechanics.

ZUSAMMENFASSUNG

Dynamische Reduktionsmodelle erlauben eine Lösung des Messungsproblems, indem sie einen ontologisch objektiven Mechanismus für den Kollaps der Wellenfunktion einführen. Dabei werden die unbeobachteten makroskopischen Überlagerungen vermieden. Neutrale Mesonen sind Teilchen-Antiteilchen oszillierende und zerfallende Systeme. In dieser Dissertation führen wir eine Analyse der beiden vielversprechendsten Kollapsmodelle, dem QMUPL Modell (Quantum Mechanics with Universal Position Localization) und massenproportionalem CSL Modell (Continuous Spontaneous Localization), durch, indem die Änderung der Mesonendynamik aufgrund eines spontanen Kollapses berechnet wurde. Dabei wurde auch die kleine Verletzung der \mathcal{CP} -Symmetrie, eine Symmetrie zwischen Materie und Antimaterie, berücksichtigt. Die Ergebnisse zeigen eine starke Abhängigkeit von Annahmen über das Rauschfeld, die den dynamischen Reduktionsmodellen zugrunde liegen. Ein Ergebnis war, dass man die Standardzerfallsdynamik in einem neutralen Mesonensystem aus der Dynamik des spontanen Kollapses ableiten kann. Dadurch wurde es möglich effektiven Kollapsraten vorherzusagen, wozu nur die gemessene Frequenz der Flavor-Oszillationen und die Zerfallskonstanten benötigt wurden. In einem weiteren Schritt wurden neutrale verschränkte Kaonenpaare betrachtet und das Wechselspiel zwischen \mathcal{CP} -Symmetrie Verletzung und spontanem Kollaps für Tests des lokalen Realismus analysiert. Diese Arbeit zeigt, dass neutrale Mesonen sehr empfindlich bezüglich Modifikationen der Standard-Quantentheorie sind und dadurch sehr mächtige Werkzeuge sind, neue physikalische Szenarien zu untersuchen und dadurch das Messungsproblem der Quantenmechanik zu beleuchten.

LIST OF PUBLICATIONS

1. K. Simonov and B. C. Hiesmayr, *Constraints on the noise in dynamical reduction models*, Phys. Lett. A **380**, 1253–1255 (2016); arXiv:1511.03252.
2. K. Simonov and B. C. Hiesmayr, *Spontaneous collapse: A solution to the measurement problem and a source of the decay in mesonic systems*, Phys. Rev. A **94**, 052128 (2016); arXiv:1606.01682.
3. S. M. Giampaolo, K. Simonov, A. Capolupo and B. C. Hiesmayr, *The Interplay between Frustration and Entanglement in Many-Body Systems*, arXiv:1607.05692 (2016).
4. K. Simonov and B. C. Hiesmayr, *Can a spontaneous collapse in flavour oscillations be tested at KLOE?*, to appear in the proceedings of the KLOE-2 Workshop on e^+e^- collision physics at 1 GeV, 26-28 October 2016, INFN – Laboratori Nazionali di Frascati, Italy, arXiv:1705.00913 (2017).

NOTATION IN THIS THESIS

Name	Value	Description
$\hat{L}_{\mathbf{x}}^i$		Localization operator of the GRW model
\hat{A}_i		Collapse operator of a general collapse model
r_C	$10^{-7} m$	Coherence length in a collapse model
d		Number of dimensions of the physical space
λ		Collapse rate in the GRW model
λ_m		Collapse rate in a general collapse model
λ_{GRW}	$10^{-16} s^{-1}$	Value of the collapse rate λ proposed by Ghirardi, Rimini and Weber
λ_{Adler}	$10^{-8 \pm 2} s^{-1}$	Value of the collapse rate λ proposed by Adler
λ_Q	$\frac{\lambda}{2r_C^2}$	Collapse rate in the QMUPL model
γ	$\lambda \cdot (\sqrt{4\pi} r_C)^d$	Collapse rate in the CSL model
λ_{CSL}	λ	Convention for λ used for the CSL model
t		Time
$ \phi_t\rangle$		State vector
$W_{i,t}$		Wiener process
$w_{i,t}$		White noise
φ		Phase of the noise
\mathbb{E}		Stochastic average
$ M^0\rangle, \bar{M}^0\rangle$		Flavor eigenstates of neutral mesons
$ M_H\rangle, M_L\rangle$		Mass eigenstates of neutral mesons
$ M_1^0\rangle, M_2^0\rangle$		\mathcal{CP} eigenstates of neutral mesons
$ K^0\rangle, \bar{K}^0\rangle$		Flavor eigenstates of neutral kaons
$ K_L\rangle, K_S\rangle$		Mass eigenstates of neutral kaons
$ K_1^0\rangle, K_2^0\rangle$		\mathcal{CP} eigenstates of neutral kaons
$\sqrt{\alpha}$		Size of a wave packet
m_μ		Absolute masses of neutral mesons
Γ_μ		Decay rates of neutral mesons
Δm		Difference of masses of neutral mesons
$\vartheta(0)$		Value of Heaviside function at zero
κ		Asymmetry of the noise

Name	Value	Description
ε		Indirect \mathcal{CP} violation parameter
$ \varepsilon $	$(2.228 \pm 0.011) \cdot 10^{-3}$	
$\arg \varepsilon$	$(43.5 \pm 0.5)^\circ$	
p	$1 + \varepsilon$	
q	$1 - \varepsilon$	
N	$\sqrt{ p ^2 + q ^2}$	
δ	$\frac{2\text{Re}\varepsilon}{1+ \varepsilon ^2} = \langle K_L K_S \rangle$	Non-orthogonality of the mass eigenstates
φ_M		Relative phase of the \mathcal{CP} eigenstates

INTRODUCTION

Quantum mechanics has proven to be an exceedingly successful theory which covers a plethora of physical phenomena at different energy scales and, up to date, no experimental data are in contradiction. However, in its standard formulation quantum theory is very counter-intuitive and meets conceptual problems. In 1935 Einstein, Podolski and Rosen (EPR) raised the question whether quantum mechanics is incomplete and tried to show its incompleteness in a gedanken experiment with a pair of particles [1]. In 1964 Bell analyzed the point of view of EPR and derived an inequality which shows that the predictions of quantum mechanics are incompatible with local realism [2]. He showed that quantum mechanics shares a counter-intuitive feature, nonlocality, “spooky action at a distance” due to Einstein. Moreover, Kochen and Specker have shown that quantum mechanics reveals contextuality [3, 4], which means that the measured value of an observable depends on the choice of compatible comeasured observables. Considering quantum mechanics as a fundamental theory also superpositions of macroscopic objects, such as cats, should exist which are obviously not observed in our daily world.

In the Copenhagen interpretation during a measurement process a breaking of the superposition is mathematically postulated, but no detailed physical process has been assigned to it. Moreover, a separation into macroscopic system (measurement apparatus) and microscopic system (quantum system) is utilized but lacks a clear definition. Ruling out unobserved macroscopic superpositions is the heart of the so-called measurement problem or macro-objectification problem [5, 6]. One out of many possible solutions are

dynamical reduction models, so-called collapse models, which introduce an ontologically objective mechanism of the wave-function collapse. Since collapse models provide definite predictions for the regime between microscopic and macroscopic they are experimentally testable. Particularly, one of the popular collapse models, the QMUPL model, has been investigated for the spontaneous radiation emission from a non-relativistic free charged particle [7, 8] and put to an intensive experimental test by X-rays [9–11]. For another popular and more physical collapse model, the CSL model, experiments with optomechanical cavities have been proposed [12–19], particularly to detect possible changes in the spectrum of light which drives a mechanical oscillator [20, 21]. In another approach a possible increase of equilibrium temperature of a mechanical oscillator produced by the spontaneous collapse was revealed [22]. For neutral mesons (K-, B-, D-meson) and neutrinos up to first order in time the effect of the mass-proportional CSL model was derived and compared to decoherence models [23, 24] by checking the experimental data [26–31]. Recently, upper bounds on collapse models have been derived for cold-atom experiments [32] and the authors of Ref. [33] have shown that reduction models can lead to a nontrivial contribution to an effective cosmological constant.

Flavour physics is a rich field within physics with many unique features, and new facilities in the near future will tackle very precisely this regime of energy. Recently, there has been great interest in using massive particle systems such as neutral mesons in testing the very foundations of quantum mechanics. Such a unique laboratory as a neutral meson system has been proposed not only to test the effect of the spontaneous collapse [23, 24], but also to stress the notions of nonlocality [34–37] and contextuality [38] as well.

In this thesis we analyze the flavor dynamics of neutral mesons in the context of collapse models and deterministic hidden variable models. The thesis is organized as follows. We start by an introduction into the measurement problem and collapse models as one of its possible solution in Chapter 2. We discuss the GRW, QMUPL and CSL collapse models and their framework, particularly their master equations and their state vector equations. Next we turn to the hidden variable models and discuss a special class of them, local hidden variable models resulting in Bell inequalities, in Chapter ???. In Chapter 3 we discuss the phenomenology of neutral mesons, the role of discrete symmetries and the Bell inequalities for a neutral kaon system. In Chapter 5, the main result of the thesis is presented. We show how for a neutral meson system the effect of the QMUPL and CSL collapse models can be included and computed through the perturbative approach up to second order in time. These computations are lengthy and

involved, therefore, some substeps are given in detail in Appendix A for the QMUPL model and in Appendix B for the CSL model including the computations with taking into account \mathcal{CP} violation, respectively. The correlation functions and their dependence on the physics of the noise field are derived in Appendix C. We present the results, the probabilities for the lifetime states and the flavor oscillating probabilities for the cases of conserved \mathcal{CP} symmetry and its tiny violation. We analyze then different possibilities, one allowing us an independent prediction of the effective collapse rate for the different types of neutral mesons which can be compared to the experimental data. The needed computations of the decay rates from the experimental data are provided in Appendix D. We proceed by giving a physical meaning to the dependence on the correlation functions of the Wiener process and finalize by developing a decoherence model that leads to the same probabilities as the CSL model, but relies on strictly different physics. In Chapter 7 we extend our analysis to a system of two entangled neutral kaons and derive Bell inequalities including effects of the CSL model. These inequalities provide bounds for the collapse rate which is a natural constant to be compatible with local realism. Last but not least we provide the conclusions and outlook in Chapter 8.

SPONTANEOUS COLLAPSE MODELS

In this chapter we review some models of spontaneous collapse, i.e. dynamical reduction models. These models are said to present a possible solution to the measurement problem of quantum mechanics. These models assume that the collapse of the wave function is an objective physical process. Thus, it provides a universal dynamics covering both microscopic and macroscopic systems. The first section reviews the measurement problem of the quantum mechanics and introduces the basic ideas underlying the collapse models including the first model, the GRW (Ghirardi–Rimini–Weber) model [39]. In the following sections we introduce the two most popular collapse models on the market, the QMUPL (Quantum Mechanics with Universal Position Localization) model [40] and the CSL (Continuous Spontaneous Localization) model [41–43].

2.1 The measurement problem and the basic concepts of collapse models

Although quantum mechanics has proven to be an exceedingly successful theory by plethora of experiments during the last century, its standard formulation meets some conceptual problems which motivates the scientific community to attempts of modifying it. For instance, one of the most important problems of quantum mechanics is tied to the superposition principle, which is one of its corner stones. A number of experiments has confirmed that it holds on the microscopic scale. However, assuming that quantum

mechanics is a fundamental theory, nothing forbids the superposition principle to hold for macroscopic objects as well. Such superpositions lead to numerous paradoxes. For instance, we do not find a table to be “here” and “there” or a cat to be “dead” and “alive” at the same time. On the other hand, let us suppose a quantum system (microscopic) being in a superposition of two eigenstates $|a_1\rangle$ and $|a_2\rangle$ of an observable \hat{A} which we can measure using a measurement apparatus (that is assumed to be macroscopic). It is supposed to hold quantum state $|M\rangle$ which corresponds to some pointer state, therefore the whole system including the observed quantum system and the measurement apparatus holds the following quantum state before the measurement

$$|\psi_{before}\rangle = (\alpha_1|a_1\rangle + \alpha_2|a_2\rangle) \otimes |M\rangle. \quad (2.1)$$

The measurement entangles the quantum system and the measurement apparatus leading to the following quantum state

$$|\psi_{after}\rangle = \alpha_1|a_1\rangle \otimes |M_1\rangle + \alpha_2|a_2\rangle \otimes |M_2\rangle, \quad (2.2)$$

which is a macroscopic superposition of two positions of the (macroscopic) pointer. Obviously, such superpositions of the macroscopic objects is not observed in our quotidian world. Ruling out them lies in the heart of the so-called measurement (or also called macro-objectification) problem of the quantum mechanics.

In the Copenhagen interpretation of quantum mechanics one usually introduces two different types of dynamics of the state of a closed quantum system

- a deterministic unitary time evolution governed by the corresponding Schrödinger equation,
- a stochastic non-unitary reduction (collapse) of the wave function caused by a measurement process which produces the Born’s rule.

In another words, the Copenhagen interpretation postulates that there exist two levels of description of the nature, macroscopic one (measurement apparatus) and microscopic one (quantum system), possessing different rules for the time evolution. However, it does not provide any precise border between these two levels. Moreover, a measurement process in the Copenhagen interpretation is postulated to force the reduction of the wave function but neither equips the process of the reduction with any underlying mechanism nor reveals whether this process has to be considered physically real.

In turn, the Copenhagen interpretation postulates the collapse but does not explain it and in fact “sweeps the difficulties under the rug”. A more consistent solution to the

measurement problem is proposed by the dynamical reduction models. They provide a new universal dynamics which covers both microscopic and macroscopic levels as well as in-between one. This dynamics includes the reduction of the wave function as an objective physical process. This process can be briefly described as spontaneous collapses of the wave function occurring randomly and permanently for any system. The wave function of a microscopic system (e.g. a particle) undergoes a collapse rarely and its evolution remains practically unchanged from that ruled by the corresponding Schrödinger equation. However, a macroscopic system consists of many particles, and its wave function will frequently undergo a collapse due to the single collapses of the wave functions of the constituent particles. The modern collapse models introduce this dynamics mainly by a modification of the standard Schrödinger equation which turns then to a non-linear stochastic differential equation (SDE). In order to recover the predictions of quantum mechanics the new modified dynamics should have the following properties

- non-linearity: the new dynamics should break superpositions on a macroscopic level, particularly during a measurement,
- stochasticity: the new dynamics should produce the quantum probabilities obeying the Born's rule,
- no superluminal signaling: the new dynamics should not be in conflict with the special relativity.

2.2 The GRW model

The first consistent dynamical reduction model which proposed the new universal dynamics was the GRW model introduced in 1985–1986 by Ghirardi, Rimini and Weber [39]. It does not carry any state vector equation but provides the following set of the postulates that rule the collapse dynamics for a system of N particles

- each particle undergoes a sudden localization at a random time t , and the wave function of the system changes due to a sudden jump in the following way

$$\phi_t(\mathbf{q}_1, \dots, \mathbf{q}_i, \dots, \mathbf{q}_N) \rightarrow \frac{\hat{L}_{\mathbf{x}}^i \phi_t(\mathbf{q}_1, \dots, \mathbf{q}_i, \dots, \mathbf{q}_N)}{\|\hat{L}_{\mathbf{x}}^i \phi_t(\mathbf{q}_1, \dots, \mathbf{q}_i, \dots, \mathbf{q}_N)\|}, \quad (2.3)$$

where $\phi_t(\mathbf{q}_1, \dots, \mathbf{q}_i, \dots, \mathbf{q}_N)$ is the wave function of the whole system, and $\hat{L}_{\mathbf{x}}^i$ is the jump operator which induces the localization of i -th particle around the point \mathbf{x} ,

- the probability of a localization of i -particle around \mathbf{x} is

$$p_i(\mathbf{x}) = \|\hat{L}_{\mathbf{x}}^i \phi_t(\mathbf{q}_1, \dots, \mathbf{q}_i, \dots, \mathbf{q}_N)\|^2, \quad (2.4)$$

- between the jumps the state of the system evolves due to Schrödinger equation, namely

$$i\hbar \frac{d}{dt} \phi_t(\mathbf{q}_1, \dots, \mathbf{q}_N) = \hat{H} \phi_t(\mathbf{q}_1, \dots, \mathbf{q}_N), \quad (2.5)$$

where \hat{H} is the standard Hamiltonian of the system,

- two new natural constants, λ , the localization rate, and r_C , coherence length of localization, are introduced,
- the localization operators of the GRW model are determined in the following way

$$\hat{L}_{\mathbf{x}}^i = \frac{1}{(\pi r_C^2)^{3/4}} e^{-\frac{(\hat{q}_i - \mathbf{x})^2}{2r_C^2}}, \quad (2.6)$$

where \hat{q}_i is the coordinate operator for i -th particle,

- the sudden localizations are distributed in time according to a Poissonian process with the rate λ .

The values of the new constants were suggested by Ghirardi, Rimini and Weber as $r_C = 10^{-7} m$ and $\lambda_{GRW} = 10^{-16} s^{-1}$. The proposed value of the coherence length lies between the typical inter-atomic scale $10^{-10} m$ and the human-size scale $10^{-4} m$. The proposed value of the localization rate is widely discussed. Particularly, Adler proposed another value of the localization rate, $\lambda_{Adler} = 10^{-8 \pm 2} s^{-1}$ in order to make collapse effective for such processes as latent image formation in photography which one can refer to as a measurement process [44, 45].

In experiments one often cannot realize pure quantum states but rather statistical mixtures which are described by density matrices. Therefore, it is important to consider a master equation which expresses the collapse dynamics through the density matrix. Indeed, a spontaneous localization of the state vector $|\phi\rangle \rightarrow \frac{\hat{L}_{\mathbf{x}}|\phi\rangle}{\|\hat{L}_{\mathbf{x}}|\phi\rangle\|}$ around point \mathbf{x} causes the following change of the corresponding density matrix, $|\phi\rangle\langle\phi| \rightarrow \frac{\hat{L}_{\mathbf{x}}|\phi\rangle\langle\phi|\hat{L}_{\mathbf{x}}}{\|\hat{L}_{\mathbf{x}}|\phi\rangle\|^2}$. Since we do not know in which point the spontaneous localization takes place the actual state changes into a mixture of states [5]

$$|\phi\rangle\langle\phi| \rightarrow \int d\mathbf{x} p(\mathbf{x}) \frac{\hat{L}_{\mathbf{x}}|\phi\rangle\langle\phi|\hat{L}_{\mathbf{x}}}{\|\hat{L}_{\mathbf{x}}|\phi\rangle\|^2} = \int d\mathbf{x} \hat{L}_{\mathbf{x}}|\phi\rangle\langle\phi|\hat{L}_{\mathbf{x}} \equiv T[|\phi\rangle\langle\phi|]. \quad (2.7)$$

This leads to the following master equation for the density matrix $\rho_t = |\phi_t\rangle\langle\phi_t|$ of the system with a given Hamiltonian \hat{H}

$$\frac{d}{dt}\hat{\rho}_t = -\frac{i}{\hbar}[\hat{H}, \hat{\rho}_t] - \lambda(\hat{\rho}_t - T[\hat{\rho}_t]), \quad (2.8)$$

which reduces to the following master equation for the matrix elements $\hat{\rho}_t(\mathbf{x}, \mathbf{y}) = \langle\mathbf{x}|\hat{\rho}_t|\mathbf{y}\rangle$ in the position basis

$$\frac{d}{dt}\hat{\rho}_t(\mathbf{x}, \mathbf{y}) = -i[\hat{H}, \hat{\rho}_t(\mathbf{x}, \mathbf{y})] - \lambda\left(1 - e^{-\frac{|\mathbf{x}-\mathbf{y}|^2}{4r_c^2}}\right)\hat{\rho}_t(\mathbf{x}, \mathbf{y}). \quad (2.9)$$

2.3 Spontaneous collapse models with a dynamical equation

The GRW model presented in the previous section introduces the collapse in the wave function through the random discrete jumps. In contrast to nowadays investigated collapse models, which describe the reduction of the wave functions as a continuous process connected to a non-linear interaction of the quantum system with an external noise field. Such models are the Quantum Mechanics with Universal Position Localization (QMUPL) model [40] and the Continuous Spontaneous Localization (CSL) model in its original [41, 42] and mass-proportional [43] versions. These models describe the collapse as a continuous process by a SDE which turns out to be a non-linear stochastic modification of the Schrödinger equation with the Hamiltonian \hat{H} of the system under investigation [46]

$$d|\phi_t\rangle = \left[-i\hat{H}dt + \sqrt{\lambda_m} \sum_{i=1}^N (\hat{A}_i - \langle\hat{A}_i\rangle_t) dW_{i,t} - \frac{\lambda_m}{2} \sum_{i=1}^N (\hat{A}_i - \langle\hat{A}_i\rangle_t)^2 dt \right] |\phi_t\rangle, \quad (2.10)$$

with $\hbar = 1$ and $\langle\hat{A}_i\rangle_t := \langle\phi_t|\hat{A}_i|\phi_t\rangle$ being the standard quantum mechanical expectation value. Here \hat{A}_i are a set of N self-adjoint commuting operators related to the collapse, $W_{i,t}$ represent a set of N independent standard Wiener processes (which lead to the white noise $w_{i,t} := \frac{d}{dt}W_{i,t}$), one for each collapse operator \hat{A}_i . The difference between the dynamics provided by various collapse models ruled by the SDE (2.10) lies mainly in the choice of the collapse operators \hat{A}_i . The constant λ_m sets the strength of the collapse processes which turns to be a new natural constant provided by the collapse model (in the same manner as the constant λ in the GRW model). Let us consider the corresponding master equation for the density matrix $\hat{\rho}_t = \mathbb{E}[|\phi_t\rangle\langle\phi_t|]$,

$$\frac{d}{dt}\hat{\rho}_t = -i[\hat{H}, \hat{\rho}_t] - \frac{\lambda_m}{2} \sum_{i=1}^N \left(\{\hat{A}_i^2, \hat{\rho}_t\} - 2\hat{A}_i\hat{\rho}_t\hat{A}_i \right), \quad (2.11)$$

where \mathbb{E} denotes averaging over the white noise and the curly brackets denotes an anti-commutator. This equation has the same form as the Gorini–Kossakowski–Sudarshan–Lindblad equation for an open system [64, 65] with the collapse operators \hat{A}_i as Lindblad operators.

Finding a solution of a SDE is a non-trivial problem. However, the equations (2.10) and (2.11) carry a very useful mathematical property which helps to find the solutions. The physical predictions of these equations are invariant under a phase change in the noise through the so-called “imaginary noise trick” [47, 48] which we generalize below in several steps. Consider the following family of the dynamical equations

$$d|\phi_t\rangle = \left[-i\hat{H}dt + \sqrt{\lambda_m} \sum_{i=1}^N (\zeta\hat{A}_i - \beta\langle\hat{A}_i\rangle_t) dW_{i,t} - \frac{\lambda_m}{2} \sum_{i=1}^N (\tilde{\zeta}\hat{A}_i^2 - 2\tilde{\beta}\hat{A}_i\langle\hat{A}_i\rangle_t + \tilde{\gamma}\langle\hat{A}_i\rangle_t^2) dt \right] |\phi_t\rangle,$$

where the coefficients $\zeta, \beta, \tilde{\zeta}, \tilde{\beta}, \tilde{\gamma}$ are arbitrary complex numbers. The corresponding family of the master equations obtains then the form

$$\begin{aligned} \frac{d}{dt}\hat{\rho}_t &= -i[\hat{H}, \hat{\rho}_t] - \frac{\lambda_m}{2} \left\{ (\tilde{\zeta}\hat{A}_i^2 - 2\tilde{\beta}\hat{A}_i\langle\hat{A}_i\rangle_t + \tilde{\gamma}\langle\hat{A}_i\rangle_t^2) \hat{\rho}_t \right\} \\ &\quad + \hat{\rho}_t \left\{ \tilde{\zeta}^* \hat{A}_i^2 - 2\tilde{\beta}^* \hat{A}_i\langle\hat{A}_i\rangle_t + \tilde{\gamma}^* \langle\hat{A}_i\rangle_t^2 \right\} + \lambda_m (\zeta\hat{A}_i - \beta\langle\hat{A}_i\rangle_t) \hat{\rho}_t (\zeta^* \hat{A}_i - \beta^* \langle\hat{A}_i\rangle_t) \\ &= -i[\hat{H}, \hat{\rho}_t] - \frac{\lambda_m}{2} \left\{ \tilde{\zeta}\hat{A}_i^2 \hat{\rho}_t + \tilde{\zeta}^* \hat{\rho}_t \hat{A}_i^2 - 2|\zeta|^2 \hat{A}_i \hat{\rho}_t \hat{A}_i \right\} \\ &\quad - \lambda_m \langle\hat{A}_i\rangle_t^2 (\text{Re } \tilde{\gamma} - |\beta|^2) \hat{\rho}_t + \lambda_m \langle\hat{A}_i\rangle_t \left\{ (\tilde{\beta} - \zeta\beta^*) \hat{A}_i \hat{\rho}_t + (\tilde{\beta}^* - \zeta^* \beta) \hat{\rho}_t \hat{A}_i \right\}. \end{aligned}$$

Due to (2.11) the last two terms should cancel out, therefore we set $\text{Re } \tilde{\gamma} = |\beta|^2$, $\tilde{\beta} = \zeta\beta^*$ and obtain the following families of the state vector equations

$$d|\phi_t\rangle = \left[-i\hat{H}dt + \sqrt{\lambda_m} \sum_{i=1}^N (\zeta\hat{A}_i - \beta\langle\hat{A}_i\rangle_t) dW_{i,t} - \frac{\lambda_m}{2} \sum_{i=1}^N \left(\tilde{\zeta}\hat{A}_i^2 - 2\zeta\beta^* \hat{A}_i\langle\hat{A}_i\rangle_t + (|\beta|^2 + \text{Im } \tilde{\gamma}) \langle\hat{A}_i\rangle_t^2 \right) dt \right] |\phi_t\rangle$$

and the density matrix equations

$$\frac{d}{dt}\hat{\rho}_t = -i[\hat{H}, \hat{\rho}_t] - \frac{\lambda_m}{2} \sum_{i=1}^N \left\{ \tilde{\zeta}\hat{A}_i^2 \hat{\rho}_t + \tilde{\zeta}^* \hat{\rho}_t \hat{A}_i^2 - 2|\zeta|^2 \hat{A}_i \hat{\rho}_t \hat{A}_i \right\},$$

The last step is to simplify the obtained families of equations by taking $\beta = 0$, $\text{Im } \tilde{\gamma} = 0$ and $\tilde{\zeta} = 1$. It results in the following state vector equation

$$d|\phi_t\rangle = \left[-i\hat{H}dt + \zeta\sqrt{\lambda_m} \sum_{i=1}^N \hat{A}_i dW_{i,t} - \frac{\lambda_m}{2} \sum_{i=1}^N \hat{A}_i^2 dt \right] |\phi_t\rangle \quad (2.12)$$

and the density matrix equation

$$\frac{d}{dt}\hat{\rho}_t = -i[\hat{H}, \hat{\rho}_t] - \frac{\lambda_m}{2} \sum_{i=1}^N \left(\{\hat{A}_i^2, \hat{\rho}_t\} - 2|\zeta|^2 \hat{A}_i \hat{\rho}_t \hat{A}_i \right). \quad (2.13)$$

Comparing the equation (2.13) with the collapse model master equation (2.11) we can see that the equation (2.13) does the same job independently of the phase φ of ζ if its absolute value is taken as $|\zeta| = 1$. Therefore, the equation (2.12) gives the same physical predictions in terms of statistical expectations or probabilities for the outcomes of measurements as the original collapse SDE (2.10). The statistics of outcomes of measurements of an observable M is expressed as averages $\mathbb{E}[\langle \phi_t | \hat{M} | \phi_t \rangle] = \text{Tr}[\hat{M} \mathbb{E}[|\phi_t\rangle\langle\phi_t|]] = \text{Tr}[\hat{M} \hat{\rho}_t]$. This invariance forms the heart of the imaginary noise trick which we can use now to simplify the dynamical equation of the collapse models under investigation

$$d|\phi_t\rangle = \left[-i\hat{H}dt + e^{i\varphi} \sqrt{\lambda_m} \sum_{i=1}^N \hat{A}_i dW_{i,t} - \frac{\lambda_m}{2} \sum_{i=1}^N \hat{A}_i^2 dt \right] |\phi_t\rangle \quad (2.14)$$

exploiting the invariance of the corresponding master equation on the phase φ of ζ .

The new state vector equation (2.14) is written in the so-called Itô form. In general, the white noise w_t represents the change in time t of the Wiener process W_t (with the definition $W_{t=0} = 0$), where the term white (uncolored) refers to independent and identically distributed growths of dW_t , with a zero expectation value and a standard deviation proportional to \sqrt{dt} . The Wiener process can be identified with a temporal integral of the white noise, $W_t = \int_{t_0}^t w_{t'} dt'$ [49]. This leads to a formal definition of the white noise as a temporal derivative $w_t := \frac{dW_t}{dt}$, although this derivative does not exist since the Wiener process W_t is nowhere differentiable [50], and in fact there is no bijection between Wiener process and noise. After all one can define a stochastic integral $\int_{t_0}^t G(t') dW_{t'}$ as a kind of Riemann–Stieltjes integral, which depends on the choice of a sampling point in the interval $[t, t + dt]$. A family of formalisms can be developed depending on the choice of the sampling point. The two popular frameworks are the Itô formalism, which chooses t (left-hand endpoint of each time subinterval), and the Stratonovich formalism, which chooses $t + \frac{dt}{2}$ (middle point of each time subinterval) [51]. The advantage of the Stratonovich formalism is that the differential and integration procedures are those familiar from ordinary calculus. Therefore, we will stick to this formalism. In the Stratonovich formalism equation (2.14) becomes a Schrödinger-like equation (linear) with a random Hamiltonian

$$i \frac{d}{dt} |\phi_t\rangle = \left[\hat{H} - e^{i\varphi} \sqrt{\lambda_m} \sum_{i=1}^N \hat{A}_i w_{i,t} \right] |\phi_t\rangle. \quad (2.15)$$

The equation (2.15) is much easier to solve and will be used later as the basic instrument for the computations. In the following we use the phase $\varphi = 0$ to simplify the computations.

2.3.1 Quantum Mechanics with Universal Position Localization (QMUPL)

The QMUPL model was introduced by Diósi in 1989 [40]. It is positioned as less realistic compared the CSL model discussed below, particularly because of formulation of the QMUPL model for distinguishable particles [6]. However, due to its simplicity it is possible to generalize it in several ways, including non-dissipativity and non-white noise field which leads to non-Markovianity of the collapse model [52–54]. The QMUPL model sets position operators in d -dimensional space as d collapse operators, $\hat{A}_i = \hat{q}_i$, which can be combined in a single vector collapse operator, $\hat{\mathbf{A}} = \hat{\mathbf{q}}$. This choice of the collapse operators leads to the following SDE for a single particle

$$d|\phi_t\rangle = \left[-i\hat{H}dt + \sqrt{\lambda_Q}(\hat{\mathbf{q}} - \langle\hat{\mathbf{q}}\rangle_t) \cdot d\mathbf{W}_t - \frac{\lambda_Q}{2}(\hat{\mathbf{q}} - \langle\hat{\mathbf{q}}\rangle_t)^2 dt \right] |\phi_t\rangle, \quad (2.16)$$

where λ_Q is the localization rate of the QMUPL model and $\mathbf{W}_t = \{W_{1,t}, \dots, W_{d,t}\}$ is the set of d Wiener process, one for each space dimension. It should be noted that in contrast to the GRW and CSL models the QMUPL model introduces only one constant λ_Q .

The master equation of the QMUPL model can be derived from one of the GRW model as a limit of small coherence length r_C . This means that the physical predictions of the QMUPL model should not differ from those of the GRW model (and the CSL model as well) for macroscopic systems. The master equation of the QMUPL model results in

$$\frac{d}{dt}\hat{\rho}_t(\mathbf{x}, \mathbf{y}) = -i[\hat{H}, \hat{\rho}_t(\mathbf{x}, \mathbf{y})] - \frac{\lambda}{4r_C^2}(\mathbf{x} - \mathbf{y})^2 \hat{\rho}_t(\mathbf{x}, \mathbf{y}), \quad (2.17)$$

where $\hat{\rho}_t(\mathbf{x}, \mathbf{y}) = \langle \mathbf{x} | \hat{\rho}_t | \mathbf{y} \rangle$. From (2.17) we can establish connection between the constants of the QMUPL and GRW models, namely $\lambda_Q = \frac{\lambda}{2r_C^2}$.

The corresponding simplified Schrödinger-like equation is

$$i\frac{d}{dt}|\phi_t\rangle = \left[\hat{H} - \sqrt{\lambda_Q}(\hat{\mathbf{q}} \cdot \mathbf{w}_t) \right] |\phi_t\rangle, \quad (2.18)$$

where $\mathbf{w}_t = \left\{ \frac{dW_{1,t}}{dt}, \dots, \frac{dW_{d,t}}{dt} \right\}$.

2.3.2 Continuous Spontaneous Localization (CSL)

The more involved CSL model was developed in its original version by Ghirardi, Pearle and Rimini in 1989–1990 [41, 42]. It is formulated through the second quantization formalism describing a system of identical particles and operates with more tricky collapse operators \hat{A}_i which act in a Fock space and therefore are replaced by a continuous set of operators $\hat{A}(\mathbf{x})$, one for each point in space, namely

$$\hat{A}(\mathbf{x}) = \sum_j \int d\mathbf{y} g(\mathbf{y} - \mathbf{x}) \hat{\psi}_j^\dagger(\mathbf{y}) \hat{\psi}_j(\mathbf{y}), \quad (2.19)$$

where $\hat{\psi}_{j,s}^\dagger(\mathbf{y})$ and $\hat{\psi}_{j,s}(\mathbf{y})$ are the creation and annihilation operators of a particle of type j and spin s in a point \mathbf{y} . The smearing function $g(\mathbf{y} - \mathbf{x})$ is usually taken to be of a Gaussian type

$$g(\mathbf{y} - \mathbf{x}) = \frac{1}{(\sqrt{2\pi} r_C)^d} e^{-(\mathbf{y} - \mathbf{x})^2 / 2r_C^2}, \quad (2.20)$$

where d reads the number of spatial dimensions and r_C is the coherence length of the CSL model which coincides with one of the GRW model. This choice of the collapse operators defines the following SDE

$$\begin{aligned} d|\phi_t\rangle &= \left[-i\hat{H} dt + \sqrt{\gamma} \int d\mathbf{x} (\hat{A}(\mathbf{x}) - \langle \hat{A}(\mathbf{x}) \rangle_t) dW_t(\mathbf{x}) \right. \\ &\quad \left. - \frac{\gamma}{2} \int d\mathbf{x} (\hat{A}(\mathbf{x}) - \langle \hat{A}(\mathbf{x}) \rangle_t)^2 dt \right] |\phi_t\rangle, \end{aligned} \quad (2.21)$$

where $W_t(\mathbf{x})$ is now an ensemble of the Wiener processes, one for each point in space, and γ is the localization rate provided by the CSL model.

The master equation of the CSL model for the system of N particles reads

$$\begin{aligned} \frac{d}{dt} \hat{\rho}_t(\mathbf{x}, \mathbf{y}) &= -i[\hat{H}, \hat{\rho}_t(\mathbf{x}, \mathbf{y})] - \frac{\gamma}{2(\sqrt{4\pi} r_C)^d} \\ &\quad \cdot \sum_{i=0}^N \sum_{j=0}^N \left[e^{-\frac{|\mathbf{x}_i - \mathbf{x}_j|^2}{4r_C^2}} + e^{-\frac{|\mathbf{y}_i - \mathbf{y}_j|^2}{4r_C^2}} - 2e^{-\frac{|\mathbf{x}_i - \mathbf{y}_j|^2}{4r_C^2}} \right] \hat{\rho}_t(\mathbf{x}, \mathbf{y}), \end{aligned} \quad (2.22)$$

where $\mathbf{x} = \{\mathbf{x}_1, \dots, \mathbf{x}_N\}$ and \mathbf{x}_i is the position of i -th particle. For the single-particle case equation (2.22) reduces to

$$\frac{d}{dt} \hat{\rho}_t(\mathbf{x}, \mathbf{y}) = -i[\hat{H}, \hat{\rho}_t(\mathbf{x}, \mathbf{y})] - \frac{\gamma}{(\sqrt{4\pi} r_C)^d} \left(1 - e^{-\frac{|\mathbf{x} - \mathbf{y}|^2}{4r_C^2}} \right) \hat{\rho}_t(\mathbf{x}, \mathbf{y}), \quad (2.23)$$

which coincides with the master equation of the GRW model. This gives rise to substitute the localization rate γ of the CSL model by the one λ of the GRW model, namely

$\gamma = \lambda \cdot (\sqrt{4\pi} r_C)^d$ which has now the units $[m^d/s]$. A characteristic of the CSL model is that all observable results will be proportional to the ratio γ/r_C^d being a rate or by including all units the strength of the interaction. Furthermore, the QMUPL model can be considered as the limit of the CSL model as well, as was mention in the previous subsection.

In 1995 Ghirardi, Grassi and Benatti proposed an important improvement of the CSL model, its mass-proportional version [43]. While the original CSL models introduces density operators as collapse operators, its mass-proportional version uses mass density operators which makes collapse dynamics dependent not only on number of particles but on their masses as well. SDE is modified in the following way

$$\hat{A}(\mathbf{x}) \rightarrow \hat{M}(\mathbf{x}) = \sum_j m_j \hat{A}_j(\mathbf{x}) = \sum_{j,s} m_j \int d\mathbf{y} g(\mathbf{y} - \mathbf{x}) \hat{\psi}_{j,s}^\dagger(\mathbf{y}) \hat{\psi}_{j,s}(\mathbf{y}), \quad (2.24)$$

where m_j is the mass of a particle of the type j . This choice of the collapse operators modifies equation (2.25) in the following way

$$\begin{aligned} d|\phi_t\rangle = & \left[-i\hat{H} dt + \frac{\sqrt{\gamma}}{m_0} \int d\mathbf{x} (\hat{M}(\mathbf{x}) - \langle \hat{M}(\mathbf{x}) \rangle_t) dW_t(\mathbf{x}) \right. \\ & \left. - \frac{\gamma}{2m_0^2} \int d\mathbf{x} (\hat{M}(\mathbf{x}) - \langle \hat{M}(\mathbf{x}) \rangle_t)^2 dt \right] |\phi_t\rangle, \end{aligned} \quad (2.25)$$

where m_0 is a reference mass which is usually chosen to be the nucleon mass.

The corresponding simplified Schrödinger-like equation is

$$i \frac{d}{dt} |\phi_t\rangle = \left[\hat{H} - \frac{\sqrt{\gamma}}{m_0} \sum_{j,s} \int d\mathbf{x} w(\mathbf{x}, t) \hat{\psi}_{j,s}^\dagger(\mathbf{x}) \hat{\psi}_{j,s}(\mathbf{x}) \right] |\phi_t\rangle, \quad (2.26)$$

where $w(\mathbf{x}, t)$ is a noise which set to be white in time and Gaussian in space,

$$\mathbb{E}[w(\mathbf{x}, t)w(\mathbf{x}', t')] = \frac{1}{(\sqrt{4\pi} r_C)^d} e^{-\frac{|\mathbf{x} - \mathbf{x}'|^2}{4r_C^2}} \delta(t - t'). \quad (2.27)$$

NEUTRAL MESON SYSTEMS

In this chapter we discuss the phenomenology of neutral mesons, which includes the flavor oscillations. We focus generally on a neutral meson $M^0 = \{K^0, D^0, B^0, B_s^0\}$ and later stick to the particular case of a neutral kaon K^0 . We discuss the discrete symmetries and their violation in the context of neutral mesons, particularly neutral kaons. Last but not least we review the formalism of generalized Bell inequalities for a system of entangled neutral kaons developed in [34–36].

3.1 Basic formalism of neutral mesons physics

A neutral meson M^0 is composed by a quark-antiquark pair bound by the strong interaction, and both the particle state $|M^0\rangle$ and the antiparticle state $|\bar{M}^0\rangle$ can decay through the weak interaction into the same final states. They can be distinguished by a flavor quantum number \mathcal{S} called strangeness [60] which is conserved by the strong interaction but violated by the weak interaction,

$$\hat{\mathcal{S}}|M^0\rangle = |M^0\rangle, \quad (3.1)$$

$$\hat{\mathcal{S}}|\bar{M}^0\rangle = -|\bar{M}^0\rangle. \quad (3.2)$$

Therefore, neutral mesons have to be considered as a two-state system. Its most general time evolution can be described by an infinite-dimensional vector in Hilbert space which includes the components of both the flavor eigenstates $|M^0\rangle$ and $|\bar{M}^0\rangle$ and all its decay products. However, finding a solution for an infinite set of coupled differential

equations is a cumbersome problem. Therefore, the dynamics of a $M^0 - \bar{M}^0$ oscillating system is usually covered by an effective Schrödinger equation within Wigner–Weisskopf approximation [61, 62] which turns out to be a proper simplification and takes into account only the components of the flavor eigenstates,

$$\frac{d}{dt}|\psi_t\rangle = -i\hat{H}_{eff}|\psi_t\rangle, \quad (3.3)$$

$$|\psi_t\rangle = a(t)|M^0\rangle + b(t)|\bar{M}^0\rangle, \quad (3.4)$$

where the phenomenological (effective) Hamiltonian $\hat{H}_{eff} = \hat{M} + \frac{i}{2}\hat{\Gamma}$ is non-Hermitian, $\hat{M} = \hat{M}^\dagger$ is the mass operator which describes the unitary part of the dynamics of a neutral meson, and $\hat{\Gamma} = \hat{\Gamma}^\dagger$ covers the decay (non-unitary part).

It can be shown that the effect of the non-Hermitian part of the Hamiltonian (decay) can be understood if the system is considered to be an open quantum system, i.e. a system which interacts with the environment which is not available in general [63]. Then the Schrödinger equation is turned to a Gorini–Kossakowski–Lindblad–Sudarshan master equation [64, 65], where a Lindblad operator implies the transition from the surviving part to the decaying part of the system under investigation. Consequently, the decay property can be incorporated via a Lindblad operator into the quantum system and can be physically understood as an interaction with a (virtual) environment. In quantum field theory this environment would refer to the QCD vacuum. This in turn shows that the total time evolution is a completely positive map. We will discuss this point in the next chapter.

Diagonalizing the phenomenological Hamiltonian leads to two different mass eigenstates ($c = 1$)

$$\hat{H}_{eff}|M_i\rangle = \left(m_i + \frac{i}{2}\Gamma_i\right)|M_i\rangle. \quad (3.5)$$

These two states $|M_L\rangle$ and $|M_H\rangle$ are eigenstates of the weak interaction and have distinct masses, without loss of generality m_L denotes the lower one (L denotes “light”, H denotes “heavy”). For all types of neutral mesons the decay rates Γ_L, Γ_H are approximately equal, except for K-mesons whose decay rates differ by a huge factor about 600. Therefore, the light mass eigenstate of a neutral kaon is denoted as the short-lived state $|M_L\rangle \rightarrow |K_S\rangle$ with lifetime $\tau_S = 0.89 \cdot 10^{-10}$ s and the heavy mass eigenstate is denoted as the long-lived state $|M_H\rangle \rightarrow |K_L\rangle$ with lifetime $\tau_L = 5.17 \cdot 10^{-8}$ s.

The flavor eigenstates are conjugated by the combined operation \mathcal{CP} ,

$$\hat{\mathcal{CP}}|M^0\rangle = e^{i\varphi_M}|\bar{M}^0\rangle, \quad (3.6)$$

$$\hat{\mathcal{CP}}|\bar{M}^0\rangle = e^{-i\varphi_M}|M^0\rangle, \quad (3.7)$$

such that $\hat{\mathcal{C}}\hat{\mathcal{P}}^2 = 1$. The strong interaction does not change the flavor quantum number, so the phase φ_M is unphysical and can be chosen arbitrarily. Usually one fixes $\varphi_M = \pi$ (and so we will do in Section 5.2). This means that \mathcal{CP} eigenstates can be defined in the following way (with this phase convention)

$$|M_1^0\rangle = \frac{1}{\sqrt{2}}(|M^0\rangle + |\bar{M}^0\rangle), \quad (3.8)$$

$$|M_2^0\rangle = \frac{1}{\sqrt{2}}(|M^0\rangle - |\bar{M}^0\rangle), \quad (3.9)$$

so that $\hat{\mathcal{C}}\hat{\mathcal{P}}|M_1^0\rangle = |M_1^0\rangle$ and $\hat{\mathcal{C}}\hat{\mathcal{P}}|M_2^0\rangle = -|M_2^0\rangle$.

Specifically for the neutral kaons we have the situation, that they can decay into two different decay channels: two pions ($\pi\pi$), with $\mathcal{CP} = +1$, or three pions ($\pi\pi\pi$) with $\mathcal{CP} = -1$. If \mathcal{CP} symmetry is conserved then the mass eigenstates can be identified with the \mathcal{CP} eigenstates such that the short-lived state decays into two pions $|K_S\rangle \rightarrow |\pi\pi\rangle$ and the long-lived state decays into three pions $|K_L\rangle \rightarrow |\pi\pi\pi\rangle$.

In general, in the case of conserved \mathcal{CP} symmetry the relation between the flavor eigenstates and mass eigenstates is given by

$$|M^0\rangle = \frac{1}{\sqrt{2}}(|M_H\rangle + |M_L\rangle), \quad (3.10a)$$

$$|\bar{M}^0\rangle = \frac{1}{\sqrt{2}}(|M_H\rangle - |M_L\rangle). \quad (3.10b)$$

Solving the effective Schrödinger equation (3.3) we obtain the following dynamics of an initial particle and antiparticle state,

$$|M^0(t)\rangle = \frac{1}{\sqrt{2}}\left(e^{-\frac{\Gamma_H}{2}t}e^{-im_H t}|M_H\rangle + e^{-\frac{\Gamma_L}{2}t}e^{-im_L t}|M_L\rangle\right), \quad (3.11a)$$

$$|\bar{M}^0(t)\rangle = \frac{1}{\sqrt{2}}\left(e^{-\frac{\Gamma_H}{2}t}e^{-im_H t}|M_H\rangle - e^{-\frac{\Gamma_L}{2}t}e^{-im_L t}|M_L\rangle\right). \quad (3.11b)$$

In this way we can find the probabilities of finding a meson or antimeson after a certain time t if a meson state $|M^0\rangle$ was produced at $t = 0$,

$$P_{M^0 \rightarrow M^0/\bar{M}^0}(t) = \frac{1}{4}\left(e^{-\Gamma_H t} + e^{-\Gamma_L t} \pm 2e^{-\frac{\Gamma_H + \Gamma_L}{2}t} \cos(t\Delta m)\right), \quad (3.12)$$

where $\Delta m = m_H - m_L$ is the difference of masses. These probabilities show that the neutral meson system reveals so-called flavor oscillations. This means that if, for example, a kaon is produced, then it oscillates into an antikaon and vice versa, also called strangeness oscillation.

3.2 \mathcal{CP} violation

The existence of antiparticles was predicted by Dirac in 1928 [66]. They are interpreted as mirror images of usual particles having the same mass and opposite electrical charge, for example, a positively charged antielectron (positron) which was successfully demonstrated in a controlled experiment by Anderson in 1933 [67]. Particles and antiparticles are produced in pairs and annihilate each other leaving high-energy photons when they come in contact. However, although in the aftermath of the Big Bang particles and antiparticles should have been created in equal amounts, we do not find as much anti-matter as matter in our visible Universe. To explain this asymmetry one has proposed two possible interpretations,

- the total baryon number \mathcal{B} of the early Universe was non-zero which means that there was already a small disbalance of matter and antimatter just after the Big Bang,
- the total baryon number \mathcal{B} of the early Universe was zero but some hypothetical set of physical processes called baryogenesis produced the asymmetry between matter and antimatter over time.

It is not clear from experimental point of view which interpretation should be preferred. However, the second one introducing the baryogenesis mechanism is usually taken. The set of three necessary conditions for such a process to produce a disbalance between matter and antimatter to occur was proposed by Sakharov in 1967 [68].

1. Such a process should necessarily violate baryon number \mathcal{B} .
2. If the charge-conjugation (\mathcal{C}) symmetry is conserved then a process which produces more baryons than antibaryons will be balanced by a mirrored process which produces more antibaryons than baryons. Thus, such a process should violate the \mathcal{C} symmetry. Moreover, it should violate the combined \mathcal{CP} symmetry to prevent a possible conservation of the total baryon number \mathcal{B} .
3. Such a process should fall out of thermal equilibrium.

The violation of \mathcal{CP} symmetry was discovered by Christenson, Cronin, Fitch and Turlay in 1963–1964 in an experiment with neutral kaons [69]. Observing the decays of long-lived kaons they have found in one of thousand events not three pions, as expected, but

two pions which exhibit the final state with $\mathcal{CP} = +1$. This can be explained in two ways. Firstly, the mass eigenstates $|K_L\rangle$ and $|K_S\rangle$ are not identical to the \mathcal{CP} eigenstates,

$$|K_L\rangle = \frac{1}{\sqrt{1+|\varepsilon|^2}} \left(\varepsilon |K_1^0\rangle + |K_2^0\rangle \right), \quad (3.13a)$$

$$|K_S\rangle = \frac{1}{\sqrt{1+|\varepsilon|^2}} \left(|K_1^0\rangle + \varepsilon |K_2^0\rangle \right). \quad (3.13b)$$

This effect exhibits indirect \mathcal{CP} violation parametrized by ε which was measured to $|\varepsilon| = (2.228 \pm 0.011) \cdot 10^{-3}$ with a phase of $\arg(\varepsilon) = (43.5 \pm 0.5)^\circ$. Taking into account the violation of the \mathcal{CP} symmetry we obtain the relation between the flavor eigenstates and mass eigenstates of a kaon,

$$|K^0\rangle = \frac{N}{2p} \left(|K_L\rangle + |K_S\rangle \right), \quad (3.14a)$$

$$|\bar{K}^0\rangle = \frac{N}{2q} \left(|K_L\rangle - |K_S\rangle \right), \quad (3.14b)$$

where $p = 1 + \varepsilon$, $q = 1 - \varepsilon$ and $N^2 = |p|^2 + |q|^2$. Since the flavor eigenstates are orthonormal, the mass eigenstates turn out to be non-orthogonal as a consequence,

$$\langle K_S | K_L \rangle = \frac{2 \operatorname{Re} \varepsilon}{1 + |\varepsilon|^2} \equiv \delta, \quad (3.15)$$

where we apply a certain phase convention to keep δ real.

Secondly, the \mathcal{CP} symmetry can be broken immediately in the decay, such that, for example, the $|K_2^0\rangle$ state decays via weak interaction into two pions. This effect leads to the direct \mathcal{CP} violation parametrized by ε' . However, as the NA48 and KTeV experiments have shown, the first effect dominates the second one, $\operatorname{Re} \frac{\varepsilon'}{\varepsilon} = (1.68 \pm 0.14) \cdot 10^{-3}$ [70–72]. In our analysis we will neglect any contribution from the direct \mathcal{CP} violation and stick to the indirect \mathcal{CP} violation.

Solving the effective Schrödinger equation (3.3) we obtain the following dynamics of the particle and antiparticle states,

$$|K^0(t)\rangle = \frac{N}{2p} \left(e^{-\frac{\Gamma_L}{2}t} e^{-im_L t} |K_L\rangle + e^{-\frac{\Gamma_S}{2}t} e^{-im_S t} |K_S\rangle \right), \quad (3.16a)$$

$$|\bar{K}^0(t)\rangle = \frac{N}{2q} \left(e^{-\frac{\Gamma_L}{2}t} e^{-im_L t} |K_L\rangle - e^{-\frac{\Gamma_S}{2}t} e^{-im_S t} |K_S\rangle \right), \quad (3.16b)$$

and the corresponding probabilities,

$$P_{K^0 \rightarrow K^0}(t) = \frac{1}{4} \left(e^{-\Gamma_L t} + e^{-\Gamma_S t} + 2e^{-\frac{\Gamma_L + \Gamma_S}{2}t} \cos(t\Delta m) \right), \quad (3.17a)$$

$$P_{K^0 \rightarrow \bar{K}^0}(t) = \frac{1}{4} \frac{|q|^2}{|p|^2} \left(e^{-\Gamma_L t} + e^{-\Gamma_S t} - 2e^{-\frac{\Gamma_L + \Gamma_S}{2}t} \cos(t\Delta m) \right). \quad (3.17b)$$

The temporal part of the evolution of mesons is not normalized for times $t > 0$ due to the non-Hermitian part of the effective Hamiltonian,

$$|M_i(t)\rangle = e^{-im_i t} e^{-\frac{\Gamma_i}{2} t} |M_i\rangle \longrightarrow \int_0^\infty \| |M_i(t)\rangle \|^2 dt = \frac{1}{\Gamma}. \quad (3.18)$$

Obviously, a normalization of the temporal part by $\sqrt{\Gamma}$ would give a similar expression as the Born rule for the spatial part and allow for a definition of a time operator [73–78]. However, taking into account the violation of \mathcal{CP} symmetry shows that this formal normalization leads to contradiction with experimental data [79]. This expresses the strikingly different roles of time and space in the quantum theory and the importance of discrete symmetries.

HIDDEN VARIABLE MODELS

In this chapter we discuss the hidden variable models, a class of deterministic theories which attempts to describe the predictions of quantum mechanics by underlying deterministic variables. We stick to the special class of local hidden variable theories, which are the hidden variable theories consistent with local realism. We discuss the Bell's theorem and the Bell inequalities in the form of CHSH inequalities and Wigner inequalities. Last but not least we discuss the Bell inequalities for entangled neutral kaons.

4.1 Local realism and Bell inequalities

The question of completeness of the quantum mechanics raised by Einstein, Podolski and Rosen (EPR) [1] opened the door to the so-called hidden variable theories. This class of deterministic theories assumes that the description of a quantum system through the quantum state $\hat{\rho}$ is not complete. It admits existence of additional underlying quantities (not necessarily inaccessible [55]), hidden variables λ , which completely determine the state of the quantum system and allow observables to have a definite value. Then the predictions of quantum mechanics can be described in the same way as statistical mechanics does, namely, as averages on the corresponding phase space of hidden states while the uncertainties arise due to practical limitations of a measurement procedure.

Let us consider a special class of hidden variable theories, precisely local hidden variable theories, and consider the EPR scenario with a source producing two particles

which are measured distantly and independently by two experimenters, Alice and Bob. Each experimenter has the ability to choose between two measurement alternatives, namely \hat{A}_1 and \hat{A}_2 for Alice and \hat{B}_1 and \hat{B}_2 for Bob, while each measurement can have an outcome either -1 or 1 . For this setup we can define a set of joint probabilities $P(ab|AB)$ that Alice gets the outcome $a \in \{-1, 1\}$ measuring $\hat{A} \in \{\hat{A}_1, \hat{A}_2\}$ and Bob gets the outcome $b \in \{-1, 1\}$ measuring $\hat{B} \in \{\hat{B}_1, \hat{B}_2\}$. Then a correlation function for the joint measurements of observables A by Alice and B by Bob can be built with use of these joint probabilities,

$$E(A, B) = \langle \hat{A}\hat{B} \rangle = \sum_{i,j} (i \cdot j) P(ij|AB). \quad (4.1)$$

A local hidden variable theory provides two important assumptions,

- the properties of the system are fixed as soon as the hidden variables λ are fixed, and the measurements just reveal these preexisting properties but do not create them (**realism**),
- the properties of space-like separated systems should be independent that results in a factorization of the joint probabilities of (4.1) (**locality**).

In this way a local hidden variable theory defines the joint probabilities in (4.1) by the following form

$$P(ab|AB) = \int_{\Lambda} d\lambda P(\lambda) \cdot P(a|A, \lambda) \cdot P(b|B, \lambda), \quad (4.2)$$

where λ is the hidden variable which lives in the phase space Λ , and the probability distribution $P(\lambda)$ is normalized. It should be noted that besides realism and locality a local hidden variable theory assumes implicitly **free will** which means that the choice of the observables A and B by Alice and Bob does not depend on hidden variables λ and vice versa. This means mathematically that $P(\lambda|A, B) = P(\lambda)$.

The famous Bell's theorem [2] states that the predictions of quantum mechanics cannot be fully reproduced by such local hidden variables theories. John Bell has shown that these theories establish strict bounds on correlations between outcomes of distant measurements which can be formulated as linear inequalities known as Bell inequalities. One of its particular forms is the CHSH (Clauser–Horne–Shimony–Holt) inequality [56].

For the considered local hidden variable models it reads

$$\begin{aligned}
 & |E(A_1, B_1) - E(A_1, B_2)| + |E(A_2, B_1) + E(A_2, B_2)| \tag{4.3} \\
 &= \sum_{i,j} \int_{\Lambda} d\lambda P(\lambda) \cdot \left\{ \left| (i \cdot j) \left(P(i|A_1, \lambda) \cdot P(j|B_1, \lambda) - P(i|A_1, \lambda) \cdot P(j|B_2, \lambda) \right) \right| \right. \\
 &\quad \left. + \left| (i \cdot j) \left(P(i|A_2, \lambda) \cdot P(j|B_1, \lambda) + P(i|A_2, \lambda) \cdot P(j|B_2, \lambda) \right) \right| \right\} \\
 &\leq \sum_{i,j} \int_{\Lambda} d\lambda P(\lambda) \cdot \max_{\lambda} \left\{ \left| (i \cdot j) \left(P(i|A_1, \lambda) \cdot P(j|B_1, \lambda) - P(i|A_1, \lambda) \cdot P(j|B_2, \lambda) \right) \right| \right. \\
 &\quad \left. + \left| (i \cdot j) \left(P(i|A_2, \lambda) \cdot P(j|B_1, \lambda) + P(i|A_2, \lambda) \cdot P(j|B_2, \lambda) \right) \right| \right\} \\
 &= 2 \int_{\Lambda} d\lambda P(\lambda),
 \end{aligned}$$

and,

$$\underbrace{|E(A_1, B_1) - E(A_1, B_2)| + |E(A_2, B_1) + E(A_2, B_2)|}_{\equiv \mathcal{E}} \leq 2. \tag{4.4}$$

One can show that these bounds can be violated for particular quantum states when the correlation functions $E(A_i, B_j)$ are calculated within quantum-mechanical mean values. Let Alice and Bob share a system of two spin- $\frac{1}{2}$ particles in the antisymmetric Bell state (e.g. in the singlet state) which is a maximally entangled state

$$|\Psi^-\rangle = \frac{1}{\sqrt{2}} \left(|\uparrow\rangle \otimes |\downarrow\rangle - |\downarrow\rangle \otimes |\uparrow\rangle \right). \tag{4.5}$$

Alice can perform the measurements of spin of her particle along \mathbf{n} and \mathbf{n}' directions, and Bob measures the spin of his particles along \mathbf{m} and \mathbf{m}' directions. Then they choose the quantization directions such that the angles between them are $\theta_{\mathbf{n}, \mathbf{m}} = \theta_{\mathbf{n}', \mathbf{m}} = \theta_{\mathbf{n}', \mathbf{m}'} = \frac{\pi}{4}$ and $\theta_{\mathbf{n}, \mathbf{m}'} = \frac{3\pi}{4}$. This choice of the quantization directions corresponds to the following choice of observables [57],

$$\begin{aligned}
 \hat{A}_1 &= \hat{A}_{\mathbf{n}} = \hat{\sigma}_x, \\
 \hat{A}_2 &= \hat{A}_{\mathbf{n}'} = \hat{\sigma}_z, \\
 \hat{B}_1 &= \hat{B}_{\mathbf{m}} = \frac{1}{\sqrt{2}} (\hat{\sigma}_z + \hat{\sigma}_x), \\
 \hat{B}_2 &= \hat{B}_{\mathbf{m}'} = \frac{1}{\sqrt{2}} (\hat{\sigma}_z - \hat{\sigma}_x).
 \end{aligned}$$

Then, calculating the correlation functions for these observables, one obtains a value of \mathcal{E} which violates the CHSH inequality,

$$\mathcal{E}_{\Psi^-}^{QM} = 2\sqrt{2} > 2. \tag{4.6}$$

Moreover, this value provides the maximal violation of the CHSH inequality and is known as the Tsirelson's bound.

Now, let us consider three quantization directions by choosing $\mathbf{n}' = \mathbf{m}'$. If we assume $E(A_{\mathbf{n}'}, B_{\mathbf{n}'}) = -1$, which means a perfect anticorrelation [35], then the CHSH inequality (4.3) reduces to the original Bell inequality [2],

$$|E(A_{\mathbf{n}}, B_{\mathbf{m}}) - E(A_{\mathbf{n}}, B_{\mathbf{n}'})| \leq E(A_{\mathbf{n}'}, B_{\mathbf{m}}). \quad (4.7)$$

Finally, one can derive the Wigner inequality by rewriting Bell inequality (4.7) in terms of joint probabilities,

$$P(\mathbf{n}, \mathbf{m}) - P(\mathbf{n}, \mathbf{n}') \leq P(\mathbf{n}', \mathbf{m}). \quad (4.8)$$

4.2 Bell inequalities for neutral kaons

Neutral kaons can be produced in entangled states at the DAΦNE collider through the decay of ϕ -mesons which in turn are produced via electron-positron collisions. In other words, through the reaction

$$e^+ e^- \rightarrow \phi \rightarrow K^0 \bar{K}^0$$

an entangled pair of kaons is created in $|\Psi^-\rangle$ Bell state at the time $t = 0$,

$$\begin{aligned} |\Psi^-\rangle &= \frac{1}{\sqrt{2}} \left(|K^0\rangle_l \otimes |\bar{K}^0\rangle_r - |\bar{K}^0\rangle_l \otimes |K^0\rangle_r \right) \\ &= \frac{N^2}{2\sqrt{2}pq} \left(|K_S\rangle_l \otimes |K_L\rangle_r - |K_L\rangle_l \otimes |K_S\rangle_r \right), \end{aligned} \quad (4.9)$$

which is antisymmetric under \mathcal{C} and \mathcal{P} symmetry operations. Then the kaons can be detected on the left and right sides apart from the source, so it is denoted by l and r indexes in (4.9).

Neutral kaons allow for a description by the quasispin picture in analogy to spin- $\frac{1}{2}$ particles and polarized photons [35, 58, 59]. In this approach the flavor eigenstates of a kaon are interpreted as the quasispin up and quasispin down states. In this way the operators which act in the quasispin space can be expressed through Pauli matrices, particularly, the strangeness operator $\hat{\mathcal{S}}$ is expressed by $\hat{\sigma}_z$ and the $\hat{\mathcal{C}}\hat{\mathcal{P}}$ operator is expressed by $-\hat{\sigma}_x$.

In analogue to Bell inequalities derived for the averaged values of spin directions along the quantization directions n and m a set of Bell inequalities can be derived for the averaged values of quasispin directions for different detection times t_a and t_b for

entangled kaons [34–36]. Thus, the free choice of detection times of the quasispin states plays the same role as the free choice of the angles for spin- $\frac{1}{2}$ particles and polarized photons. Moreover, there is a freedom of choice of the particular quasispin states of a kaon, therefore we can choose as quasispin up and quasispin down states not only the flavor eigenstates $|K^0\rangle, |\bar{K}^0\rangle$, but the mass eigenstates $|K_L\rangle, |K_S\rangle$ and the \mathcal{CP} eigenstates $|K_1^0\rangle, |K_2^0\rangle$ as well.

It should be noted that one has to extend the Hilbert space of two kaons $\mathcal{H}^r \otimes \mathcal{H}^l$ to include the decay products and avoid a decrease of the total state. Thus, one assumes the following time evolution of the mass eigenstates,

$$|K_i(t)\rangle = e^{-im_i t} e^{-\frac{\Gamma_i}{2} t} |K_i\rangle + |\Omega_i(t)\rangle, \quad (4.10)$$

which includes $|\Omega_i(t)\rangle$, the state of all decay products which is orthogonal to the kaon mass eigenstates and satisfies the following relation,

$$\langle \Omega_i(t) | \Omega_j(t) \rangle = \begin{cases} 1 - e^{-\Gamma_i t}, & i = j, \\ \delta \cdot \left(1 - e^{i\Delta m t} e^{-\frac{\Gamma_L + \Gamma_S}{2} t} \right), & i \neq j. \end{cases}$$

Now we can consider a set of observables $O^\eta(k_n, t_a)$ which have the value $+1$ if one in a measurement at time t_a detects the quasispin state k_n on the side η ($\eta = l$ for the left side and $\eta = r$ for the right side) and the value -1 if the particle decayed. This leads to a definition of the correlation function $O(k_n, t_a; k_m, t_b)$ which gets the value $+1$ if one in a measurement detects the quasispin states k_n at time t_a on one side and k_m at time t_b on the other side or detects none of them and the value -1 if one in a measurement detects only one of the two quasispin states. Now the locality assumption divides the correlation function into a product of the observables,

$$O(k_n, t_a; k_m, t_b) \equiv O^r(k_n, t_a) \cdot O^l(k_m, t_b). \quad (4.11)$$

Then considering N measurements of the observable O one can derive the CHSH inequality for its expectation values [34, 35],

$$|E(k_n, t_a; k_m, t_b) - E(k_n, t_a; k_{m'}, t_d)| + |E(k_{n'}, t_c; k_{m'}, t_d) + E(k_{n'}, t_c; k_m, t_b)| \leq 2, \quad (4.12)$$

where $E(k_n, t_a; k_m, t_b) = \frac{1}{N} \sum_{i=1}^N O_i(k_n, t_a; k_m, t_b)$ and O_i is the measured value of O in the i -th experiment. Consequently, one defines a set of four probabilities,

- $P_{nm}(Y, t_a; Y, t_b)$ for detecting the quasispin state k_n at time t_a on the left side and the quasispin state k_m at time t_b on the left-hand side,

- $P_{nm}(Y, t_a; N, t_b)$ for detecting the quasispin state k_n at time t_a on the left side and no quasispin state k_m at time t_b on the left-hand side,
- $P_{nm}(N, t_a; Y, t_b)$ for detecting no quasispin state k_n at time t_a on the left side and the quasispin state k_m at time t_b on the left-hand side,
- $P_{nm}(N, t_a; N, t_b)$ for detecting no quasispin state k_n at time t_a on the left side and no quasispin state k_m at time t_b on the left-hand side,

and plugging them into the (4.12) one obtains the CHSH inequality for the probabilities [34, 35],

$$|P_{nm}(Y, t_a; Y, t_b) + P_{nm}(N, t_a; N, t_b) - P_{nm'}(Y, t_a; Y, t_d) - P_{nm'}(N, t_a; N, t_d)| \quad (4.13)$$

$$\leq 1 \pm \left\{ -1 + P_{n'm}(Y, t_c; Y, t_b) + P_{n'm}(N, t_c; N, t_b) - P_{n'm'}(Y, t_c; Y, t_d) - P_{n'm'}(N, t_c; N, t_d) \right\}.$$

Finally, choosing in (4.13) the plus sign and putting $n' = m'$ and $t_c = t_d$ one obtains a Wigner-type Bell inequality for three quasispin states [34, 35],

$$P_{nm}(Y, t_a; Y, t_b) \leq P_{nn'}(Y, t_a; Y, t_c) + P_{n'm}(Y, t_c; Y, t_b) + h(k_n, k_m, k_{n'}; t_a, t_b, t_c), \quad (4.14)$$

where $h(k_n, k_m, k_{n'}; t_a, t_b, t_c) = -P_{nm}(N, t_a; N, t_b) + P_{nn'}(N, t_a; N, t_c) + P_{n'm}(N, t_c; N, t_b) + P_{n'n'}(N, t_c; N, t_c)$ is the correction function which turns into zero at $t_a = t_b = 0$. This inequality we will use in our analysis of the collapse models.

The Wigner-type Bell inequality (4.14) reveals a crucial role of the violation of \mathcal{CP} symmetry in the local hidden variables models context. Choosing two sets of the quasispin states $k_n = K_S, k_m = \bar{K}^0, k_{n'} = K_1^0$ and $k_n = K_S, k_m = K^0, k_{n'} = K_1^0$, one can derive from (4.14) two inequalities for the transition probabilities $P_{ij}(Y, t_a; Y, t_b)$ which turn into bounds for the \mathcal{CP} violation parameter δ defined in (3.15),

$$\delta \leq 0,$$

$$\delta \geq 0,$$

which turns into the equality [36, 37]

$$\delta = 0. \quad (4.15)$$

This means that a local hidden variable theory implies a conservation of \mathcal{CP} symmetry, and its violation leads to a violation of the Bell inequalities.

SPONTANEOUS COLLAPSE IN FLAVOR OSCILLATIONS

In this chapter we apply two popular collapse models introduced above, the QMUPL model and the mass-proportional CSL model, to the neutral meson system and compute the effect of spontaneous collapse through a perturbative approach, namely Dyson series, following the method discussed in [23, 25, 48, 80, 81]. Then we discuss the obtained results and provide a review them from the open quantum system's point of view. Last but not least we extend the analysis of spontaneous collapse in a neutral meson system by taking into account the violation of \mathcal{CP} symmetry.

5.1 Perturbative calculation of the probabilities

In this section we aim to apply the two collapse models, the QMUPL model and the mass-proportional CSL model, to the dynamics of the neutral meson system described by the phenomenological Hamiltonian as discussed above. The observables of our interest are the transition probabilities from mass eigenstates to mass eigenstates, $P_{M_\mu \rightarrow M_\nu}(t)$, and from flavor eigenstates to flavor eigenstates, $P_{M^0 \rightarrow M^0/\bar{M}^0}(t)$, which are intensively studied in experiments. These probabilities are computed under the assumption that we start at time $t_0 = 0$ with a mass eigenstate $|M_\mu\rangle$ or flavor eigenstate $|M^0\rangle$,

$$P_{M_\mu \rightarrow M_\nu}(t) = \sum_{\mathbf{p}_f} \mathbb{E} |\langle M_\nu, \mathbf{p}_f | M_\mu(t), \mathbf{p}_i \rangle|^2,$$

$$P_{M^0 \rightarrow M^0/\bar{M}^0}(t) = \sum_{\mathbf{p}_f} \mathbb{E} |\langle M^0/\bar{M}^0, \mathbf{p}_f | M^0(t), \mathbf{p}_i \rangle|^2,$$

where \mathbf{p}_i is the momentum of the initial state.

As we have shown in equation (2.15), the collapse models modify the Hamiltonian of the system in the following way

$$\hat{H} \rightarrow \hat{H} - \sqrt{\lambda} \sum_{i=1}^N \hat{A}_i w_{i,t} := \hat{H} + \hat{N}(t), \quad (5.2)$$

where $\varphi = 0$ is taken for simplicity, and the explicit form of the operators \hat{A}_i is defined by the corresponding collapse model. We treat the term $N(t)$ which describes the interaction with the noise field as a perturbation. This allows us to use a perturbation theory in order to compute the transition probabilities.

To obtain these probabilities we need to compute the transition amplitudes for all the mass eigenstates. For that we move first to the interaction picture [23, 25, 48, 80, 81]

$$\begin{aligned} T_{\mu\nu}(\mathbf{p}_f, \mathbf{p}_i, \alpha; t) &:= \langle M_\nu, \mathbf{p}_f | M_\mu(t), \mathbf{p}_i, \alpha \rangle \\ &= e^{-im_\mu t} \langle M_\nu, \mathbf{p}_f | \hat{U}_I(t) | M_\mu, \mathbf{p}_i, \alpha \rangle, \end{aligned} \quad (5.3)$$

where the evolution operator $\hat{U}_I(t)$ is the corresponding one in the interaction picture. The evolution operator can be expanded into a Dyson series, and we compute the transition amplitudes up to fourth perturbative order

$$\begin{aligned} T_{\mu\nu}(\mathbf{p}_f, \mathbf{p}_i; t) &\simeq e^{-im_\mu t} \left(T_{\mu\nu}^{(0)}(\mathbf{p}_f, \mathbf{p}_i; t) + T_{\mu\nu}^{(1)}(\mathbf{p}_f, \mathbf{p}_i; t) + T_{\mu\nu}^{(2)}(\mathbf{p}_f, \mathbf{p}_i; t) \right. \\ &\quad \left. + T_{\mu\nu}^{(3)}(\mathbf{p}_f, \mathbf{p}_i; t) + T_{\mu\nu}^{(4)}(\mathbf{p}_f, \mathbf{p}_i; t) \right), \end{aligned} \quad (5.4)$$

where

$$T_{\mu\nu}^{(0)}(\mathbf{p}_f, \mathbf{p}_i; t_0) = \langle M_\nu, \mathbf{p}_f | M_\mu, \mathbf{p}_i \rangle, \quad (5.5a)$$

$$\begin{aligned} T_{\mu\nu}^{(n)}(\mathbf{p}_f, \mathbf{p}_i; t_0) &= (-i)^n \int_0^{t_0} dt_1 \dots \int_0^{t_{n-1}} dt_n \\ &\quad \cdot \langle M_\nu, \mathbf{p}_f | \prod_{j=1}^n \left(\hat{N}_I(t_j) \right) | M_\mu, \mathbf{p}_i \rangle \text{ for } n = 1, 2, 3, 4, \end{aligned} \quad (5.5b)$$

where $\hat{N}_I(t)$ is the noise term in the interaction picture. The detailed computations of each term of the Dyson series (5.4) we provide in the Appendix A for the QMUPL model and in the Appendix B for the mass-proportional CSL model.

5.1.1 The neutral meson dynamics predicted by the QMUPL model

For the QMUPL model we define the initial state as a wave packet in position picture with a width $\sqrt{\alpha}$ in d -dimensional space and a momentum \mathbf{p}_i , while the final state is

typically assumed to be a momentum eigenstate. We start with the 1-dimensional case as the simplest one and then generalize the results to the d -dimensional case. As was mentioned in the previous chapter, in the QMUPL model the collapse operators \hat{A}_i are chosen to be the position operators \hat{q}_i . In order to describe the collapse dynamics in the case of neutral mesons we extend the collapse operators \hat{A}_i by a flavor part

$$\hat{\mathbf{A}}_{QMUPL} = \hat{\mathbf{q}} \otimes \left[\frac{m_H}{m_0} |M_H\rangle \langle M_H| + \frac{m_L}{m_0} |M_L\rangle \langle M_L| \right], \quad (5.6a)$$

and, consequently, the potential $\hat{N}(t)$ of the Schrödinger-like equation (2.15) becomes

$$\hat{N}_{QMUPL}(t) = -\sqrt{\lambda} (\mathbf{w}_t \cdot \hat{\mathbf{q}}) \otimes \left[\frac{m_H}{m_0} |M_H\rangle \langle M_H| + \frac{m_L}{m_0} |M_L\rangle \langle M_L| \right]. \quad (5.6b)$$

We consider \mathbf{w}_t as a white (uncolored) noise field and the corresponding correlation function is $\mathbb{E}[\mathbf{w}_t \cdot \mathbf{w}_{t'}] = \delta(t - t')$. Then putting the transition amplitudes and performing necessary computations we obtain the transition probabilities up to second order in time and collapse constants,

$$P_{M_\mu \rightarrow M_\nu}^{QMUPL}(t) = \delta_{\mu\nu} \left(1 - \Lambda_\mu^{QMUPL} \cdot t + 3 \cdot \frac{1}{2} (\Lambda_\mu^{QMUPL})^2 \cdot t^2 \right) \cdot e^{-\Gamma_\mu t}, \quad (5.7a)$$

$$\begin{aligned} P_{M^0 \rightarrow M^0/M^0}^{QMUPL}(t) &= \frac{1}{4} \left\{ \sum_{i=H,L} e^{-\Gamma_i t} \left(1 - \Lambda_i^{QMUPL} \cdot t + 3 \cdot \frac{1}{2} (\Lambda_i^{QMUPL})^2 \cdot t^2 \right) \right. \\ &\quad \left. \pm 2 \cos(\Delta m t) e^{-\frac{\Gamma_H + \Gamma_L}{2} t} \cdot \left(1 - \left[\frac{\alpha \lambda \Delta m^2}{2} \frac{1}{2m_0^2} + \frac{\Lambda_H^{QMUPL} + \Lambda_L^{QMUPL}}{2} \right] \cdot t \right. \right. \\ &\quad \left. \left. + 3 \cdot \frac{1}{2} \left[\frac{\alpha \lambda \Delta m^2}{2} \frac{1}{2m_0^2} + \frac{\Lambda_H^{QMUPL} + \Lambda_L^{QMUPL}}{2} \right]^2 \cdot t^2 \right) \right\}, \quad (5.7b) \end{aligned}$$

where $\Delta m = m_H - m_L$ is the difference of masses, $\Lambda_\mu^{QMUPL} = \frac{\alpha \lambda}{2} \cdot \frac{m_\mu^2}{m_0^2} \cdot (1 - 2\vartheta(0))$, and $\vartheta(0)$ is the value of the Heaviside function at zero.

We see that the mass eigenstates do not oscillate as it is the case in the standard approach. The effect of the collapse on the meson time evolution leads to terms containing absolute masses of the mesons which never appear in the standard quantum theory. Moreover, it gives an “inverted” ordering, namely the decay rate that is larger than the other one is connected to the heavier mass. This in turns means that the eigenstate of the heavier mass decays earlier. The standard theory does not give any such restrictions.

The computations for the QMUPL model show that the transition probabilities are independent of space dimensionality d . Moreover, the second order in time shows an additional factor 3 which is independent of dimensionality as well. This factor is produced by the choice of a Gaussian wave packet as an initial state and its integration over all

final momenta. In turn the collapse effect cannot be assumed to be an exponential one in general. Due to such a dynamic the effect of the QMUPL model becomes in principle observable.

5.1.2 The neutral meson dynamics predicted by the CSL model

For the mass-proportional CSL model we define the initial state as a plane wave with a momentum \mathbf{p}_i and investigate the d -dimensional case immediately. In this case we choose the following collapse operators and potential for the two mass eigenstates of the neutral meson system

$$\hat{A}_{CSL}(\mathbf{x}) = \int d\mathbf{y} g(\mathbf{y} - \mathbf{x}) \left(\frac{m_H}{m_0} \hat{\psi}_H^\dagger(\mathbf{y}) \hat{\psi}_H(\mathbf{y}) + \frac{m_L}{m_0} \hat{\psi}_L^\dagger(\mathbf{y}) \hat{\psi}_L(\mathbf{y}) \right), \quad (5.8a)$$

$$\hat{N}_{CSL}(t) = -\sqrt{\gamma} \int d\mathbf{y} w_t(\mathbf{y}) \left(\frac{m_H}{m_0} \hat{\psi}_H^\dagger(\mathbf{y}) \hat{\psi}_H(\mathbf{y}) + \frac{m_L}{m_0} \hat{\psi}_L^\dagger(\mathbf{y}) \hat{\psi}_L(\mathbf{y}) \right), \quad (5.8b)$$

where the correlation functions of the mass-proportional CSL noise $w_t(\mathbf{x})$ are given by

$$\mathbb{E}[w_t(\mathbf{x})w_s(\mathbf{y})] = F(\mathbf{x} - \mathbf{y})\delta(t - s), \quad (5.9)$$

where $F(\mathbf{x}) = \frac{1}{(\sqrt{4\pi}r_C)^d} e^{-\mathbf{x}^2/4r_C^2}$. Collecting all the necessary terms we obtain the probabilities of interest (see Appendix B),

$$P_{M_\mu \rightarrow M_\nu}^{CSL}(t) = \delta_{\mu\nu} \left(1 - \Gamma_\mu^{CSL} \cdot t + \frac{1}{2} (\Gamma_\mu^{CSL})^2 \cdot t^2 \right) \cdot e^{-\Gamma_\mu t}, \quad (5.10a)$$

$$\begin{aligned} P_{M^0 \rightarrow M^0/\bar{M}^0}^{CSL}(t) &= \frac{1}{4} \left\{ \sum_{i=H,L} e^{-\Gamma_i t} \left(1 - \Gamma_i^{CSL} \cdot t + \frac{1}{2} (\Gamma_i^{CSL})^2 \cdot t^2 \right) \right. \\ &\quad \left. \pm 2 \cos(\Delta m t) e^{-\frac{\Gamma_H + \Gamma_L}{2} t} \cdot \left(1 - \left[\frac{\gamma}{(\sqrt{4\pi}r_C)^d} \frac{\Delta m^2}{2m_0^2} + \frac{\Gamma_H^{CSL} + \Gamma_L^{CSL}}{2} \right] \cdot t \right. \right. \\ &\quad \left. \left. + \frac{1}{2} \left[\frac{\gamma}{(\sqrt{4\pi}r_C)^d} \frac{\Delta m^2}{2m_0^2} + \frac{\Gamma_H^{CSL} + \Gamma_L^{CSL}}{2} \right]^2 \cdot t^2 \right) \right\}, \quad (5.10b) \end{aligned}$$

where $\Gamma_\mu^{CSL} = \frac{\gamma}{(\sqrt{4\pi}r_C)^d} \cdot \frac{m_\mu^2}{m_0^2} \cdot (1 - 2\vartheta(0))$.

In strong contrast to the CSL model, where we can expect that the dynamics of a mass eigenstate propagating in free space is exponential, so

$$P_{M_{\mu=L/H} \rightarrow M_{\nu=L/H}}^{CSL}(t) = \delta_{\mu\nu} e^{-(\Gamma_\mu^{CSL} + \Gamma_\mu)t}. \quad (5.11)$$

Last but not least the choice of $\vartheta(0) \in [0, 1]$ coming from the correlation functions of the Wiener processes leads to positive ($\vartheta(0) \in [0, \frac{1}{2})$), zero ($\vartheta(0) = \frac{1}{2}$) or negative ($\vartheta(0) \in [\frac{1}{2}, 1]$) values of Γ^{CSL} .

Again, for the CSL model we assume that the higher orders in time lead to an exponential behavior, which we have proven up to the second order in time

$$P_{M^0 \rightarrow M^0/\bar{M}^0}^{CSL}(t) = \frac{e^{-(\Gamma_L + \Gamma_L^{CSL})t} + e^{-(\Gamma_H + \Gamma_H^{CSL})t}}{4} \cdot \left\{ 1 \pm \frac{\cos(\Delta m t)}{\cosh\left(\frac{(\Gamma_L + \Gamma_L^{CSL}) - (\Gamma_H + \Gamma_H^{CSL})}{2} \cdot t\right)} \cdot e^{-\frac{\gamma}{(\sqrt{4\pi} r_C)^d} \frac{(\Delta m)^2}{2m_0^2} t} \right\}. \quad (5.12)$$

This is an interesting result since it disentangles two effects of the collapse model. A damping of the interference term proportional to the mass difference squared $(\Delta m)^2$, which is independent of the choice of the Heaviside function $\vartheta(0)$ and additional energy terms Γ_i^{CSL} proportional to the absolute masses, which depend on the Heaviside function. These additional energy terms play the same role as the decay constants (added by hands) in standard quantum theory.

5.2 Including the \mathcal{CP} violation effects to the predictions of the CSL model

Now we take into account non-orthogonality of the mass eigenstates due to the violation of \mathcal{CP} symmetry in a neutral kaon system, $\langle K_L | K_S \rangle = \delta$, and apply the same perturbative approach used in the previous sections to compute the transition probabilities for kaons. We start with transition probabilities for the mass eigenstates, which reveal now a more involved form for the mass-proportional CSL model (see Appendix B), and neglect the freedom of choosing the value of the Heaviside function in zero by fixing $\vartheta(0) = \frac{1}{2}$,

$$P_{K_L \rightarrow K_L}^{CSL}(t) = e^{-\Gamma_L t} \left\{ 1 - \delta^2 (1 - \delta^2) \frac{\gamma}{(\sqrt{4\pi} r_C)^d} \frac{m_S^2}{m_0^2} \cdot \Lambda_{\mathcal{CP}}^{CSL}(t) \cdot t \right\}, \quad (5.13)$$

$$P_{K_L \rightarrow K_S}^{CSL}(t) = \delta^2 e^{-\Gamma_L t} \left\{ 1 - (1 - \delta^2) \frac{\gamma}{(\sqrt{4\pi} r_C)^d} \frac{m_L m_S}{m_0^2} \cdot \Lambda_{\mathcal{CP}}^{CSL}(t) \cdot t \right\}, \quad (5.14)$$

$$P_{K_S \rightarrow K_S}^{CSL}(t) = \delta^2 e^{-\Gamma_S t} \left\{ 1 - (1 - \delta^2) \frac{\gamma}{(\sqrt{4\pi} r_C)^d} \frac{m_L m_S}{m_0^2} \cdot \Lambda_{\mathcal{CP}}^{CSL}(t) \cdot t \right\}, \quad (5.15)$$

$$P_{K_S \rightarrow K_L}^{CSL}(t) = e^{-\Gamma_S t} \left\{ 1 - \delta^2 (1 - \delta^2) \frac{\gamma}{(\sqrt{4\pi} r_C)^d} \frac{m_L^2}{m_0^2} \cdot \Lambda_{\mathcal{CP}}^{CSL}(t) \cdot t \right\}, \quad (5.16)$$

where $\Lambda_{\mathcal{CP}}^{CSL}(t) = 1 - \frac{1}{4} \frac{\gamma}{(\sqrt{4\pi} r_C)^d} \frac{(\Delta m)^2 + 4\delta^2 m_L m_S}{m_0^2} \cdot t$. We see that the effect of the CSL collapse on the kaon time evolution in the presence of the \mathcal{CP} violation leads to terms containing

absolute masses. Moreover, their contribution to the evolution of the mass eigenstates is not more exponential as we have seen in the previous subsection.

Collecting all the necessary transition probabilities for the mass eigenstates we obtain the transition probabilities for the flavor eigenstates,

$$\begin{aligned}
 P_{K^0 \rightarrow K^0}^{CSL}(t) &= \frac{1}{4} \left\{ e^{-\Gamma_L t} + e^{-\Gamma_S t} \right. \\
 &\quad - \delta(1-\delta) \frac{\gamma}{(\sqrt{4\pi} r_C)^d} \frac{(\Delta m)^2}{m_0^2} (m_L e^{-\Gamma_S t} - m_S e^{-\Gamma_L t}) \cdot \Lambda_{\mathcal{CP}}^{CSL}(t) \cdot t \\
 &\quad \left. + 2e^{-\frac{\Gamma_L + \Gamma_S}{2} t} \cos[t\Delta m] \left(1 - \frac{1-\delta}{2} \frac{\gamma}{(\sqrt{4\pi} r_C)^d} \cdot \Lambda_{\mathcal{CP}}^{CSL}(t) \cdot t \right) \right\}, \quad (5.17)
 \end{aligned}$$

$$\begin{aligned}
 P_{K^0 \rightarrow \bar{K}^0}^{CSL}(t) &= \frac{1}{4} \frac{1-\delta}{1+\delta} \left\{ e^{-\Gamma_L t} + e^{-\Gamma_S t} \right. \\
 &\quad + \delta(1+\delta) \frac{\gamma}{(\sqrt{4\pi} r_C)^d} \frac{(\Delta m)^2}{m_0^2} (m_L e^{-\Gamma_S t} - m_S e^{-\Gamma_L t}) \cdot \Lambda_{\mathcal{CP}}^{CSL}(t) \cdot t \\
 &\quad \left. + 2e^{-\frac{\Gamma_L + \Gamma_S}{2} t} \cos[t\Delta m] \left(1 - \frac{1+\delta}{2} \frac{\gamma}{(\sqrt{4\pi} r_C)^d} \cdot \Lambda_{\mathcal{CP}}^{CSL}(t) \cdot t \right) \right\}. \quad (5.18)
 \end{aligned}$$

In this way \mathcal{CP} violation combined with the collapse effect brings an extra contribution proportional to the absolute masses which changes the evolution of a neutral kaon system in a non-trivial way. In contrast to the case of unbroken \mathcal{CP} symmetry (5.12), breaking the \mathcal{CP} symmetry entangles two effects of the mass-proportional CSL model, the damping of the interference term and the additional energy terms, such that the behavior of the transition probability is no longer exponential.

5.3 Interpretation of the results via the CSL model

In the next step we investigate whether the collapse dynamics leading to the above result can explain the full dynamics of the neutral meson systems without defining decay constants (by hands) due to Wigner–Weisskopf approximation.

At accelerator facilities the following asymmetry term $A(t)$ is experimentally intensively investigated

$$A^{exp}(t) = \frac{P_{M^0 \rightarrow M^0}^{exp}(t) - P_{M^0 \rightarrow \bar{M}^0}^{exp}(t)}{P_{M^0 \rightarrow M^0}^{exp}(t) + P_{M^0 \rightarrow \bar{M}^0}^{exp}(t)} = \frac{\cos(\Delta m t)}{\cosh(\frac{\Delta \Gamma}{2} \cdot t)}, \quad (5.19)$$

where $\Delta \Gamma = \Gamma_L - \Gamma_H$. The CSL model predicts the asymmetry term in the following form

for the unbroken \mathcal{CP} symmetry

$$\begin{aligned}
 A^{CSL}(t) &= \frac{P_{M^0 \rightarrow M^0}^{CSL}(t) - P_{M^0 \rightarrow \bar{M}^0}^{CSL}(t)}{P_{M^0 \rightarrow M^0}^{CSL}(t) + P_{M^0 \rightarrow \bar{M}^0}^{CSL}(t)} \\
 &= \frac{\cos(\Delta m t)}{\cosh\left(\frac{(\Gamma_L + \Gamma_L^{CSL}) - (\Gamma_H + \Gamma_H^{CSL})}{2} \cdot t\right)} \cdot e^{-\frac{\gamma}{(\sqrt{4\pi} r_C)^d} \frac{(\Delta m)^2}{2m_0^2} t},
 \end{aligned} \tag{5.20}$$

and in the presence of \mathcal{CP} violation in a neutral kaon system

$$\begin{aligned}
 A_{\mathcal{CP}}^{CSL}(t) &= \frac{\delta + \frac{\cos(\Delta m t)}{\cosh(\frac{\Delta\Gamma}{2} \cdot t)}}{1 + \delta \frac{\cos(\Delta m t)}{\cosh(\frac{\Delta\Gamma}{2} \cdot t)}} \cdot \left(1 - \frac{1 - \delta^2}{2} \frac{\gamma}{(\sqrt{4\pi} r_C)^d} \frac{\Delta m^2}{m_0^2} \cdot \Lambda_{\mathcal{CP}}^{CSL}(t) \cdot t\right) \\
 &\quad - \frac{\delta \tanh(\frac{\Delta\Gamma}{2} \cdot t)}{1 + \delta \frac{\cos(\Delta m t)}{\cosh(\frac{\Delta\Gamma}{2} \cdot t)}} \cdot \frac{1 - \delta^2}{2} \frac{\gamma}{(\sqrt{4\pi} r_C)^d} \frac{m_L^2 - m_S^2}{m_0^2} \cdot \Lambda_{\mathcal{CP}}^{CSL}(t) \cdot t,
 \end{aligned} \tag{5.21}$$

which for small times reduces to

$$A_{\mathcal{CP}}^{CSL}(t) \approx \frac{\delta + \cos[t\Delta m]}{1 + \delta \cos[t\Delta m]} \left(1 - \frac{1 - \delta^2}{2} \frac{\gamma}{(\sqrt{4\pi} r_C)^d} \frac{\Delta m^2}{m_0^2} \cdot \Lambda_{\mathcal{CP}}^{CSL}(t) \cdot t\right). \tag{5.22}$$

From (5.21) and (5.22) we observe that the \mathcal{CP} violation combined with the CSL collapse effect brings an extra contribution proportional to the absolute masses and leads to a non-trivial asymmetry term.

From (5.20) with assumed unbroken \mathcal{CP} symmetry we observe that the damping term proportional to $\frac{\gamma}{(\sqrt{4\pi} r_C)^d} \frac{(\Delta m)^2}{2m_0^2}$ is in principle measurable. As we have discussed in Section 2.1 the standard proposed value for the mass-proportional CSL model is $\lambda_{CSL} := \frac{\gamma}{(\sqrt{4\pi} r_C)^d} \approx 10^{-(8\pm 2)} s^{-1}$ (Adler [44]) or $\approx 10^{-16} s^{-1}$ (GRW [39]). Here the coherence length is assumed to be of the order $10^{-5} cm$ and $d = 3$ and from that the collapse strength γ can be deduced. For more details on the allowed parameter space for r_C and γ consider, e.g., Ref. [82]. Let us also note that the best experimental upper bound is currently obtained by X-rays [9] being five orders away from the proposed value of Adler, i.e. $10^{-12} s^{-1}$.

Plugging in these two values (Adler/GRW) and the measured mass differences we find damping rates of the order $10^{-38} s^{-1}/10^{-46} s^{-1}$ for K -mesons, $10^{-30} s^{-1}/10^{-38} s^{-1}$ for B_d -mesons, $10^{-30} s^{-1}/10^{-38} s^{-1}$ for B_s mesons and $10^{-34} s^{-1}/10^{-42} s^{-1}$ for D mesons (see also Ref. [24]). The choice of the reference mass m_0 being either the neutron mass or the rest mass of the respective neutral meson does not affect the values considerably. This is not directly observable since it corresponds to a lifetime much greater than the

decay rates of the respective neutral meson. Consequently, the effect of the spontaneous collapse on the interference can be safely neglected.

The idea behind the choice of m_0 , being generally a free parameter of the CSL model, is that for ordinary matter the mass ratio corresponds to an average number of constituents of the composite object [83]; the bigger the object, the stronger the effect of spontaneous localization. The choice in the meson system stems from our assumption that if collapse models are relevant in Nature then they have to hold for all physical systems. For the meson system this mass ratio $\frac{m_\mu}{m_0}$ decreases if m_0 is of the order of a nucleon or the rest mass of the mesons system, i.e. has the opposite behavior. Thus, it may seem more reasonable to have for particles lighter than those that make up the ordinary matter the inverted ratio. If we do so then the damping factor of the interference term becomes $\frac{1}{2}\lambda_{CSL}\frac{\Delta m^2 m_0^2}{m_H^2 m_L^2}$, which is only computable if we know the absolute masses.

The second modification due to the mass proportional CSL model compared to the standard approach is for the decay rates, i.e. $\Gamma_\mu + \Gamma_\mu^{CSL}$. Here Γ_μ are the standard decay rates introduced to the system by the Wigner–Weisskopf approximation. The collapse contribution is connected to the absolute mass (playing no role in the standard approach) and the value of the Heaviside function at zero, i.e. $\Gamma_\mu^{CSL} = \lambda_{CSL} \cdot \frac{m_\mu^2}{m_0^2} \cdot (1 - 2\vartheta(0))$ or in the inverted scenario $\Gamma_\mu^{CSL} = \lambda_{CSL} \cdot \frac{m_0^2}{m_\mu^2} \cdot (1 - 2\vartheta(0))$.

Taking this one step further is to ask whether collapse models could solely be responsible for the decaying part of the neutral mesons, i.e. the dynamics of the spontaneous location induces the decay of the mass eigenstates. For that we set $\Gamma_\mu^{exp} \equiv \Gamma_\mu^{CSL}$. Certainly Γ^{CSL} needs to be positive, i.e. $\vartheta(0) \in [0, \frac{1}{2}]$, to obey equations (5.11). Then we obtain

$$\frac{\Gamma_L^{CSL} - \Gamma_H^{CSL}}{\Gamma_L^{CSL} + \Gamma_H^{CSL}} \stackrel{\vartheta(0) \neq \frac{1}{2}}{=} \pm \frac{m_L^2 - m_H^2}{m_L^2 + m_H^2} = \begin{cases} \text{K-mesons: } 0.996506 \begin{cases} +1.2760 \cdot 10^{-5} \\ -1.2760 \cdot 10^{-5} \end{cases} \\ \text{D-mesons: } 0.00645 \begin{cases} +0.0007 \\ -0.0009 \end{cases} \\ \text{B}_d\text{-mesons: } 0.0005 \begin{cases} +0.0050 \\ -0.0050 \end{cases} \\ \text{B}_s\text{-mesons: } 0.06912 \begin{cases} +7.7058 \cdot 10^{-4} \\ -7.7058 \cdot 10^{-4} \end{cases} \end{cases} \quad (5.23)$$

The experimental values for the experimentally measured decay constants (right-hand side of the above equation) are taken from the particle data book [84]. The method how to deduce from the experimental values measured the decay rates is described in Appendix D since it differs slightly for each meson. The minus sign holds for the inverted

	$\Gamma_L^{\text{exp}} [s^{-1}]$	$\Gamma_H^{\text{exp}} [s^{-1}]$	$\Delta m^{\text{exp}} [\hbar s^{-1}]$	$m_L [\hbar s^{-1}]$	$m_H [\hbar s^{-1}]$
<i>K</i> -mesons	$1.117 \cdot 10^{10}$	$1.955 \cdot 10^7$	$0.529 \cdot 10^{10}$	$2.311 \cdot 10^8$	$5.524 \cdot 10^9$
<i>D</i> -mesons	$2.454 \cdot 10^{12}$	$2.423 \cdot 10^{12}$	$0.950 \cdot 10^{10}$	$1.468 \cdot 10^{12}$	$1.477 \cdot 10^{12}$
<i>B_d</i> -mesons	$6.582 \cdot 10^{11}$	$6.576 \cdot 10^{11}$	$0.510 \cdot 10^{12}$	$1.020 \cdot 10^{15}$	$1.020 \cdot 10^{15}$
<i>B_s</i> -mesons	$7.072 \cdot 10^{11}$	$6.158 \cdot 10^{11}$	$1.776 \cdot 10^{13}$	$2.477 \cdot 10^{14}$	$2.655 \cdot 10^{14}$

Table 5.1: Experimental values of the decay rates, the mass difference and the computed values of the absolute masses for the neutral mesons system.

scenario. Together with the experimentally obtained value of $\Delta m := m_H - m_L$, this allows to compute the absolute values of the masses $m_{H/L}$ via

$$\frac{\Gamma_L^{CSL} - \Gamma_H^{CSL}}{\Gamma_L^{CSL} + \Gamma_H^{CSL}} = \pm \frac{m_L^2 - (m_L + \Delta m)^2}{m_L^2 + (m_L + \Delta m)^2} = \pm \left(-1 + \frac{m_L^2}{m_L^2 + m_L \Delta m + \frac{1}{2}(\Delta m)^2} \right). \quad (5.24)$$

In the case we have $m_H > m_L$ ($\Delta m > 0$) we observe that the right-hand side of (5.24) becomes negative (if we do not reverse the mass ratio). Thus, the two involved masses cannot be both positive. This is because the collapse models relate the decay rates with the corresponding masses directly proportionally: the heavier the mass the larger the decay rate, the smaller the lifetime.

This is physically intuitive from the collapse model perspective since heavier masses should be affected stronger by the spontaneous factorization. The counter-intuitive effect for applying that to neutral mesons decay is that the more massive state should decay faster. In literature there can be found experiments [85, 86] for *K*-mesons assigned to measure the sign of Δm and, herewith, if the heavier mass connects also to the lower decay rate (longer lifetime) and vice versa. The results are a positive sign of Δm , i.e. the heavier mass decays slower. Note that not for all mesons the sign has been determined. In summary, for positive mass differences $\Delta m > 0$ we cannot find positive masses.

In the reversed scenario positive values for the absolute masses are obtained and listed in table 5.1. Note that the numerical values are very sensitive to the errors and the method to determine the decay constants which are very different to the specific mesons and the experiments considered. We stick here to the values published by the particle data group in their summary and review papers [84].

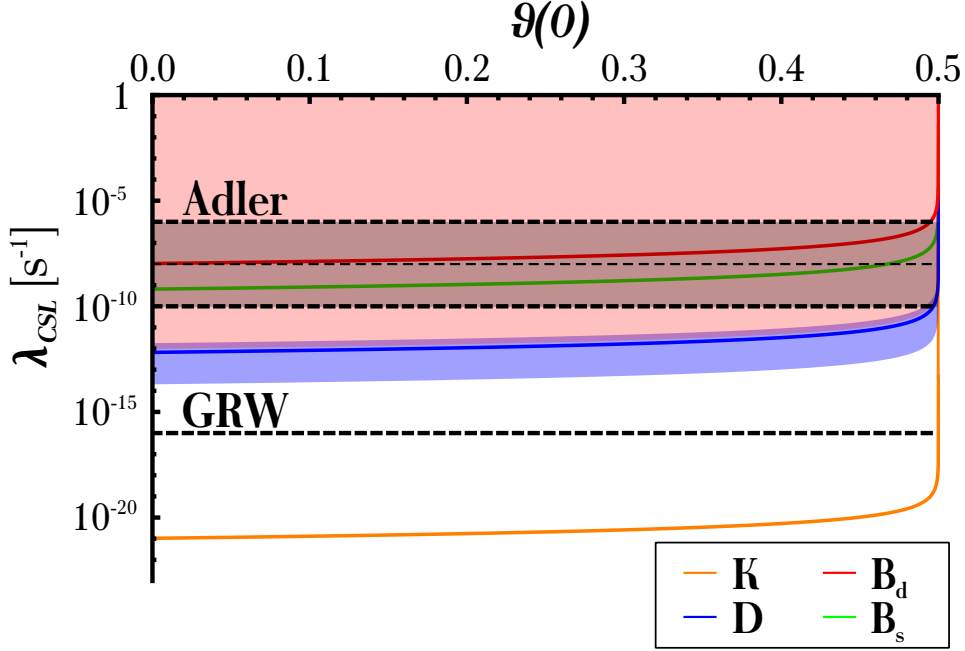


Figure 5.1: These plots show the values of $\vartheta(0)$ versus the deduced collapse rate based on the input parameters $\Gamma_H^{\text{exp}}, \Gamma_L^{\text{exp}}, \Delta m^{\text{exp}}$ for the different types of neutral mesons (including experimental errors highlighted by the shaded areas). As a reference mass the respective rest mass of the neutral mesons is assumed.

Now we can use these values of absolute masses to estimate λ_{CSL} by

$$\begin{aligned} \lambda_{CSL}^{\text{estimated}} &:= \Gamma_{\mu}^{\text{exp}} \cdot \frac{m_{\mu}^2}{m_0^2} \frac{1}{(1-2\vartheta(0))} \\ &= \frac{1}{(\sqrt{\Gamma_L^{-1}} - \sqrt{\Gamma_H^{-1}})^2} \frac{(\Delta m)^2}{m_0^2} \frac{1}{(1-2\vartheta(0))}. \end{aligned} \quad (5.25)$$

The predicted values of λ_{CSL} are plotted in Fig. 5.1 and their lower bounds are plotted in Fig. 5.2 for the different meson types. Interestingly, these values correspond to the ones assumed by Adler, except for the K-meson system which is closer to the one of GRW (even weaker).

Fixing the collapse rate to the one proposed by GRW requires that $\vartheta(0)$ converges to $\frac{1}{2}$, only in the Adler case values $\neq \frac{1}{2}$ are allowed. Taking the scenario with reversed masses seriously we have also to consider the modified contribution to the interference term, i.e.

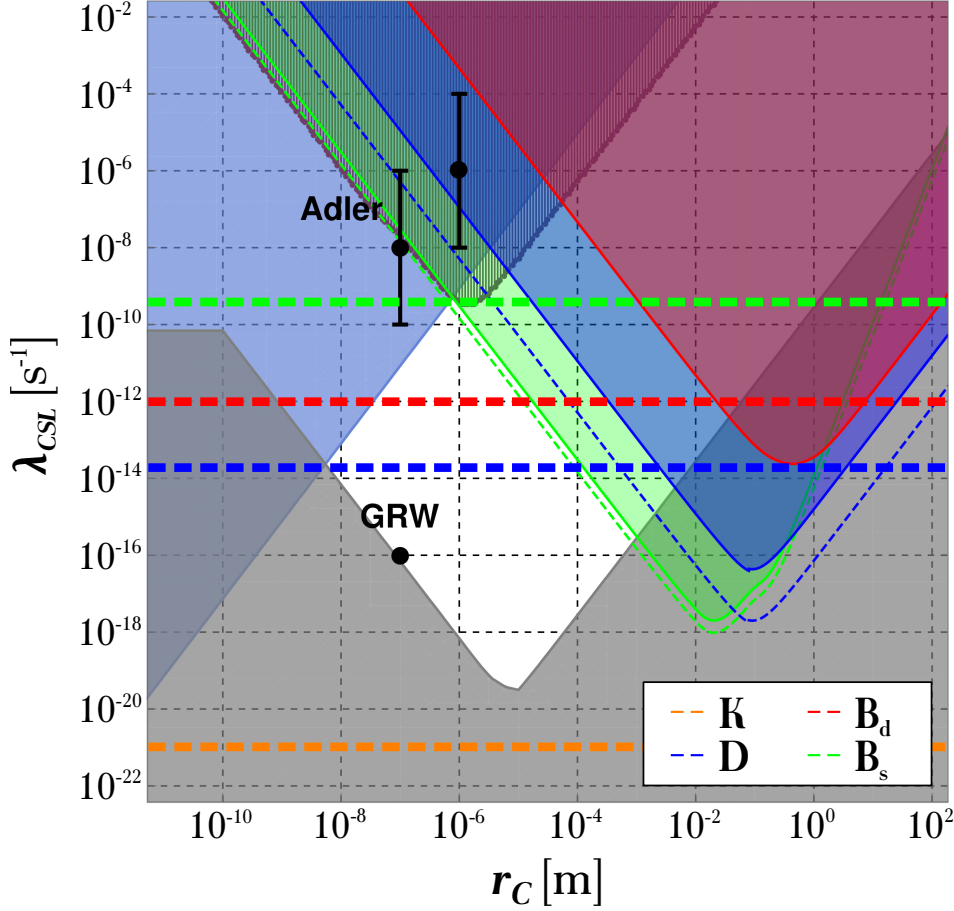


Figure 5.2: Bounds on the natural constants of the CSL model based on LIGO, LISA Pathfinder and AURIGA experiments (blue, green, and red lines), X-ray experiments (light blue line) [9], ultracold cantilever experiments (purple line) [87] and theoretical estimations (grey line) [88]. The lines refer to our computations of λ_{CSL} for the neutral meson system. Note that r_C is not bound. The other plots are taken from Ref. [89].

$$\begin{aligned}
 & \frac{1}{2} \lambda_{CSL} \frac{\Delta m^2 m_0^2}{m_H^2 m_L^2} \\
 &= \frac{1}{2} \lambda_{CSL} \frac{m_0^2}{(\Delta m)^2} \Gamma_H \Gamma_L (\sqrt{\Gamma_L^{-1}} - \sqrt{\Gamma_H^{-1}})^4 \\
 &= \frac{1}{2} \frac{\lambda_{CSL}}{\lambda_{CSL}^{\text{estimated}}} \frac{1}{1 - 2\vartheta(0)} (\sqrt{\Gamma_L} - \sqrt{\Gamma_H})^2.
 \end{aligned} \tag{5.26}$$

This term is negligible for all types of neutral mesons due to the tiny decay difference assuming the other values to be of order 1 except for the K-meson system. In this case

we have a very sensitive tradeoff between obtaining the experimental values of the decay constant and the damping of the interference term. The best limit on such a possible modification of the interference term comes from the entangled K-meson system [28], however, this is not directly comparable.

In summary a full description of the decay and oscillation properties in the dynamics of neutral mesons can be obtained demanding certain properties of collapse models.

5.4 The mathematical and physical meanings of $\vartheta(0)$

Let us note that the freedom of choosing the Heaviside function in the interval $\vartheta(0) \in [0, 1]$ comes from the action of the classical noise underlying any collapse model. One assumes that the stochastic noise average of two Wiener processes is given by a delta distribution, $\mathbb{E}[\mathbf{w}_t \cdot \mathbf{w}_s] = \delta(t - s)$. This in turn is the assumption of the white noise scenario, i.e. the assumption of a constant power spectral density. In our derivation we had to compute the following type of time integrals

$$\int_0^t ds \delta(t - s) = \begin{cases} \vartheta(t) - \vartheta(0) = 1 - \vartheta(0) & \text{for } t - s \geq 0, \\ \vartheta(0) - \vartheta(-t) = \vartheta(0) & \text{for } t - s \leq 0, \end{cases}$$

with $\int_{-\infty}^{\infty} \delta(t) dt = 1$. Note that the dependence on $\vartheta(0)$ occurs only in case one matches amplitudes of different orders within the expansion. Assuming the independence of the time direction $\delta(t) = \delta(-t)$ leads to $\vartheta(0) = \frac{1}{2}$. In this case the collapse quantities Λ^{QMUPL} , Γ^{CSL} become zero, respectively. No effect of the collapse field arises in the evolution of the mass eigenstates. Consequently, in this case also no dependence on absolute masses (m_H, m_L) is proposed in line with the standard quantum mechanical approach.

Now let us consider an approximation of the white noise ξ_t which reveals the correlation function $\mathbb{E}[\xi_t \xi_s] = f(t - s)$. In fact we can consider a family of approximations parametrized by constant κ which sets the asymmetry of the noise,

$$f_\varepsilon(t_1 - t_2, \kappa) = \frac{1}{\varepsilon} \frac{1}{\kappa + \frac{1}{\kappa}} e^{-\frac{|t_1 - t_2|}{\varepsilon} \cdot \kappa \cdot \text{sgn}(t_1 - t_2)}. \quad (5.27)$$

This family of approximations whose correlation functions are plotted in Fig. 5.3 includes a special symmetrical case $\kappa = 1$ which is usually considered in textbooks,

$$f_\varepsilon(t_1 - t_2, 1) \equiv f_\varepsilon^S(t_1 - t_2) = \frac{1}{2\varepsilon} e^{-\frac{|t_1 - t_2|}{\varepsilon}}. \quad (5.28)$$

Analogously to the temporal integral of the noise, $\int_0^t w_s ds = W_t$, which is the Wiener process, the temporal integral of the approximation ξ_t of the white noise converges to

the Wiener process in the mean square,

$$\text{qm-lim}_{\varepsilon \rightarrow 0} \int_0^t \xi_s ds = W_t. \quad (5.29)$$

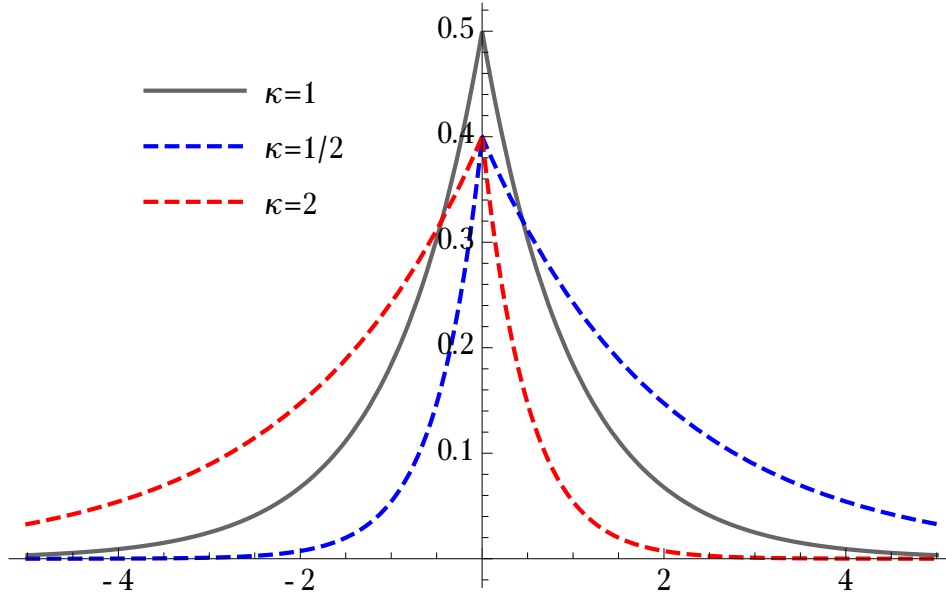


Figure 5.3: The plots of the correlation functions of the approximation ξ_t of the white noise for symmetrical choice $\kappa = 1$ and asymmetrical ones $\kappa = \frac{1}{2}$ and $\kappa = 2$.

Now we can show that the value $\vartheta(0)$ is connected to the asymmetry of the approximation of the white noise. For that purpose we compute the following integrals from Appendix C where delta function is changed by the approximated correlation function $f_\varepsilon(t_1 - t_2; \kappa)$,

$$C_{11}(t) = \int_0^t dt_1 \int_0^t dt_2 f_\varepsilon(t_1 - t_2; \kappa), \quad (5.30)$$

$$C_{20}(t) = \int_0^t dt_1 \int_0^{t_1} dt_2 f_\varepsilon(t_1 - t_2; \kappa). \quad (5.31)$$

Computing these integrals for the approximated noise with the correlation function $f_\varepsilon(t_1 - t_2; \kappa)$ and the white noise with the correlation function $\delta(t_1 - t_2)$, we obtain the following table,

	Asymmetric approximation	Symmetric approximation	White noise
$C_{11}(t)$	$t - \frac{\varepsilon}{\kappa + \kappa^3} [1 - e^{-\frac{\kappa t}{\varepsilon}} + (1 - e^{-\frac{t}{\kappa \varepsilon}}) \kappa^4]$	$t - \varepsilon [1 - e^{-t/\varepsilon}]$	t
$C_{20}(t)$	$\frac{1}{1 + \kappa^2} t - \frac{\varepsilon}{\kappa + \kappa^3} [1 - e^{-\frac{\kappa t}{\varepsilon}}]$	$\frac{1}{2} t - \frac{\varepsilon}{2} [1 - e^{-t/\varepsilon}]$	$(1 - \vartheta(0))t$

Comparing these results one can see that the value of $\vartheta(0)$ is defined by the asymmetry of the distribution in the following way,

$$\vartheta(0) = \frac{\kappa^2}{1 + \kappa^2}. \quad (5.32)$$

In this way the limit (5.29) means that the collapse equation (2.14) is not changed under changing the asymmetry of the approximation of the white noise and thus the parameter $\vartheta(0)$. Moreover, it should be noted that in general the noise does not really need to be of Gaussian nature, however only a continuity of its integral is enough to be postulated [49].

A value $\vartheta(0) \neq \frac{1}{2}$ can be interpreted as the freedom that the time evolved states in the expansions in the “out” (“bra”) and the “in” (“ket”) states do depend on the particular time ordering within the expansion. Only in this case the interaction with the classical noise field leads to contributions not solely affecting the interference term with respect to the chosen basis. Consequently, here is the point where the physics of the noise field strongly enters the discussion. In particular non-white noise fields will change the very dynamics of neutral mesons, that in turn will be testable in principle.

COMPARISON OF THE PREDICTIONS OF THE MASS-PROPORTIONAL CSL MODEL WITH ANOTHER APPROACHES

To append a possibility to understand and test in experiment the new physics proposed by collapse models for the meson dynamics, let us compare the results obtained in the previous subsections with the dynamics provided by the Schrödinger–Newton equation and decoherence models.

6.1 Semi-classical gravity

The Schrödinger–Newton equation [92–95] ($\hbar = 1$)

$$i \frac{d}{dt} \psi(t, \mathbf{r}) = \left(-\frac{1}{2m} \nabla^2 - Gm^2 \int d^3 \mathbf{r}' \frac{|\psi(t, \mathbf{r}')|^2}{|\mathbf{r} - \mathbf{r}'|} \right) \psi(t, \mathbf{r}), \quad (6.1)$$

where m is a gravitational mass and G is the gravitational constant, is a non-linear extension of the Schrödinger equation. It includes a potential which yields non-relativistic self-gravitation interaction and can be seen as a non-relativistic limit of classical gravity. From the collapse models point of view the Schrödinger–Newton equation is a model, which describes the dynamics for the spatial localization of the wave function. It is expected to describe the gravitational interaction for quantum matter [96, 97].

In [98] the Schrödinger–Newton equation was applied to the neutral meson system, particularly neutral kaons. Due to the non-trivial coupling between the spatial and the flavor wave functions the authors have considered two possible assumptions:

1. Both mass eigenstates $|M_H\rangle$ and $|M_L\rangle$ are described by the one unique spatial wave function,
2. The mass eigenstates $|M_H\rangle$ and $|M_L\rangle$ are described by different spatial wave functions.

Analyzing both scenarios of the Schrödinger–Newton dynamics for a K-meson one obtains a shift of the difference of masses Δm [98],

$$\Delta m \rightarrow (1 - \eta \cdot \Delta_{SN})\Delta m, \quad (6.2)$$

where $\eta = 1$ holds if the first assumption is met and $\eta = 2$ if the second one is met. The shift Δ_{SN} depends on the invariant mass of the neutral kaon $m_K = (497.614 \pm 0.024)\text{MeV}/c^2$,

$$\Delta_{SN} = \sqrt{\frac{2}{\pi}} \frac{Gm_K}{c^2 a}, \quad (6.3)$$

where c is the speed of light and a is a width which is assumed to be large.

Comparing the effect of the Schrödinger–Newton dynamics in a neutral kaon system with the results obtained for the mass-proportional CSL model, we observe that the semi-classical gravity described by the Schrödinger–Newton equation changes the frequency of the flavor oscillations, thus changing the predictions on the oscillating behavior of a neutral kaon system. On the contrary, the CSL collapse leads to effects on both phenomena, oscillation and decay.

6.2 Decoherence models

Decoherence models [99–105] describe the loss of quantum coherence due to the interaction of a quantum system with environment. In the context of the measurement problem they describe the evolution of a quantum superposition into a statistical mixture of states recovering the Born rule but not explaining the measurement process itself. In contrast to decoherence models collapse models propose a mechanism, ontic reduction of the wave function, which explains the measurement process. Let us see which decoherence model for a neutral meson system would in principle lead to the same predictions as the mass-proportional CSL model.

Before to discuss the decoherence models we repeat some properties of the non-Hermitian Hamiltonian that is the standard starting point in describing the meson phenomenology. Neutral meson systems violate the \mathcal{CP} symmetry for the mass matrix and have a non-vanishing lifetime difference described by the decay matrix. This leads to an effective Hamiltonian which is even not a normal operator.

In the Wigner–Weisskopf approach, by diagonalizing the Hamiltonian, the non-orthogonal “stationary” states M_H, M_L are obtained. These states have complex eigenvalues whose real (imaginary) part does not coincide with the eigenvalues of the mass (decay) matrix.

The mesonic systems can also be described as an open quantum mechanical system [63, 90, 91], which allows to describe its dynamics by completely positive time evolution and thus conserving probabilities. In particular, the following Gorini-Kossakowski-Lindblad-Sudarshan (GKLS) master equation [64, 65] does the job [63]

$$\begin{aligned} \frac{d}{dt}\hat{\rho}(t) &= -i[\hat{\mathcal{H}}, \hat{\rho}(t)] \\ &\quad - \frac{1}{2} \sum_{i=0}^f \left(\hat{\mathcal{L}}_i^\dagger \hat{\mathcal{L}}_i \hat{\rho}(t) + \hat{\rho}(t) \hat{\mathcal{L}}_i^\dagger \hat{\mathcal{L}}_i - 2\hat{\mathcal{L}}_i \hat{\rho}(t) \hat{\mathcal{L}}_i^\dagger \right), \end{aligned} \quad (6.4)$$

where we define $\hat{\rho}$ to live on a Hilbert space with a direct product structure $H_{tot} = H_s \oplus H_d$ (s corresponds to the surviving part and d of the decaying part of the system). Particularly, for a neutral meson system the total Hilbert space H_{tot} needs at least 4 dimensions. The Hamiltonian $\hat{\mathcal{H}}$ and all Lindblad operators $\hat{\mathcal{L}}$ in H_{tot} are defined to act only onto the surviving part of the system, i.e.

$$\hat{\mathcal{H}} = \begin{pmatrix} \hat{M} & 0 \\ 0 & 0 \end{pmatrix}, \quad \hat{\mathcal{L}}_{i>0} = \begin{pmatrix} \hat{L}_i & 0 \\ 0 & 0 \end{pmatrix}, \quad (6.5)$$

whereas the zero Lindblad operator entangles the surviving part with the decaying part

$$\hat{\mathcal{L}}_0 = \begin{pmatrix} 0 & 0 \\ \hat{L}_0 & 0 \end{pmatrix}, \quad (6.6)$$

where the operator $\hat{L}_0 : H_s \rightarrow H_d$ defines the decay operator of the effective Hamiltonian \hat{H}_{eff} in (3.3) as $\hat{\Gamma} = \hat{L}_0^\dagger \hat{L}_0$. Given these definitions the total density matrix

$$\hat{\rho}(t) = \begin{pmatrix} \hat{\rho}_{ss}(t) & \hat{\rho}_{sd}(t) \\ \hat{\rho}_{sd}^\dagger(t) & \hat{\rho}_{dd}(t) \end{pmatrix} \quad (6.7)$$

is normalized for all times. The differential equation decouples for the “parts” of the system. Hence, the solution of the survive-to-decay part $\hat{\rho}_{sd}(t)$ has no physical significance

and the time dependence of the decay-to-decay contribution $\hat{\rho}_{dd}(t)$ depends solely on the survive-to-survive part $\hat{\rho}_{ss}(t)$, i.e.

$$\hat{\rho}_{dd}(t) = \hat{L}_0 \int_0^t \hat{\rho}_{ss}(s) ds \hat{L}_0^\dagger. \quad (6.8)$$

For clarity, let us rewrite the relevant differential equations explicitly (for Hermitian Lindblad generators)

$$\begin{aligned} \hat{\rho}_{ss}(t) &= -i[\hat{H}, \hat{\rho}_{ss}(t)] - \frac{1}{2}\{\hat{L}_0, \hat{\rho}_{ss}(t)\} \\ &\quad - \frac{1}{2} \sum_{i>0} \{\{\hat{L}_i, \hat{\rho}_{ss}(t)\} - 2\hat{L}_i \hat{\rho}_{ss}(t) \hat{L}_i\}, \end{aligned} \quad (6.9)$$

where $\hat{L}_0 = \text{diag}\left\{\sqrt{\Gamma_L + \Gamma_L^{CSL}}, \sqrt{\Gamma_H + \Gamma_H^{CSL}}\right\}$ is given in the mass eigenstate basis.

Introducing a Lindblad generator $\hat{L}_1 = \sqrt{\frac{\gamma}{(\sqrt{4\pi}r_C)^d}} \left(\frac{m_L}{m_0} |M_L\rangle\langle M_L| + \frac{m_H}{m_0} |M_H\rangle\langle M_H| \right)$ formally leads to the same probabilities, see Eq. (5.12). This has the following physical intuitive picture: the state vector undergoes a random unitary transformation in the time dt

$$\begin{aligned} \hat{U}(\phi)|\psi(t)\rangle &= e^{-i\phi\hat{G}} |\psi(t)\rangle \\ &= (\mathbb{1} - i\phi\hat{G} - \frac{1}{2}\phi^2\hat{G}^2 + \dots)|\psi(t)\rangle \end{aligned} \quad (6.10)$$

with a Gaussian probability distribution with a width proportional to dt , namely with probability ($\int_{-\infty}^{\infty} p(\phi) d\phi = 1$)

$$p(\phi) = \frac{1}{\sqrt{2\pi}\sigma} \cdot e^{-\frac{\phi^2}{2\sigma^2}}, \quad (6.11)$$

where we choose the width equal to $\sigma = \sqrt{\frac{\gamma}{(\sqrt{4\pi}r_C)^d} \cdot dt}$. Since we assume small dt we can neglect safely the higher order terms and find for the density matrix at time $t + dt$

$$\begin{aligned} \hat{\rho}(t+dt) &= \int_{-\infty}^{+\infty} d\phi p(\phi) \hat{U}(\phi) \cdot \hat{\rho}(t) \cdot \hat{U}^\dagger(\phi) \\ &= \int_{-\infty}^{+\infty} d\phi p(\phi) \left\{ \hat{\rho}(t) - \frac{\phi^2}{2} (\{\hat{G}^2, \hat{\rho}(t)\} - 2\hat{G} \hat{\rho}(t) \hat{G}) \right\} \\ &= \hat{\rho}(t) - \frac{\sigma^2}{2} (\{\hat{G}^2, \hat{\rho}(t)\} - 2\hat{G} \hat{\rho}(t) \hat{G}). \end{aligned} \quad (6.12)$$

This differential equation is equivalent to the one in the Lindblad form with \hat{L}_1 if we choose for $\hat{G} = \sum_i \frac{m_i}{m_0} |M_i\rangle\langle M_i|$ (compare with the flavor part of our collapse operators in (5.6a) and (5.8a)). Even though we formally arrive at the same formulae for the

dynamics (5.12), let us stress that in this case no ontic collapse is assumed, in particular the spatial part of the wave function played no role. Moreover, the dependence on the “decay rate” Γ_i^{CSL} is not generated by the dynamics, but introduced by hand through the Lindblad operators. It is physically not clear how to motivate such a Lindblad operator. However, it explains why the interference term in the flavor oscillation probabilities depends on $(\Delta m)^2$, this is a general feature of any random unitary noise with a Gaussian distribution.

SPONTANEOUS COLLAPSE AND BELL INEQUALITIES

In this chapter we extend our analysis of the collapse models to the case of a system of two entangled neutral kaons. At first we perform a perturbative calculation of joint 2-particle probabilities for the mass-proportional CSL model. Then we use the calculated probabilities in the Bell inequalities for the neutral kaons discussed in Section 4.2.

7.1 Calculation of the 2-particle probabilities including spontaneous collapse

As we have highlighted in Section 4.2 neutral kaons are produced at the DAΦNE collider in an entangled antisymmetric state,

$$|I\rangle = \frac{1}{\sqrt{2}} \left(|K^0\rangle \otimes |\bar{K}^0\rangle - |\bar{K}^0\rangle \otimes |K^0\rangle \right). \quad (7.1)$$

In this way the observables of our interest are the probabilities of measuring the state F_l at time t_l on the left side and the state F_r at time t_r on the right side which we denote as $P(F_l, F_r; t_l, t_r)$. We assume that we start at time $t_0 = 0$ with the entangled state $|I\rangle$ with momenta \mathbf{p}_l and $-\mathbf{p}_l$, and compose the transition probabilities in the same way as done in Section 5.1,

$$P(F_l, F_r; t_l, t_r) = \sum_{\mathbf{p}_l, \mathbf{p}_r} \mathbb{E} |\langle F_l, F_r; \mathbf{p}_l, \mathbf{p}_r | I(t_l, t_r) \rangle|^2,$$

where we take flavor eigenstates $|K^0\rangle, |\bar{K}^0\rangle$, mass eigenstates $|K_L\rangle, |K_S\rangle$ and \mathcal{CP} eigenstates $|K_1^0\rangle, |K_2^0\rangle$ as the possible final states $|F_l\rangle, |F_r\rangle$, and the time evolution of each of two particles includes the collapse due to the Hamiltonian (5.2) for the mass-proportional CSL model. Particularly, these probabilities were computed in [23] up to the first order in time for the choice $F_l = F_r = K^0$,

$$\begin{aligned}
 P_{K^0, K^0}(Y, t_l; Y, t_r) &= \frac{1}{8} \left(e^{-(\Gamma_L t_l + \Gamma_S t_r)} + e^{-(\Gamma_S t_l + \Gamma_L t_r)} \right. \\
 &\quad \left. + 2e^{-\frac{\Gamma_L + \Gamma_S}{2}(t_l + t_r)} e^{-\frac{\lambda_{CSL}}{2} \frac{(\Delta m)^2}{m_0^2} (t_l + t_r)} \cos[\Delta m(t_l - t_r)] \right). \tag{7.2}
 \end{aligned}$$

We are interested in investigation of the Wigner-type Bell inequalities for kaons (4.14), therefore we perform the perturbative calculations up to the second perturbative order for two sets of probabilities which include the quasispin states K_S, \bar{K}^0, K_1^0 and K_S, K^0, K_1^0 .

Since we work with kaons, we can perform the calculations with $\vartheta(0) = \frac{1}{2}$ due to the results summarized in Fig. 5.1. Moreover, we use the inverted mass ration $\frac{m_0}{m_\mu}$ in the calculations to conserve the positive absolute masses of kaons. Collecting all the necessary components and setting the equal times $t_l = t_r = t$ of measurement on the right and left sides we obtain the following results for the first set of probabilities,

$$P_{K_S, \bar{K}^0}(Y, t; Y, t) = \frac{|p|^2}{2N^2} \left[1 + 2\lambda_{CSL}^2 (1 - \delta^2)^2 \frac{m_0^4}{m_L^2 m_S^2} t^2 \right] e^{-(\Gamma_L + \Gamma_S)t}, \tag{7.3}$$

$$P_{K_S, K_1^0}(Y, t; Y, t) = \frac{|pe^{i\varphi_M} - q|^2}{4N^2} \left[1 + 2\lambda_{CSL}^2 (1 - \delta^2)^2 \frac{m_0^4}{m_L^2 m_S^2} t^2 \right] e^{-(\Gamma_L + \Gamma_S)t}, \tag{7.4}$$

$$P_{K_1^0, \bar{K}^0}(Y, t; Y, t) = \frac{1}{4} \left[1 + 2\lambda_{CSL}^2 (1 - \delta^2)^2 \frac{m_0^4}{m_L^2 m_S^2} t^2 \right] e^{-(\Gamma_L + \Gamma_S)t}, \tag{7.5}$$

$$\begin{aligned}
 h(K_S, K_1^0, \bar{K}^0; t) &= 2 - P_{K_S, \bar{K}^0}(Y, t; Y, t) + P_{K_S, K_1^0}(Y, t; Y, t) + P_{K_1^0, \bar{K}^0}(Y, t; Y, t) \\
 &\quad - \frac{1}{1 - \delta^2} \frac{2}{1 + |\varepsilon|^2} \left\{ e^{-\Gamma_S t} + |\varepsilon|^2 e^{-\Gamma_L t} - 2\delta \operatorname{Re}(\varepsilon e^{-i\Delta m t}) e^{-\frac{\Gamma_L + \Gamma_S}{2} t} \right\}, \tag{7.6}
 \end{aligned}$$

and the second one,

$$P_{K_S, K^0}(Y, t; Y, t) = \frac{|q|^2}{2N^2} \left[1 + 2\lambda_{CSL}^2 (1 - \delta^2)^2 \frac{m_0^4}{m_L^2 m_S^2} t^2 \right] e^{-(\Gamma_L + \Gamma_S)t}, \quad (7.7)$$

$$P_{K_S, K_1^0}(Y, t; Y, t) = \frac{|pe^{i\varphi_M} - q|^2}{4N^2} \left[1 + 2\lambda_{CSL}^2 (1 - \delta^2)^2 \frac{m_0^4}{m_L^2 m_S^2} t^2 \right] e^{-(\Gamma_L + \Gamma_S)t}, \quad (7.8)$$

$$P_{K_1^0, K^0}(Y, t; Y, t) = \frac{1}{4} \left[1 + 2\lambda_{CSL}^2 (1 - \delta^2)^2 \frac{m_0^4}{m_L^2 m_S^2} t^2 \right] e^{-(\Gamma_L + \Gamma_S)t}, \quad (7.9)$$

$$h(K_S, K_1^0, K^0; t_l) = 2 - P_{K_S, K^0}(Y, t; Y, t) + P_{K_S, K_1^0}(Y, t; Y, t) + P_{K_1^0, K^0}(Y, t; Y, t) \quad (7.10)$$

$$- \frac{1}{1 - \delta^2} \frac{2}{1 + |\varepsilon|^2} \left\{ e^{-\Gamma_S t} + |\varepsilon|^2 e^{-\Gamma_L t} - 2\delta \operatorname{Re}(\varepsilon e^{-i\Delta m t}) e^{-\frac{\Gamma_L + \Gamma_S}{2} t} \right\}.$$

Collecting the contributions of the effect of the mass-proportional CSL model we see that the spontaneous collapse affects all the probabilities in the same way by adding a new term, which contains absolute values of masses.

7.2 Bell inequalities including spontaneous collapse

Before we plug the probabilities into the Bell inequalities we introduce some abbreviation,

$$c(K_S, K_1^0, \bar{K}^0; t) := e^{(\Gamma_L + \Gamma_S)t} - \frac{1}{1 - \delta^2} \frac{1}{1 + |\varepsilon|^2} \left\{ |\varepsilon|^2 e^{\Gamma_S t} + e^{\Gamma_L t} - 2\delta \operatorname{Re}(\varepsilon e^{-i\Delta m t}) e^{\frac{\Gamma_L + \Gamma_S}{2} t} \right\},$$

$$K(\delta, t) := 2\lambda_{CSL}^2 (1 - \delta^2)^2 \frac{m_0^4}{m_L^2 m_S^2} t^2,$$

Then, plugging in the probabilities obtained in the previous section to (4.14) we obtain two inequalities,

$$\frac{1 + K(\delta, t)}{2N^2} \left(\operatorname{Re}(pq^* e^{i\varphi_M}) - |q|^2 \right) \leq c(K_S, K_1^0, \bar{K}^0; t), \quad (7.11)$$

$$\frac{1 + K(\delta, t)}{2N^2} \left(\operatorname{Re}(pq^* e^{i\varphi_M}) - |p|^2 \right) \leq c(K_S, K_1^0, K^0; t). \quad (7.12)$$

As we have discussed in Section 3.2 one can tune the phase φ_M arbitrarily. Therefore, we fix φ_M such to compensate the phase of pq^* . Then, taking into account that $\delta = (|p|^2 - |q|^2)/N^2$ and $c(K_S, K_1^0, \bar{K}^0; t) = c(K_S, K_1^0, K^0; t) \equiv c(t)$, we obtain two Bell inequalities for the collapse contribution $K(\delta, t)$,

$$K(\delta, t) \leq \frac{2c(t)}{\delta} \frac{|p| + |q|}{|q|} - 1, \quad (7.13)$$

$$K(\delta, t) \geq -\frac{2c(t)}{\delta} \frac{|p| + |q|}{|p|} - 1, \quad (7.14)$$

or, rewriting them including the collapse rate λ_{CSL}^2 ,

$$\lambda_{CSL}^2 \leq \frac{1}{2(1-\delta^2)^2 t^2} \frac{m_L^2 m_S^2}{m_0^4} \left(\frac{2c(t)}{\delta} \frac{|p|+|q|}{|q|} - 1 \right), \quad (7.15)$$

$$\lambda_{CSL}^2 \geq -\frac{1}{2(1-\delta^2)^2 t^2} \frac{m_L^2 m_S^2}{m_0^4} \left(\frac{2c(t)}{\delta} \frac{|p|+|q|}{|p|} + 1 \right). \quad (7.16)$$

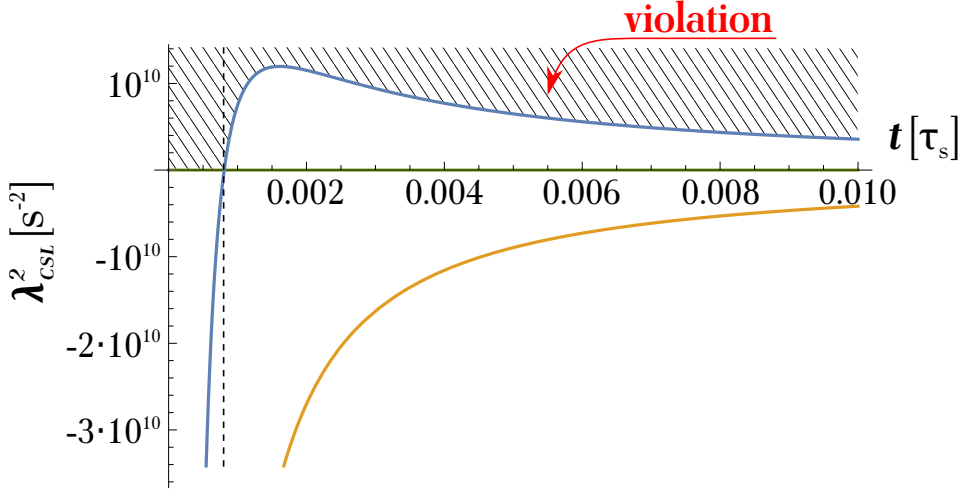


Figure 7.1: The plots of the upper (blue line) and lower (orange line) bounds for λ_{CSL}^2 established by a local hidden variables model. The green line represents the GRW and Adler value of λ_{CSL}^2 and the vertical dotted line separates the region where these values violate the Bell inequalities. The rest mass of kaon is assumed as a reference mass m_0 .

In this way we see that a local hidden variables model establishes time-dependent bounds for the square of the collapse rate. These bounds are plotted in Fig. 7.1 for the measured value of the \mathcal{CP} violation parameter δ in a neutral meson system [84]. Moreover, the violation of \mathcal{CP} symmetry plays a crucial role here since it establishes these bounds. Particularly, if \mathcal{CP} symmetry is conserved ($\delta = 0$), then any value of the collapse rate is compatible with local realism, while increasing the \mathcal{CP} violation leads to increasing of the region where GRW and Adler values of the collapse rate violate the Bell inequalities.

However, the measured value of the \mathcal{CP} violation parameter δ in a neutral kaon system establishes a region of violation of the local realism by all the values of λ_{CSL} , which lies in a short-time scale as shown in Fig. 7.1. The time scale around τ_S provides violation of the local realism for the values of the collapse constant $\lambda_{CSL} \gtrsim 10^1$.

CONCLUSIONS AND OUTLOOK

In this thesis we have focused on two popular dynamical reduction models, QMUPL (Quantum Mechanics with Universal Position Localization) and mass-proportional CSL (Continuous Spontaneous Localization) models, and analyzed their effects to the neutral meson system. These models provide a physical mechanism for the collapse in order to solve the measurement problem in the quantum mechanics. Taking these models seriously they have to also affect systems at higher energies, in particular, neutral mesons, which have shown to be proper systems for testing the foundations of quantum mechanics.

The challenges in deriving the possible effect of spontaneous collapse in a neutral meson system were manifold. To tackle the problem we considered the two-state phenomenological Hamiltonian which describes the flavor oscillations and assumed the (white) noise implied by the collapse models as a small perturbation by utilizing the Dyson series. Since the dynamical reduction models assume the collapse to happen in the spatial part of the state, we had to choose proper collapse operators relating the flavor space (where the oscillations takes place) with the spatial space. The transition probabilities were calculated up to fourth perturbative order. These high orders were necessary in order to distinguish between exponential behavior (observed for the CSL model without taking into account \mathcal{CP} violation) and non-exponential behavior (observed for the CSL model by taking into account \mathcal{CP} violation and the QMUPL model). This gives insight into the physics of the noise field underlying the collapse mechanism.

Calculating the transition probabilities we have observed a dependence on the choice

of the value of the Heaviside function at zero, $\vartheta(0)$, which shows up in the amplitudes connecting different orders in the Dyson expansion. These amplitudes contain the integrals of correlation functions of two or more Wiener processes. Mathematically, the value of the Heaviside function at zero can be in the interval $\vartheta(0) \in [0, 1]$. Only the value $\vartheta(0) = \frac{1}{2}$ provides an evolution of the lifetime states which do not depend on the collapse in the spatial part. Any value $\vartheta(0) \neq \frac{1}{2}$ leads to a dependence on the absolute masses (energies) of the eigenstates of the time evolution. Absolute masses of the lifetime states do not show up in the standard quantum approach. The effect due to the QMUPL model leads to a non-exponential behavior and is therefore in principle observable. Since this deviation from standard dynamics has not (yet) been observed, experiments provide upper bounds on the absolute masses of the lifetime states in this case. In the CSL model the absolute masses of the lifetime states would not be directly measurable since they would effectively contribute to the decay constants.

By including the tiny violation of the \mathcal{CP} symmetry to the predictions of the CSL model the time evolution changes in a non-trivial way and shows non-exponential behavior. Particularly, the asymmetry term, which is intensively investigated in experiments, undergoes an exponential damping if the \mathcal{CP} symmetry is assumed to be unbroken, while taking into account the \mathcal{CP} violation leads to a non-trivial polynomial contribution based on the collapse dynamics.

We have analyzed whether spontaneous localization could be considered as the only source of decay in the neutral meson dynamics. We have related the measured decay constants with the absolute masses appearing due to the computed contribution of the collapse effect. At first, we have seen that the choice of the sign of the mass difference plays an important role, which relates the longer-lived state to the more massive state or the lighter one. Experiments for K-mesons favor the first relation. However, this relation is in contrast to the principles of collapse models, which assume a more massive system to be localized faster since the ultimate aim is to let macroscopic superpositions disappear. To obtain positive absolute masses we have identified the strength of generation of a heavy mass eigenstate with the lower mass and vice versa. Doing so, we can compute the absolute masses and, herewith, fully describe the decay mechanism of neutral mesons based on the collapse mechanism. Or alternatively, one can predict the value of the collapse rate. This rate is computed solely by the experimental input parameters of the mass difference and the two decay rates, the latter two depending on the value for $\vartheta(0)$. The range is compatible with the values of the collapse rate proposed by Adler or Ghirardi, Rimini, and Weber except for the K-meson system.

In order to obtain an insight into any deviations from the standard dynamics in the experiment which could differ from those provided by the dynamical reduction models we have compared collapse dynamics with potential effects provided by semi-classical gravity and decoherence models.

The Schrödinger–Newton equation provides another mathematical framework which describes a spatial localization of the wave function. In this case the collapse is due to a non-relativistic gravitational mechanism. Comparing the results provided by the Schrödinger–Newton equation with the collapse dynamics, we observe that the gravitational mechanism changes flavor oscillation behavior while a spontaneous collapse provides a damping of flavor oscillation and can describe the decay property of the system.

To compare the collapse dynamics with the decoherence models we have defined a master equation within standard quantum mechanics that leads to the same probabilities in finding a meson or antimeson at time t . We have extended the Hilbert space to include the decay components based on [36] and have solved the GKLS master equation with Gaussian noise proportional to the masses. This illustrates the dependence of the damping on the squared mass difference since it is a general feature of systems undergoing a random Gaussian distributed unitary noise.

Last but not least we have expanded the analysis to systems of two neutral kaons including the violation of the \mathcal{CP} symmetry. We have used the perturbative approach to derive the Wigner-type Bell inequalities for two kaons undergoing a collapse based on the mass-proportional CSL model. We have found that the values of the collapse rate compatible with a local hidden variable model are bounded above, and this time-dependent upper bound is established by the violation of \mathcal{CP} symmetry. Moreover, we have found a time scale where any collapse rate violates local realism.

In summary, the dynamical reduction models – proposed to be a possible solution of the measurement problem – lead to novel testable predictions. Appending spontaneous collapse to neutral mesons allows new physics to be tested at an energy regime not provided by other quantum systems, in addition to the peculiarity of providing a superposition of two different mass eigenstates. Precision data from experiments such as KLOE will further restrict or even rule out certain collapse scenarios. On the theoretical side, our computations are performed for a white noise scenario. Therefore, it is a future challenge to extend them to a more realistic non-white noise scenario, which could change the dynamics noticeably. Furthermore, investigating other types of Bell inequalities could reveal testable predictions of the dynamical reduction models compatible with the value

of \mathcal{CP} violation given by the Nature and contribute to the understanding of the role of \mathcal{CP} violation and entanglement in Nature.

ACKNOWLEDGEMENTS

I would like to thank Dr. Beatrix C. Hiesmayr for having been my supervisor for this work, helping me a lot in understanding of physics, and giving me a lot of useful and interesting opportunities and experiences.

I would like to thank University of Vienna and Austrian Science Fund FWF (Project FWF-P67283) for giving us excellent facilities and opportunity to do this work.

I would like to thank Dr. Sandro Donadi for the long and fruitful discussions on the models of spontaneous collapse and sharing his work experience.

I would like to thank Dr. Catalina Curceanu for useful conversations and for having invited me to the conferences in Erice and Frascati on the foundations of quantum mechanics which have given me a chance to have useful discussions with many experts on the topic of my research.

I would like to thank Dr. Salvatore Marco Giampaolo for a number of useful discussions and sharing his knowledge and experience in condensed matter physics.

I would like to thank Dr. Angelo Bassi and Dr. Kristian Piscicchia for discussions on the models of spontaneous collapse in Frascati.

I would like to thank Prof. Detlef Dürr for having invited to me to Munich for a useful discussion on collapse models and good free time in LMU.

I would like to thank Prof. Paweł Moskal and Prof. Lajos Diósi for useful discussions on quantum mechanics.

Chciałbym podziękować mojej rodzinie, szczególnie moim rodzicom – Andrzejowi i Oldze oraz mojemu bratu Mykytowi za nieocenione wsparcie, wspaniały wpływ, jaki mieli

CHAPTER 9. ACKNOWLEDGEMENTS

na mnie przez lata, i za to, że cały czas są ze mną i wspierają mnie na duchu.

To conclude, I would like to thank Dr. Giacomo Guarnieri, Dr. Andrea Smirne, Dr. Nicolai Friis and Dr. Marcus Huber for conversations about physics and good free time.



COMPUTATIONS FOR THE QMUPL MODEL

A.1 Transition probabilities for the mass eigenstates

We start the computations of the transition probabilities for the QMUPL model with the 1-dimensional case. The five terms (5.5a)–(5.5b) form the transition amplitude up to fourth order of the Dyson series which we calculate here. Inserting the definition (5.6b) for the $\hat{N}_{QMUPL}(t)$ operator (1-dimensional case) and calculating the flavor part of matrix elements, we obtain the following expression for the components up to n -th order of the transition amplitudes

$$T_{\mu\nu}^{(n)}(p_f, p_i, \alpha; t) = e^{-im_\mu t} F^{(n)}(t) \left(i\sqrt{\lambda} \frac{m_\mu}{m_0} \right)^n \cdot \langle p_f | \hat{q}^n | p_i, \alpha \rangle \delta_{\mu\nu}, \quad (\text{A.1})$$

where

$$\begin{aligned} F^{(0)}(t_0) &= 1, \\ F^{(n)}(t_0) &= \int_0^{t_0} dt_1 \dots \int_0^{t_{n-1}} dt_n \prod_{j=1}^n w(t_j). \end{aligned}$$

The transition amplitudes derive to

$$\langle p_f | \hat{q}^n | p_i, \alpha \rangle = \sqrt{2\sqrt{\alpha\pi}} e^{-\frac{\alpha}{2}(p_f - p_i)^2} \cdot \zeta(n) \quad (\text{A.2})$$

with

$$\begin{aligned}
 \zeta(0) &= 1, \\
 \zeta(1) &= (-i)\alpha(p_f - p_i), \\
 \zeta(2) &= \alpha(1 - \alpha(p_f - p_i)^2), \\
 \zeta(3) &= (-i)\alpha^2(3(p_f - p_i) - \alpha(p_f - p_i)^3), \\
 \zeta(4) &= \alpha^2(3 - 6\alpha(p_f - p_i)^2 + \alpha^2(p_f - p_i)^4).
 \end{aligned}$$

The next step is to compute the transition probability which consists of three terms

$$P_{M_\mu \rightarrow M_\nu}(\alpha; t) = P_{M_\mu \rightarrow M_\nu}^{(0)}(\alpha; t) + P_{M_\mu \rightarrow M_\nu}^{(1)}(\alpha; t) + P_{M_\mu \rightarrow M_\nu}^{(2)}(\alpha; t), \quad (\text{A.3})$$

which decompose in terms of the transition amplitudes to

$$P_{M_\mu \rightarrow M_\nu}^{(0)}(\alpha; t) = \frac{1}{2\pi} \int dp_f \mathbb{E} \left[T_{\mu\nu}^{(0)}(p_f, p_i, \alpha; t) T_{\mu\nu}^{(0)*}(p_f, p_i, \alpha; t) \right], \quad (\text{A.4a})$$

$$\begin{aligned}
 P_{M_\mu \rightarrow M_\nu}^{(1)}(\alpha; t) &= \frac{1}{2\pi} \int dp_f \mathbb{E} \left[T_{\mu\nu}^{(0)}(p_f, p_i, \alpha; t) T_{\mu\nu}^{(2)*}(p_f, p_i, \alpha; t) \right. \\
 &\quad \left. + T_{\mu\nu}^{(2)}(p_f, p_i, \alpha; t) T_{\mu\nu}^{(0)*}(p_f, p_i, \alpha; t) + T_{\mu\nu}^{(1)}(p_f, p_i, \alpha; t) T_{\mu\nu}^{(1)*}(p_f, p_i, \alpha; t) \right], \quad (\text{A.4b})
 \end{aligned}$$

$$\begin{aligned}
 P_{M_\mu \rightarrow M_\nu}^{(2)}(\alpha; t) &= \frac{1}{2\pi} \int dp_f \mathbb{E} \left[T_{\mu\nu}^{(0)}(p_f, p_i, \alpha; t) T_{\mu\nu}^{(4)*}(p_f, p_i, \alpha; t) \right. \\
 &\quad \left. + T_{\mu\nu}^{(4)}(p_f, p_i, \alpha; t) T_{\mu\nu}^{(0)*}(p_f, p_i, \alpha; t) + T_{\mu\nu}^{(1)}(p_f, p_i, \alpha; t) T_{\mu\nu}^{(3)*}(p_f, p_i, \alpha; t) \right. \\
 &\quad \left. + T_{\mu\nu}^{(3)}(p_f, p_i, \alpha; t) T_{\mu\nu}^{(1)*}(p_f, p_i, \alpha; t) + T_{\mu\nu}^{(2)}(p_f, p_i, \alpha; t) T_{\mu\nu}^{(2)*}(p_f, p_i, \alpha; t) \right]. \quad (\text{A.4c})
 \end{aligned}$$

The first term gives

$$P_{M_\mu \rightarrow M_\nu}^{(0)}(\alpha; t) = \frac{2\sqrt{\alpha\pi}}{2\pi} \int dp_f e^{-\alpha(p_f - p_i)^2} \delta_{\mu\nu} = \delta_{\mu\nu}. \quad (\text{A.5})$$

For the first order in time we need

$$\begin{aligned}
 &\frac{1}{2\pi} \int dp_f \mathbb{E} \left[T_{\mu\nu}^{(0)*}(p_f, p_i, \alpha; t) T_{\mu\nu}^{(2)}(p_f, p_i, \alpha; t) + T_{\mu\nu}^{(2)*}(p_f, p_i, \alpha; t) T_{\mu\nu}^{(0)}(p_f, p_i, \alpha; t) \right] \\
 &= -2\delta_{\mu\nu} \frac{\lambda m_\mu^2}{m_0^2} \int_0^t dt_1 \int_0^{t_1} dt_2 \mathbb{E}[w(t_1)w(t_2)] \cdot \frac{2\alpha\sqrt{\alpha\pi}}{2\pi} \int dp_f \left[1 - \alpha(p_f - p_i)^2 \right] e^{-\alpha(p_f - p_i)^2} \\
 &= -\delta_{\mu\nu} (\alpha\lambda) \frac{m_\mu^2}{m_0^2} (1 - \vartheta(0)) \cdot t,
 \end{aligned}$$

where the computation of the two-point correlation function $\int_0^t dt_1 \int_0^{t_1} dt_2 \mathbb{E}[w(t_1)w(t_2)]$ is explicitly derived in the Appendix C.

The second term derives to

$$\begin{aligned}
& \frac{1}{2\pi} \int dp_f \mathbb{E} \left[T_{\mu\nu}^{(1)*}(p_f, p_i, \alpha; t) T_{\mu\nu}^{(1)}(p_f, p_i, \alpha; t) \right] \\
&= \delta_{\mu\nu} \frac{\lambda m_\mu^2}{m_0^2} \int_0^t dt_1 \int_0^t dt_2 \mathbb{E}[w(t_1)w(t_2)] \cdot \frac{2\alpha^2 \sqrt{\alpha\pi}}{2\pi} \int dp_f (p_f - p_i)^2 e^{-\alpha(p_f - p_i)^2} \\
&= \delta_{\mu\nu} \frac{\alpha}{2} \frac{\lambda m_\mu^2}{m_0^2} \cdot t,
\end{aligned}$$

where the two-point correlation function $\int_0^t dt_1 \int_0^t dt_2 \mathbb{E}[w(t_1)w(t_2)]$ is derived in the Appendix C (note the difference in the integration limits).

Consequently, the transition probabilities in first order in time t result in

$$P_{M_\mu \rightarrow M_\nu}^{(1)}(\alpha; t) = -\delta_{\mu\nu} \frac{\alpha}{2} \frac{\lambda m_\mu^2}{m_0^2} (1 - 2\vartheta(0)) \cdot t. \quad (\text{A.6})$$

To obtain the solution in the second order in time t we have to compute the five components, $T^{(0)*}T^{(4)}$, $T^{(4)*}T^{(0)}$, $T^{(1)*}T^{(3)}$, $T^{(3)*}T^{(1)}$ and $T^{(2)*}T^{(2)}$, where we have for the first time to evaluate a four point function in the noise which is done in detail in Appendix C. We compute

$$\begin{aligned}
& \frac{1}{2\pi} \int dp_f \mathbb{E} \left[T_{\mu\nu}^{(0)*}(p_f, p_i, \alpha; t) T_{\mu\nu}^{(4)}(p_f, p_i, \alpha; t) + T_{\mu\nu}^{(0)*}(p_f, p_i, \alpha; t) T_{\mu\nu}^{(4)}(p_f, p_i, \alpha; t) \right] \\
&= 2\delta_{\mu\nu} \frac{\lambda^2 m_\mu^4}{m_0^4} C_{4,0}^{(2)}(t) \cdot \frac{2\alpha^2 \sqrt{\alpha\pi}}{2\pi} \int dp_f \left[3 - 6\alpha(p_f - p_i)^2 + \alpha^2(p_f - p_i)^4 \right] e^{-\alpha(p_f - p_i)^2} \\
&= \delta_{\mu\nu} \frac{3\alpha^2}{2} \frac{\lambda^2 m_\mu^4}{m_0^4} C_{4,0}^{(2)}(t) \\
&= \delta_{\mu\nu} \frac{3\alpha^2}{2} \frac{\lambda^2 m_\mu^4}{m_0^4} \cdot \frac{1}{2} (1 - \vartheta(0))^2 \cdot t^2,
\end{aligned}$$

and

$$\begin{aligned}
& \frac{1}{2\pi} \int dp_f \mathbb{E} \left[T_{\mu\nu}^{(1)*}(p_f, p_i, \alpha; t) T_{\mu\nu}^{(3)}(p_f, p_i, \alpha; t) + T_{\mu\nu}^{(3)*}(p_f, p_i, \alpha; t) T_{\mu\nu}^{(1)}(p_f, p_i, \alpha; t) \right] \\
&= -2\delta_{\mu\nu} \frac{\lambda^2 m_\mu^4}{m_0^4} C_{3,1}^{(2)}(t) \cdot \frac{2\alpha^3 \sqrt{\alpha\pi}}{2\pi} \int dp_f \left[3 - \alpha(p_f - p_i)^2 \right] (p_f - p_i)^2 e^{-\alpha(p_f - p_i)^2} \\
&= -\delta_{\mu\nu} \frac{3\alpha^2}{2} \frac{\lambda^2 m_\mu^4}{m_0^4} C_{3,1}^{(2)}(t) \\
&= -\delta_{\mu\nu} \frac{3\alpha^2}{2} \frac{\lambda^2 m_\mu^4}{m_0^4} \cdot (1 - \vartheta(0)) \cdot t^2,
\end{aligned}$$

and

$$\begin{aligned}
 & \frac{1}{2\pi} \int d\mathbf{p}_f \mathbb{E} \left[T_{\mu\nu}^{(2)*}(\mathbf{p}_f, \mathbf{p}_i, \alpha; t) T_{\mu\nu}^{(2)}(\mathbf{p}_f, \mathbf{p}_i, \alpha; t) \right] \\
 &= \delta_{\mu\nu} \frac{\lambda^2 m_\mu^4}{m_0^4} C_{2,2}^{(2)}(t) \cdot \frac{2\alpha^2 \sqrt{\alpha\pi}}{2\pi} \int d\mathbf{p}_f \left[1 - \alpha(\mathbf{p}_f - \mathbf{p}_i)^2 \right]^2 e^{-\alpha(\mathbf{p}_f - \mathbf{p}_i)^2} \\
 &= \delta_{\mu\nu} \frac{3\alpha^2 \lambda^2 m_\mu^4}{4 m_0^4} C_{2,2}^{(2)}(t) \\
 &= \delta_{\mu\nu} \frac{3\alpha^2 \lambda^2 m_\mu^4}{4 m_0^4} \cdot \left((1 - \vartheta(0))^2 + \frac{1}{2} \right) \cdot t^2.
 \end{aligned}$$

where $C_{4,0}^{(2)}(t)$, $C_{3,1}^{(2)}(t)$ and $C_{2,2}^{(2)}(t)$ correspond to the integrals of the 4-point correlation functions of the noise field, which are calculated in Appendix C.

Summing up, we obtain the transition probabilities in second order time t

$$\begin{aligned}
 P_{M_\mu \rightarrow M_\nu}^{(2)}(\alpha; t) &= \delta_{\mu\nu} \frac{3\alpha^2 \lambda^2 m_\mu^4}{4 m_0^4} \left(2\vartheta(0)(\vartheta(0) - 1) + \frac{1}{2} \right) \cdot t^2 \\
 &= \delta_{\mu\nu} \frac{3\alpha^2 \lambda^2 m_\mu^4}{8 m_0^4} (1 - 2\vartheta(0))^2 \cdot t^2.
 \end{aligned} \tag{A.7}$$

Finally, collecting all the terms (A.5)–(A.7), we obtain the transition probabilities for mass eigenstates up to second order in time t

$$P_{M_\mu \rightarrow M_\nu}(\alpha; t) = \delta_{\mu\nu} \left[1 - \frac{\alpha \lambda m_\mu^2}{2 m_0^2} (1 - 2\vartheta(0)) t + \frac{3\alpha^2 \lambda^2 m_\mu^4}{8 m_0^4} (1 - 2\vartheta(0))^2 t^2 \right]. \tag{A.8}$$

A.2 d -dimensional case

In the case of d -dimensional space the components (5.5a)–(5.5b) of transition amplitudes have to be generalized in the following way

$$T_{\mu\nu}^{(n)}(\mathbf{p}_f, \mathbf{p}_i, \alpha; t) = e^{-im_\mu t} \tilde{F}^{(n)}(\mathbf{p}_f, \mathbf{p}_i, \alpha; t) \left(i\sqrt{\lambda} \frac{m_\mu}{m_0} \right)^n \delta_{\mu\nu}, \tag{A.9}$$

where

$$\begin{aligned}
 \tilde{F}^{(0)}(\mathbf{p}_f, \mathbf{p}_i, \alpha; t_0) &= \langle \mathbf{p}_f | \mathbf{p}_i, \alpha \rangle, \\
 \tilde{F}^{(n)}(\mathbf{p}_f, \mathbf{p}_i, \alpha; t_0) &= \int_0^{t_0} dt_1 \dots \int_0^{t_{n-1}} dt_n \langle \mathbf{p}_f | \prod_{j=1}^n (\hat{\mathbf{q}} \cdot \mathbf{w}(t_j)) | \mathbf{p}_i, \alpha \rangle.
 \end{aligned}$$

Here one can think of basically two different ways the noise would act onto the system. Either a factorization in any of the possible dimensions happens and contributes to the

first order in time, or a factorization of the wave function has to occur in all dimensions simultaneously. The second one seems to be less natural to assume. Since we assume white noise and an initial Gaussian wave function in all dimensions, however, integrals give the same value and the only difference is how often the integral occurs. Therefore, we stick to the first case.

Explicitly, we find

$$\begin{aligned}
\tilde{F}_0(\mathbf{p}_f, \mathbf{p}_i, \alpha; t) &= \left(2\sqrt{\alpha\pi}\right)^{d/2} e^{-\frac{\alpha}{2}(\mathbf{p}_f - \mathbf{p}_i)^2}, \\
\tilde{F}_1(\mathbf{p}_f, \mathbf{p}_i, \alpha; t) &= -i \cdot \left(2\sqrt{\alpha\pi}\right)^{d/2} \alpha \int_0^t dt_1 \left(\mathbf{p}_f - \mathbf{p}_i\right) \cdot \mathbf{w}(t_1) e^{-\frac{\alpha}{2}(\mathbf{p}_f - \mathbf{p}_i)^2}, \\
\tilde{F}_2(\mathbf{p}_f, \mathbf{p}_i, \alpha; t) &= \left(2\sqrt{\alpha\pi}\right)^{d/2} \alpha \int_0^t dt_1 \int_0^{t_1} dt_2 \left[\left(\mathbf{w}(t_1) \cdot \mathbf{w}(t_2)\right) \right. \\
&\quad \left. - \alpha \left(\mathbf{p}_f - \mathbf{p}_i\right) \cdot \mathbf{w}(t_1)\right] \left(\mathbf{p}_f - \mathbf{p}_i\right) \cdot \mathbf{w}(t_2) \Big] e^{-\frac{\alpha}{2}(\mathbf{p}_f - \mathbf{p}_i)^2}, \\
\tilde{F}_3(\mathbf{p}_f, \mathbf{p}_i, \alpha; t) &= -i \cdot \left(2\sqrt{\alpha\pi}\right)^{d/2} \alpha^2 \int_0^t dt_1 \int_0^{t_1} dt_2 \int_0^{t_2} dt_3 \left[\left(\mathbf{p}_f - \mathbf{p}_i\right) \cdot \mathbf{w}(t_1)\right] \left(\mathbf{w}(t_2) \cdot \mathbf{w}(t_3)\right) \\
&\quad + \left(\mathbf{p}_f - \mathbf{p}_i\right) \cdot \mathbf{w}(t_2)\right] \left(\mathbf{w}(t_1) \cdot \mathbf{w}(t_3)\right) + \left(\mathbf{p}_f - \mathbf{p}_i\right) \cdot \mathbf{w}(t_3)\right] \left(\mathbf{w}(t_1) \cdot \mathbf{w}(t_2)\right) \\
&\quad - \alpha \left(\mathbf{p}_f - \mathbf{p}_i\right) \cdot \mathbf{w}(t_1)\right] \left(\mathbf{p}_f - \mathbf{p}_i\right) \cdot \mathbf{w}(t_2)\right] \left(\mathbf{p}_f - \mathbf{p}_i\right) \cdot \mathbf{w}(t_3)\right] e^{-\frac{\alpha}{2}(\mathbf{p}_f - \mathbf{p}_i)^2}, \\
\tilde{F}_4(\mathbf{p}_f, \mathbf{p}_i, \alpha; t) &= \left(2\sqrt{\alpha\pi}\right)^{d/2} \alpha^2 \int_0^t dt_1 \int_0^{t_1} dt_2 \int_0^{t_2} dt_3 \int_0^{t_3} dt_4 \left[\left(\mathbf{w}(t_1) \cdot \mathbf{w}(t_2)\right)\right] \left(\mathbf{w}(t_3) \cdot \mathbf{w}(t_4)\right) \\
&\quad + \left(\mathbf{w}(t_1) \cdot \mathbf{w}(t_3)\right)\right] \left(\mathbf{w}(t_2) \cdot \mathbf{w}(t_4)\right) + \left(\mathbf{w}(t_1) \cdot \mathbf{w}(t_4)\right)\right] \left(\mathbf{w}(t_2) \cdot \mathbf{w}(t_3)\right) \\
&\quad - \alpha \left(\mathbf{p}_f - \mathbf{p}_i\right) \cdot \mathbf{w}(t_1)\right] \left(\mathbf{p}_f - \mathbf{p}_i\right) \cdot \mathbf{w}(t_2)\right] \left(\mathbf{w}(t_3) \cdot \mathbf{w}(t_4)\right) \\
&\quad - \alpha \left(\mathbf{p}_f - \mathbf{p}_i\right) \cdot \mathbf{w}(t_1)\right] \left(\mathbf{p}_f - \mathbf{p}_i\right) \cdot \mathbf{w}(t_3)\right] \left(\mathbf{w}(t_2) \cdot \mathbf{w}(t_4)\right) \\
&\quad - \alpha \left(\mathbf{p}_f - \mathbf{p}_i\right) \cdot \mathbf{w}(t_1)\right] \left(\mathbf{p}_f - \mathbf{p}_i\right) \cdot \mathbf{w}(t_4)\right] \left(\mathbf{w}(t_2) \cdot \mathbf{w}(t_3)\right) \\
&\quad - \alpha \left(\mathbf{p}_f - \mathbf{p}_i\right) \cdot \mathbf{w}(t_2)\right] \left(\mathbf{p}_f - \mathbf{p}_i\right) \cdot \mathbf{w}(t_3)\right] \left(\mathbf{w}(t_1) \cdot \mathbf{w}(t_4)\right) \\
&\quad - \alpha \left(\mathbf{p}_f - \mathbf{p}_i\right) \cdot \mathbf{w}(t_2)\right] \left(\mathbf{p}_f - \mathbf{p}_i\right) \cdot \mathbf{w}(t_4)\right] \left(\mathbf{w}(t_1) \cdot \mathbf{w}(t_3)\right) \\
&\quad - \alpha \left(\mathbf{p}_f - \mathbf{p}_i\right) \cdot \mathbf{w}(t_3)\right] \left(\mathbf{p}_f - \mathbf{p}_i\right) \cdot \mathbf{w}(t_4)\right] \left(\mathbf{w}(t_1) \cdot \mathbf{w}(t_2)\right) \\
&\quad + \alpha^2 \left(\mathbf{p}_f - \mathbf{p}_i\right) \cdot \mathbf{w}(t_1)\right] \left(\mathbf{p}_f - \mathbf{p}_i\right) \cdot \mathbf{w}(t_2)\right] \left(\mathbf{p}_f - \mathbf{p}_i\right) \cdot \mathbf{w}(t_3)\right] \left(\mathbf{p}_f - \mathbf{p}_i\right) \cdot \mathbf{w}(t_4)\right] \\
&\quad \cdot e^{-\frac{\alpha}{2}(\mathbf{p}_f - \mathbf{p}_i)^2},
\end{aligned}$$

and herewith the probabilities

$$\begin{aligned}
 P_{M_\mu \rightarrow M_\nu}^{(0)}(\alpha; t) &= \delta_{\mu\nu}, \\
 P_{M_\mu \rightarrow M_\nu}^{(1)}(\alpha; t) &= -\delta_{\mu\nu} \frac{\alpha}{2} \frac{\lambda m_\mu^2}{m_0^2} (1 - 2\vartheta(0))t, \\
 P_{M_\mu \rightarrow M_\nu}^{(2)}(\alpha; t) &= \delta_{\mu\nu} \frac{3\alpha^2}{4} \frac{\lambda^2 m_\mu^4}{m_0^4} \left(2\vartheta(0)(\vartheta(0) - 1) + \frac{1}{2} \right) t^2,
 \end{aligned}$$

which are identical to the ones of the 1-dimensional case and, consequently, lead to the same transition probabilities.

A.3 Transition probabilities for the flavor states

Transition amplitude for a flavor state can be expanded in the following way:

$$\begin{aligned}
 T_{M^0 \rightarrow M^0/\bar{M}^0}(\mathbf{p}_f, \mathbf{p}_i, \alpha; t) &= \langle M^0/\bar{M}^0, \mathbf{p}_f | M^0(t), \mathbf{p}_i, \alpha \rangle \\
 &= \sum_{\mu, \nu} \alpha_\mu \beta_\nu^* \langle M_\nu, \mathbf{p}_f | M_\mu(t), \mathbf{p}_i, \alpha \rangle \\
 &= \sum_{\mu, \nu} \alpha_\mu \beta_\nu^* T_{\mu\nu}(\mathbf{p}_f, \mathbf{p}_i, \alpha; t),
 \end{aligned}$$

where $\mu, \nu = H, L$ and $\alpha_H = \alpha_L = \beta_H = \frac{1}{\sqrt{2}}$, $\beta_L = \pm \frac{1}{\sqrt{2}}$ (plus sign refers to a meson, minus sign refers to an antimeson). In the same manner, transition probability for a flavor state can be defined as

$$\begin{aligned}
 P_{M^0 \rightarrow M^0/\bar{M}^0}(\alpha; t) &= \sum_{\mu, \nu, \mu', \nu'} \alpha_\mu \beta_\nu^* \alpha_{\mu'}^* \beta_{\nu'} \frac{1}{(2\pi)^d} \int d\mathbf{p}_f \mathbb{E}[T_{\mu\nu}(\mathbf{p}_f, \mathbf{p}_i, \alpha; t) T_{\mu'\nu'}^*(\mathbf{p}_f, \mathbf{p}_i, \alpha; t)] \\
 &\equiv \sum_{\mu, \nu, \mu', \nu'} \alpha_\mu \beta_\nu^* \alpha_{\mu'}^* \beta_{\nu'} P_{\mu\nu\mu'\nu'}(\alpha; t).
 \end{aligned} \tag{A.10}$$

Furthermore, since each transition amplitude $T_{\mu\nu}(\mathbf{p}_f, \mathbf{p}_i, \alpha; t)$ contains a Kronecker delta $\delta_{\mu\nu}$, as can be seen from (A.1) and (A.9), we can leave just one index in an amplitude and correspondingly two indexes in probabilities $P_{\mu\nu\mu'\nu'}(\alpha; t)$

$$\begin{aligned}
 P_{M^0 \rightarrow M^0/\bar{M}^0}(\alpha; t) &= \sum_{\mu, \mu'} \alpha_\mu \beta_\mu^* \alpha_{\mu'}^* \beta_{\mu'} P_{\mu\mu'}(\alpha; t) \\
 &= \frac{1}{4} (P_{HH}(\alpha; t) \pm P_{HL}(\alpha; t) \pm P_{LH}(\alpha; t) + P_{LL}(\alpha; t)).
 \end{aligned} \tag{A.11}$$

Using the transition probabilities which were calculated above we obtain the terms for the transition probability, with same indexes P_{aa} and different ones P_{ab}

$$P_{aa}(\alpha; t) = 1 - \frac{\alpha}{2} \frac{\lambda m_a^2}{m_0^2} (1 - 2\vartheta(0)) t + \frac{3\alpha^2}{8} \frac{\lambda^2 m_a^4}{m_0^4} (1 - 2\vartheta(0))^2 t^2, \quad (\text{A.12})$$

$$\begin{aligned} P_{ab}(\alpha; t) &= e^{-i(m_a - m_b)t} \left\{ 1 - \frac{\alpha}{2} \frac{\lambda}{m_0^2} \left((m_a^2 + m_b^2) (1 - \vartheta(0)) - m_a m_b \right) t \right. \\ &\quad + \frac{3\alpha^2}{8} \frac{\lambda^2}{m_0^4} \left[(m_a^4 + m_b^4) (1 - \vartheta(0))^2 - 2(m_a^3 m_b + m_a m_b^3) (1 - \vartheta(0)) \right. \\ &\quad \left. \left. + 2m_a^2 m_b^2 \left((1 - \vartheta(0))^2 + \frac{1}{2} \right) \right] t^2 \right\}. \end{aligned} \quad (\text{A.13})$$

Putting the terms together we finally obtain the transition probability for the flavor states

$$\begin{aligned} P_{M^0 \rightarrow M^0/\bar{M}^0}(\alpha; t) &= \frac{1}{2} \left\{ 1 - \frac{\alpha}{4} \frac{\lambda(m_H^2 + m_L^2)}{m_0^2} (1 - 2\vartheta(0)) \cdot t \right. \\ &\quad + \frac{3\alpha^2}{16} \frac{\lambda^2(m_H^4 + m_L^4)}{m_0^4} (1 - 2\vartheta(0))^2 \cdot t^2 \\ &\quad \pm \left[1 - \frac{1}{2} \frac{\lambda\alpha}{m_0^2} \left((m_H^2 + m_L^2) (1 - \vartheta(0)) - m_H m_L \right) \cdot t \right. \\ &\quad + \frac{3}{8} \frac{\lambda^2\alpha^2}{m_0^4} \left((m_H^4 + m_L^4) (1 - \vartheta(0))^2 - 2m_H m_L (m_H^2 + m_L^2) (1 - \vartheta(0)) \right. \\ &\quad \left. \left. + 2m_H^2 m_L^2 \left((1 - \vartheta(0))^2 + \frac{1}{2} \right) \right) \cdot t^2 \right] \cdot \cos \left[(m_H - m_L)t \right] \left. \right\}. \end{aligned} \quad (\text{A.14})$$

Taking the decay into account we obtain

$$\begin{aligned} P_{M^0 \rightarrow M^0/\bar{M}^0}(\alpha; t) &= \frac{1}{4} \left\{ e^{-\Gamma_H t} + e^{-\Gamma_L t} \right. \\ &\quad - \frac{1}{2} \frac{\lambda\alpha}{m_0^2} (m_H^2 e^{-\Gamma_H t} + m_L^2 e^{-\Gamma_L t}) (1 - 2\vartheta(0)) \cdot t \\ &\quad + \frac{3}{8} \frac{\lambda^2\alpha^2}{m_0^4} (m_H^4 e^{-\Gamma_H t} + m_L^4 e^{-\Gamma_L t}) (1 - 2\vartheta(0))^2 \cdot t^2 \\ &\quad \pm 2 \left[1 - \frac{1}{2} \frac{\lambda\alpha}{m_0^2} \left((m_H^2 + m_L^2) (1 - \vartheta(0)) - m_H m_L \right) \cdot t \right. \\ &\quad + \frac{3}{8} \frac{\lambda^2\alpha^2}{m_0^4} \left((m_H^4 + m_L^4) (1 - \vartheta(0))^2 - 2m_H m_L (m_H^2 + m_L^2) (1 - \vartheta(0)) \right. \\ &\quad \left. \left. + 2m_H^2 m_L^2 \left((1 - \vartheta(0))^2 + \frac{1}{2} \right) \right) \cdot t^2 \right] \cdot \cos \left[(m_H - m_L)t \right] \cdot e^{-\frac{\Gamma_H + \Gamma_L}{2} t} \left. \right\}. \end{aligned} \quad (\text{A.15})$$

COMPUTATIONS FOR THE CSL MODEL

B.1 Transition probabilities for mass eigenstates

For the CSL model we also have five terms which form the transition amplitude up to fourth order of the Dyson series. Putting the expressions for the \hat{N}_I operators in we obtain:

$$T_{\mu\nu}^{(n)}(\mathbf{p}_f, \mathbf{p}_i, \alpha; t) = e^{-im_\mu t} (i\sqrt{\gamma})^n K_{\mu\nu}^{(n)}(\mathbf{p}_f, \mathbf{p}_i, \alpha; t),$$

where

$$K_{\mu\nu}^{(0)}(\mathbf{p}_f, \mathbf{p}_i, \alpha; t_0) = \langle M_\nu, \mathbf{p}_f | M_\mu, \mathbf{p}_i, \alpha \rangle, \quad (\text{B.1})$$

$$K_{\mu\nu}^{(n)}(\mathbf{p}_f, \mathbf{p}_i, \alpha; t_0) = \int_0^{t_0} dt_1 \cdots \int_0^{t_{n-1}} dt_n \int d\mathbf{x}_1 \cdots \int d\mathbf{x}_n \quad (\text{B.2})$$

$$\cdot \langle M_\nu, \mathbf{p}_f | \prod_{j=1}^n \left(w(t_j, \mathbf{x}_j) \cdot \sum_{k=H,L} \frac{m_k}{m_0} \hat{\psi}_I^{k\dagger}(t_j, \mathbf{x}_j) \hat{\psi}_I^k(t_j, \mathbf{x}_j) \right) | M_\mu, \mathbf{p}_i, \alpha \rangle.$$

Accordingly, we will calculate the matrix elements in the same manner as done in [23]. At first, we make an expansion of field operators into a superposition of plane waves

$$\hat{\psi}_I^k(t, \mathbf{x}) = \frac{1}{\sqrt{L^d}} \sum_{\mathbf{q}} \hat{b}_{\mathbf{q}} e^{-i(E_q^{(k)} t - \mathbf{q} \cdot \mathbf{x})}, \quad (\text{B.3})$$

where the energy of a meson of mass m_k and momentum \mathbf{q} is taken in non-relativistic limit, $E_q^{(k)} = \sqrt{\mathbf{q}^2 + m_k^2} \approx m_k$. Here the system is assumed to be quantized in a box of size

L with using periodic boundary conditions. While calculating the transition amplitudes and probabilities we take the limit $L \rightarrow \infty$ and perform an integration by momentum $\frac{1}{\sqrt{L^d}} \sum_{\mathbf{q}} \rightarrow \frac{1}{\sqrt{(2\pi)^d}} \int d\mathbf{q}$.

Using the coordinate representation and calculating the matrix elements, we obtain components of the transition amplitudes in the following form

$$\begin{aligned}
 K_{\mu\nu}^{(0)}(\mathbf{p}_f, \mathbf{p}_i, \alpha; t) &= (2\sqrt{\alpha\pi})^{d/2} e^{-\frac{\alpha}{2}(\mathbf{p}_f - \mathbf{p}_i)^2} \delta_{\mu\nu}, \\
 K_{\mu\nu}^{(1)}(\mathbf{p}_f, \mathbf{p}_i, \alpha; t) &= \frac{m_\mu}{m_0} \left[\left(\frac{1}{\sqrt{\alpha\pi}} \right)^{d/2} \int_0^t dt_1 \int d\mathbf{x}_1 w(t_1, \mathbf{x}_1) \cdot e^{-i(\mathbf{p}_f - \mathbf{p}_i)\mathbf{x}_1} e^{-\frac{\mathbf{x}_1^2}{2\alpha}} \right] \delta_{\mu\nu}, \\
 K_{\mu\nu}^{(2)}(\mathbf{p}_f, \mathbf{p}_i, \alpha; t) &= \frac{m_\mu^2}{m_0^2} \frac{1}{(2\pi)^d} \int d\mathbf{q}_1 \left[\left(\frac{1}{\sqrt{\alpha\pi}} \right)^{d/2} \int_0^t dt_1 \int_0^{t_1} dt_2 \iint d\mathbf{x}_1 d\mathbf{x}_2 \right. \\
 &\quad \left. \cdot w(t_1, \mathbf{x}_1) w(t_2, \mathbf{x}_2) \cdot e^{-i(\mathbf{p}_f - \mathbf{q}_1)\mathbf{x}_1} e^{-i(\mathbf{q}_1 - \mathbf{p}_i)\mathbf{x}_2} e^{-\frac{\mathbf{x}_2^2}{2\alpha}} \right] \delta_{\mu\nu}, \\
 K_{\mu\nu}^{(3)}(\mathbf{p}_f, \mathbf{p}_i, \alpha; t) &= \frac{m_\mu^3}{m_0^3} \frac{1}{(2\pi)^{2d}} \iint d\mathbf{q}_1 d\mathbf{q}_2 \left[\left(\frac{1}{\sqrt{\alpha\pi}} \right)^{d/2} \int_0^t dt_1 \int_0^{t_1} dt_2 \int_0^{t_2} dt_3 \iiint d\mathbf{x}_1 d\mathbf{x}_2 d\mathbf{x}_3 \right. \\
 &\quad \left. \cdot w(t_1, \mathbf{x}_1) w(t_2, \mathbf{x}_2) w(t_3, \mathbf{x}_3) \cdot e^{-i(\mathbf{p}_f - \mathbf{q}_1)\mathbf{x}_1} e^{-i(\mathbf{q}_1 - \mathbf{q}_2)\mathbf{x}_2} e^{-i(\mathbf{q}_2 - \mathbf{p}_i)\mathbf{x}_3} e^{-\frac{\mathbf{x}_3^2}{2\alpha}} \right] \delta_{\mu\nu}, \\
 K_{\mu\nu}^{(4)}(\mathbf{p}_f, \mathbf{p}_i, \alpha; t) &= \frac{m_\mu^4}{m_0^4} \frac{1}{(2\pi)^{3d}} \iiint d\mathbf{q}_1 d\mathbf{q}_2 d\mathbf{q}_3 \\
 &\quad \cdot \left[\left(\frac{1}{\sqrt{\alpha\pi}} \right)^{d/2} \int_0^t dt_1 \int_0^{t_1} dt_2 \int_0^{t_2} dt_3 \int_0^{t_3} dt_4 \iiint d\mathbf{x}_1 d\mathbf{x}_2 d\mathbf{x}_3 d\mathbf{x}_4 \right. \\
 &\quad \left. \cdot w(t_1, \mathbf{x}_1) w(t_2, \mathbf{x}_2) w(t_3, \mathbf{x}_3) w(t_4, \mathbf{x}_4) \cdot e^{-i(\mathbf{p}_f - \mathbf{q}_1)\mathbf{x}_1} e^{-i(\mathbf{q}_1 - \mathbf{q}_2)\mathbf{x}_2} e^{-i(\mathbf{q}_2 - \mathbf{q}_3)\mathbf{x}_3} e^{-i(\mathbf{q}_3 - \mathbf{p}_i)\mathbf{x}_4} e^{-\frac{\mathbf{x}_4^2}{2\alpha}} \right] \delta_{\mu\nu}.
 \end{aligned}$$

The next step is to compute the transition probability which consists of three terms

$$P_{M_\mu \rightarrow M_\nu}(t) = P_{M_\mu \rightarrow M_\nu}^{(0)}(t) + P_{M_\mu \rightarrow M_\nu}^{(1)}(t) + P_{M_\mu \rightarrow M_\nu}^{(2)}(t), \quad (\text{B.5})$$

where each term corresponds to zeroth, first and second order by time

$$P_{M_\mu \rightarrow M_\nu}^{(0)}(\mathbf{p}_i, \alpha; t) = \frac{1}{(2\pi)^d} \int d\mathbf{p}_f \mathbb{E} \left[T_{\mu\nu}^{(0)}(\mathbf{p}_f, \mathbf{p}_i, \alpha; t) T_{\mu\nu}^{(0)*}(\mathbf{p}_f, \mathbf{p}_i, \alpha; t) \right], \quad (\text{B.6a})$$

$$P_{M_\mu \rightarrow M_\nu}^{(1)}(\mathbf{p}_i, \alpha; t) = \frac{1}{(2\pi)^d} \int d\mathbf{p}_f \mathbb{E} \left[T_{\mu\nu}^{(0)}(\mathbf{p}_f, \mathbf{p}_i, \alpha; t) T_{\mu\nu}^{(2)*}(\mathbf{p}_f, \mathbf{p}_i, \alpha; t) \right. \\ \left. + T_{\mu\nu}^{(2)}(\mathbf{p}_f, \mathbf{p}_i, \alpha; t) T_{\mu\nu}^{(0)*}(\mathbf{p}_f, \mathbf{p}_i, \alpha; t) + T_{\mu\nu}^{(1)}(\mathbf{p}_f, \mathbf{p}_i, \alpha; t) T_{\mu\nu}^{(1)*}(\mathbf{p}_f, \mathbf{p}_i, \alpha; t) \right], \quad (\text{B.6b})$$

$$P_{M_\mu \rightarrow M_\nu}^{(2)}(\mathbf{p}_i, \alpha; t) = \frac{1}{(2\pi)^d} \int d\mathbf{p}_f \mathbb{E} \left[T_{\mu\nu}^{(0)}(\mathbf{p}_f, \mathbf{p}_i, \alpha; t) T_{\mu\nu}^{(4)*}(\mathbf{p}_f, \mathbf{p}_i, \alpha; t) \right. \\ \left. + T_{\mu\nu}^{(4)}(\mathbf{p}_f, \mathbf{p}_i, \alpha; t) T_{\mu\nu}^{(0)*}(\mathbf{p}_f, \mathbf{p}_i, \alpha; t) + T_{\mu\nu}^{(1)}(\mathbf{p}_f, \mathbf{p}_i, \alpha; t) T_{\mu\nu}^{(3)*}(\mathbf{p}_f, \mathbf{p}_i, \alpha; t) \right. \\ \left. + T_{\mu\nu}^{(3)}(\mathbf{p}_f, \mathbf{p}_i, \alpha; t) T_{\mu\nu}^{(1)*}(\mathbf{p}_f, \mathbf{p}_i, \alpha; t) + T_{\mu\nu}^{(2)}(\mathbf{p}_f, \mathbf{p}_i, \alpha; t) T_{\mu\nu}^{(2)*}(\mathbf{p}_f, \mathbf{p}_i, \alpha; t) \right]. \quad (\text{B.6c})$$

First term is trivial and given by:

$$P_{M_\mu \rightarrow M_\nu}^{(0)}(t) = \left(\frac{2\sqrt{\alpha\pi}}{2\pi} \right)^d \int d\mathbf{p}_f e^{-\alpha(\mathbf{p}_f - \mathbf{p}_i)^2} \delta_{\mu\nu} = \delta_{\mu\nu}. \quad (\text{B.7})$$

Second term consists of three components, $T_{\mu\nu}^{(0)*} T_{\mu\nu}^{(2)}$, $T_{\mu\nu}^{(2)*} T_{\mu\nu}^{(0)}$ and $T_{\mu\nu}^{(1)*} T_{\mu\nu}^{(1)}$, where the first two components result in

$$\frac{1}{(2\pi)^d} \int d\mathbf{p}_f \mathbb{E} \left[T_{\mu\nu}^{(0)*}(\mathbf{p}_f, \mathbf{p}_i, \alpha; t) T_{\mu\nu}^{(2)}(\mathbf{p}_f, \mathbf{p}_i, \alpha; t) + T_{\mu\nu}^{(2)*}(\mathbf{p}_f, \mathbf{p}_i, \alpha; t) T_{\mu\nu}^{(0)}(\mathbf{p}_f, \mathbf{p}_i, \alpha; t) \right] \\ = -2\delta_{\mu\nu} \frac{\gamma m_\mu^2}{m_0^2} \left(\frac{\sqrt{2}(\alpha\pi)^{1/4}}{(2\pi)^2(\alpha\pi)^{1/4}} \right)^d \iint d\mathbf{p}_f d\mathbf{q} \iint d\mathbf{x}_1 d\mathbf{x}_2 \cos \left[(\mathbf{p}_f - \mathbf{q})\mathbf{x}_1 + (\mathbf{q} - \mathbf{p}_i)\mathbf{x}_2 \right] e^{-\frac{\mathbf{x}_2^2}{2\alpha}} \\ \cdot e^{-\frac{\alpha}{2}(\mathbf{p}_f - \mathbf{p}_i)^2} \int_0^t dt_1 \int_0^{t_1} dt_2 \mathbb{E}[w(t_1, \mathbf{x}_1)w(t_2, \mathbf{x}_2)] \\ = -\delta_{\mu\nu} \gamma \frac{m_\mu^2}{m_0^2} \frac{1}{(\sqrt{4\pi} r_C)^d} \left(\frac{\sqrt{2}}{(2\pi)^2} \right)^d \iint d\mathbf{p}_f d\mathbf{q} \iint d\mathbf{x}_1 d\mathbf{x}_2 e^{-\frac{(\mathbf{x}_1 - \mathbf{x}_2)^2}{4r_C^2}} \left[e^{i(\mathbf{p}_f - \mathbf{q})\mathbf{x}_1} e^{i(\mathbf{q} - \mathbf{p}_i)\mathbf{x}_2} \right. \\ \left. + e^{-i(\mathbf{p}_f - \mathbf{q})\mathbf{x}_1} e^{-i(\mathbf{q} - \mathbf{p}_i)\mathbf{x}_2} \right] e^{-\frac{\mathbf{x}_2^2}{2\alpha}} e^{-\frac{\alpha}{2}(\mathbf{p}_f - \mathbf{p}_i)^2} \cdot C_{2,0}^{(1)}(t) \\ = -2\delta_{\mu\nu} \frac{1}{(\sqrt{4\pi} r_C)^d} \frac{\gamma m_\mu^2}{m_0^2} (1 - \vartheta(0)) \cdot t.$$

The third component equals to

$$\frac{1}{(2\pi)^d} \int d\mathbf{p}_f \mathbb{E} \left[T_{\mu\nu}^{(1)*}(\mathbf{p}_f, \mathbf{p}_i, \alpha; t) T_{\mu\nu}^{(1)}(\mathbf{p}_f, \mathbf{p}_i, \alpha; t) \right] \\ = \delta_{\mu\nu} \frac{\gamma m_\mu^2}{m_0^2} \left(\frac{1}{2\pi\sqrt{\alpha\pi}} \right)^d \int d\mathbf{p}_f \iint d\mathbf{x}_1 d\mathbf{x}_2 e^{-i(\mathbf{p}_f - \mathbf{p}_i)(\mathbf{x}_1 - \mathbf{x}_2)} e^{-\frac{\mathbf{x}_1^2 + \mathbf{x}_2^2}{2\alpha}} \int_0^t dt_1 \int_0^t dt_2 \mathbb{E}[w(t_1, \mathbf{x}_1)w(t_2, \mathbf{x}_2)] \\ = \delta_{\mu\nu} \frac{\gamma m_\mu^2}{m_0^2} \frac{1}{(\sqrt{4\pi} r_C)^d} \left(\frac{1}{2\pi\sqrt{\alpha\pi}} \right)^d \int d\mathbf{p}_f \iint d\mathbf{x}_1 d\mathbf{x}_2 e^{-\frac{(\mathbf{x}_1 - \mathbf{x}_2)^2}{4r_C^2}} e^{-i(\mathbf{p}_f - \mathbf{p}_i)(\mathbf{x}_1 - \mathbf{x}_2)} e^{-\frac{\mathbf{x}_1^2 + \mathbf{x}_2^2}{2\alpha}} \cdot C_{1,1}^{(1)}(t) \\ = \delta_{\mu\nu} \frac{1}{(\sqrt{4\pi} r_C)^d} \frac{\gamma m_\mu^2}{m_0^2} \cdot t.$$

Consequently,

$$P_{M_\mu \rightarrow M_\nu}^{(1)}(t) = -\delta_{\mu\nu} \frac{1}{(\sqrt{4\pi} r_C)^d} \frac{\gamma m_\mu^2}{m_0^2} (1 - 2\vartheta(0)) t. \quad (\text{B.8})$$

The computations of the integrals $C_{2,0}^{(1)}(t)$ and $C_{1,1}^{(1)}(t)$ which contain 2-point correlation functions of the noise field, can be found in the Appendix C.

Second term consists of five components, $T^{(0)*} T^{(4)}$, $T^{(4)*} T^{(0)}$, $T^{(1)*} T^{(3)}$, $T^{(3)*} T^{(1)}$ and $T^{(2)*} T^{(2)}$, where the first two components result in

$$\begin{aligned} & \frac{1}{(2\pi)^d} \int d\mathbf{p}_f \mathbb{E} \left[T_{\mu\nu}^{(0)*}(\mathbf{p}_f, \mathbf{p}_i, \alpha; t) T_{\mu\nu}^{(4)}(\mathbf{p}_f, \mathbf{p}_i, \alpha; t) + T_{\mu\nu}^{(4)*}(\mathbf{p}_f, \mathbf{p}_i, \alpha; t) T_{\mu\nu}^{(0)}(\mathbf{p}_f, \mathbf{p}_i, \alpha; t) \right] \\ &= 2\delta_{\mu\nu} \frac{\gamma^2 m_\mu^4}{m_0^4} \left(\frac{\sqrt{2}(\alpha\pi)^{1/4}}{(2\pi)^4(\alpha\pi)^{1/4}} \right)^d \iiint d\mathbf{p}_f d\mathbf{q}_1 d\mathbf{q}_2 d\mathbf{q}_3 \iiint d\mathbf{x}_1 d\mathbf{x}_2 d\mathbf{x}_3 d\mathbf{x}_4 \\ & \quad \cdot \cos \left[(\mathbf{p}_f - \mathbf{q}_1)\mathbf{x}_1 + (\mathbf{q}_1 - \mathbf{q}_2)\mathbf{x}_2 + (\mathbf{q}_2 - \mathbf{q}_3)\mathbf{x}_3 + (\mathbf{q}_3 - \mathbf{p}_i)\mathbf{x}_4 \right] e^{-\frac{\mathbf{x}_4^2}{2\alpha}} e^{-\frac{\alpha}{2}(\mathbf{p}_f - \mathbf{p}_i)^2} \\ & \quad \cdot \int_0^t dt_1 \int_0^{t_1} dt_2 \int_0^{t_2} dt_3 \int_0^{t_3} dt_4 \mathbb{E} [w(t_1, \mathbf{x}_1) w(t_2, \mathbf{x}_2) w(t_3, \mathbf{x}_3) w(t_4, \mathbf{x}_4)] \\ &= \delta_{\mu\nu} \frac{1}{(4\pi r_C^2)^d} \frac{\gamma^2 m_\mu^4}{m_0^4} \left(\frac{\sqrt{2}}{(2\pi)^4} \right)^d \iiint d\mathbf{p}_f d\mathbf{q}_1 d\mathbf{q}_2 d\mathbf{q}_3 \iiint d\mathbf{x}_1 d\mathbf{x}_2 d\mathbf{x}_3 d\mathbf{x}_4 \\ & \quad \cdot \left[e^{i(\mathbf{p}_f - \mathbf{q}_1)\mathbf{x}_1} e^{i(\mathbf{q}_1 - \mathbf{q}_2)\mathbf{x}_2} e^{i(\mathbf{q}_2 - \mathbf{q}_3)\mathbf{x}_3} e^{i(\mathbf{q}_3 - \mathbf{p}_i)\mathbf{x}_4} + e^{-i(\mathbf{p}_f - \mathbf{q}_1)\mathbf{x}_1} e^{-i(\mathbf{q}_1 - \mathbf{q}_2)\mathbf{x}_2} e^{-i(\mathbf{q}_2 - \mathbf{q}_3)\mathbf{x}_3} e^{-i(\mathbf{q}_3 - \mathbf{p}_i)\mathbf{x}_4} \right] e^{-\frac{\mathbf{x}_4^2}{2\alpha}} \\ & \quad \cdot e^{-\frac{\alpha}{2}(\mathbf{p}_f - \mathbf{p}_i)^2} \left[e^{-\frac{(\mathbf{x}_1 - \mathbf{x}_2)^2}{4r_C^2}} e^{-\frac{(\mathbf{x}_3 - \mathbf{x}_4)^2}{4r_C^2}} U_1^{4,0}(t) + e^{-\frac{(\mathbf{x}_1 - \mathbf{x}_3)^2}{4r_C^2}} e^{-\frac{(\mathbf{x}_2 - \mathbf{x}_4)^2}{4r_C^2}} U_2^{4,0}(t) + e^{-\frac{(\mathbf{x}_1 - \mathbf{x}_4)^2}{4r_C^2}} e^{-\frac{(\mathbf{x}_2 - \mathbf{x}_3)^2}{4r_C^2}} U_3^{4,0}(t) \right] \\ &= \delta_{\mu\nu} \frac{1}{(4\pi r_C^2)^d} \frac{\gamma^2 m_\mu^4}{m_0^4} \left(\frac{\sqrt{2}}{(2\pi)^4} \right)^d \iiint d\mathbf{p}_f d\mathbf{q}_1 d\mathbf{q}_2 d\mathbf{q}_3 \iiint d\mathbf{x}_1 d\mathbf{x}_2 d\mathbf{x}_3 d\mathbf{x}_4 \\ & \quad \cdot \left[e^{i(\mathbf{p}_f - \mathbf{q}_1)\mathbf{x}_1} e^{i(\mathbf{q}_1 - \mathbf{q}_2)\mathbf{x}_2} e^{i(\mathbf{q}_2 - \mathbf{q}_3)\mathbf{x}_3} e^{i(\mathbf{q}_3 - \mathbf{p}_i)\mathbf{x}_4} + e^{-i(\mathbf{p}_f - \mathbf{q}_1)\mathbf{x}_1} e^{-i(\mathbf{q}_1 - \mathbf{q}_2)\mathbf{x}_2} e^{-i(\mathbf{q}_2 - \mathbf{q}_3)\mathbf{x}_3} e^{-i(\mathbf{q}_3 - \mathbf{p}_i)\mathbf{x}_4} \right] \\ & \quad \cdot e^{-\frac{\mathbf{x}_4^2}{2\alpha}} e^{-\frac{\alpha}{2}(\mathbf{p}_f - \mathbf{p}_i)^2} e^{-\frac{(\mathbf{x}_1 - \mathbf{x}_2)^2}{4r_C^2}} e^{-\frac{(\mathbf{x}_3 - \mathbf{x}_4)^2}{4r_C^2}} \cdot \frac{1}{2} (1 - \vartheta(0))^2 t^2 \\ &= 2\delta_{\mu\nu} \frac{1}{(4\pi r_C^2)^d} \frac{\gamma^2 m_\mu^4}{m_0^4} \cdot \frac{1}{2} (1 - \vartheta(0))^2 \cdot t^2, \end{aligned}$$

the second two components result in

$$\begin{aligned}
 & \frac{1}{(2\pi)^d} \int d\mathbf{p}_f \mathbb{E} \left[T_{\mu\nu}^{(1)*}(\mathbf{p}_f, \mathbf{p}_i, \alpha; t) T_{\mu\nu}^{(3)}(\mathbf{p}_f, \mathbf{p}_i, \alpha; t) + T_{\mu\nu}^{(3)*}(\mathbf{p}_f, \mathbf{p}_i, \alpha; t) T_{\mu\nu}^{(1)}(\mathbf{p}_f, \mathbf{p}_i, \alpha; t) \right] \\
 &= -2\delta_{\mu\nu} \frac{\gamma^2 m_\mu^4}{m_0^4} \left(\frac{1}{(2\pi)^3 \sqrt{\alpha\pi}} \right)^d \iiint d\mathbf{p}_f d\mathbf{q}_1 d\mathbf{q}_2 \iiint d\mathbf{x}_1 d\mathbf{x}_2 d\mathbf{x}_3 d\mathbf{x}_4 \\
 & \quad \cdot \cos \left[(\mathbf{p}_f - \mathbf{q}_1) \cdot \mathbf{x}_1 + (\mathbf{q}_1 - \mathbf{q}_2) \cdot \mathbf{x}_2 + (\mathbf{q}_2 - \mathbf{p}_i) \cdot \mathbf{x}_3 - (\mathbf{p}_f - \mathbf{p}_i) \cdot \mathbf{x}_4 \right] e^{-\frac{\mathbf{x}_3^2 + \mathbf{x}_4^2}{2\alpha}} \\
 & \quad \cdot \int_0^t dt_1 \int_0^{t_1} dt_2 \int_0^{t_2} dt_3 \int_0^t dt_4 \mathbb{E} [w(t_1, \mathbf{x}_1) w(t_2, \mathbf{x}_2) w(t_3, \mathbf{x}_3) w(t_4, \mathbf{x}_4)] \\
 &= -\delta_{\mu\nu} \frac{1}{(4\pi r_C^2)^d} \frac{\gamma^2 m_\mu^4}{m_0^4} \left(\frac{1}{(2\pi)^3 \sqrt{\alpha\pi}} \right)^d \iiint d\mathbf{p}_f d\mathbf{q}_1 d\mathbf{q}_2 \iiint d\mathbf{x}_1 d\mathbf{x}_2 d\mathbf{x}_3 d\mathbf{x}_4 \\
 & \quad \cdot \left[e^{i(\mathbf{p}_f - \mathbf{q}_1) \cdot \mathbf{x}_1} e^{i(\mathbf{q}_1 - \mathbf{q}_2) \cdot \mathbf{x}_2} e^{i(\mathbf{q}_2 - \mathbf{p}_i) \cdot \mathbf{x}_3} e^{-i(\mathbf{p}_f - \mathbf{p}_i) \cdot \mathbf{x}_4} + e^{-i(\mathbf{p}_f - \mathbf{q}_1) \cdot \mathbf{x}_1} e^{-i(\mathbf{q}_1 - \mathbf{q}_2) \cdot \mathbf{x}_2} e^{-i(\mathbf{q}_2 - \mathbf{p}_i) \cdot \mathbf{x}_3} e^{i(\mathbf{p}_f - \mathbf{p}_i) \cdot \mathbf{x}_4} \right] e^{-\frac{\mathbf{x}_3^2 + \mathbf{x}_4^2}{2\alpha}} \\
 & \quad \cdot \left[e^{-\frac{(\mathbf{x}_1 - \mathbf{x}_2)^2}{4r_C^2}} e^{-\frac{(\mathbf{x}_3 - \mathbf{x}_4)^2}{4r_C^2}} U_1^{3,1}(t) + e^{-\frac{(\mathbf{x}_1 - \mathbf{x}_3)^2}{4r_C^2}} e^{-\frac{(\mathbf{x}_2 - \mathbf{x}_4)^2}{4r_C^2}} U_2^{3,1}(t) + e^{-\frac{(\mathbf{x}_1 - \mathbf{x}_4)^2}{4r_C^2}} e^{-\frac{(\mathbf{x}_2 - \mathbf{x}_3)^2}{4r_C^2}} U_3^{3,1}(t) \right] \\
 &= -\delta_{\mu\nu} \frac{1}{(4\pi r_C^2)^d} \frac{\gamma^2 m_\mu^4}{m_0^4} \left(\frac{1}{(2\pi)^3 \sqrt{\alpha\pi}} \right)^d \iiint d\mathbf{p}_f d\mathbf{q}_1 d\mathbf{q}_2 \iiint d\mathbf{x}_1 d\mathbf{x}_2 d\mathbf{x}_3 d\mathbf{x}_4 \\
 & \quad \cdot \left[e^{i(\mathbf{p}_f - \mathbf{q}_1) \cdot \mathbf{x}_1} e^{i(\mathbf{q}_1 - \mathbf{q}_2) \cdot \mathbf{x}_2} e^{i(\mathbf{q}_2 - \mathbf{p}_i) \cdot \mathbf{x}_3} e^{-i(\mathbf{p}_f - \mathbf{p}_i) \cdot \mathbf{x}_4} + e^{-i(\mathbf{p}_f - \mathbf{q}_1) \cdot \mathbf{x}_1} e^{-i(\mathbf{q}_1 - \mathbf{q}_2) \cdot \mathbf{x}_2} e^{-i(\mathbf{q}_2 - \mathbf{p}_i) \cdot \mathbf{x}_3} e^{i(\mathbf{p}_f - \mathbf{p}_i) \cdot \mathbf{x}_4} \right] e^{-\frac{\mathbf{x}_3^2 + \mathbf{x}_4^2}{2\alpha}} \\
 & \quad \cdot \left[e^{-\frac{(\mathbf{x}_1 - \mathbf{x}_2)^2}{4r_C^2}} e^{-\frac{(\mathbf{x}_3 - \mathbf{x}_4)^2}{4r_C^2}} + e^{-\frac{(\mathbf{x}_1 - \mathbf{x}_4)^2}{4r_C^2}} e^{-\frac{(\mathbf{x}_2 - \mathbf{x}_3)^2}{4r_C^2}} \right] \cdot \frac{1}{2} (1 - \vartheta(0)) t^2 \\
 &= -2\delta_{\mu\nu} \frac{1}{(4\pi r_C^2)^d} \frac{\gamma^2 m_\mu^4}{m_0^4} (1 - \vartheta(0)) \cdot t^2,
 \end{aligned}$$

and the last component equals to

$$\begin{aligned}
 & \frac{1}{(2\pi)^d} \int d\mathbf{p}_f \mathbb{E} \left[T_{\mu\nu}^{(2)*}(\mathbf{p}_f, \mathbf{p}_i, \alpha; t) T_{\mu\nu}^{(2)}(\mathbf{p}_f, \mathbf{p}_i, \alpha; t) \right] \\
 &= \delta_{\mu\nu} \frac{\gamma^2 m_\mu^4}{m_0^4} \left(\frac{1}{(2\pi)^3 \sqrt{\alpha\pi}} \right)^d \iiint d\mathbf{p}_f d\mathbf{q}_1 d\mathbf{q}_2 \iiint d\mathbf{x}_1 d\mathbf{x}_2 d\mathbf{x}_3 d\mathbf{x}_4 \\
 & \quad \cdot e^{-i(\mathbf{p}_f - \mathbf{q}_1)\mathbf{x}_1} e^{-i(\mathbf{q}_1 - \mathbf{p}_i)\mathbf{x}_2} e^{-\frac{\mathbf{x}_2^2}{2\alpha}} e^{i(\mathbf{p}_f - \mathbf{q}_2)\mathbf{x}_3} e^{i(\mathbf{q}_2 - \mathbf{p}_i)\mathbf{x}_4} e^{-\frac{\mathbf{x}_4^2}{2\alpha}} \\
 & \quad \cdot \int_0^t dt_1 \int_0^{t_1} dt_2 \int_0^{t_2} dt_3 \int_0^{t_3} dt_4 \mathbb{E}[w(t_1, \mathbf{x}_1)w(t_2, \mathbf{x}_2)w(t_3, \mathbf{x}_3)w(t_4, \mathbf{x}_4)] \\
 &= \delta_{\mu\nu} \frac{1}{(4\pi r_C^2)^d} \frac{\gamma^2 m_\mu^4}{m_0^4} \left(\frac{1}{(2\pi)^3 \sqrt{\alpha\pi}} \right)^d \iiint d\mathbf{p}_f d\mathbf{q}_1 d\mathbf{q}_2 \iiint d\mathbf{x}_1 d\mathbf{x}_2 d\mathbf{x}_3 d\mathbf{x}_4 \\
 & \quad \cdot e^{-i(\mathbf{p}_f - \mathbf{q}_1)\mathbf{x}_1} e^{-i(\mathbf{q}_1 - \mathbf{p}_i)\mathbf{x}_2} e^{-\frac{\mathbf{x}_2^2}{2\alpha}} e^{-i(\mathbf{p}_f - \mathbf{q}_1)\mathbf{x}_1} e^{-i(\mathbf{q}_1 - \mathbf{p}_i)\mathbf{x}_2} e^{-\frac{\mathbf{x}_2^2}{2\alpha}} e^{i(\mathbf{p}_f - \mathbf{q}_2)\mathbf{x}_3} e^{i(\mathbf{q}_2 - \mathbf{p}_i)\mathbf{x}_4} e^{-\frac{\mathbf{x}_4^2}{2\alpha}} \\
 & \quad \cdot \left[e^{-\frac{(\mathbf{x}_1 - \mathbf{x}_2)^2}{4r_C^2}} e^{-\frac{(\mathbf{x}_3 - \mathbf{x}_4)^2}{4r_C^2}} U_1^{2,2}(t) + e^{-\frac{(\mathbf{x}_1 - \mathbf{x}_3)^2}{4r_C^2}} e^{-\frac{(\mathbf{x}_2 - \mathbf{x}_4)^2}{4r_C^2}} U_2^{2,2}(t) + e^{-\frac{(\mathbf{x}_1 - \mathbf{x}_4)^2}{4r_C^2}} e^{-\frac{(\mathbf{x}_2 - \mathbf{x}_3)^2}{4r_C^2}} U_3^{2,2}(t) \right] \\
 &= \delta_{\mu\nu} \frac{1}{(4\pi r_C^2)^d} \frac{\gamma^2 m_\mu^4}{m_0^4} \left(\frac{1}{(2\pi)^3 \sqrt{\alpha\pi}} \right)^d \iiint d\mathbf{p}_f d\mathbf{q}_1 d\mathbf{q}_2 \iiint d\mathbf{x}_1 d\mathbf{x}_2 d\mathbf{x}_3 d\mathbf{x}_4 \\
 & \quad \cdot e^{-i(\mathbf{p}_f - \mathbf{q}_1)\mathbf{x}_1} e^{-i(\mathbf{q}_1 - \mathbf{p}_i)\mathbf{x}_2} e^{-\frac{\mathbf{x}_2^2}{2\alpha}} e^{-i(\mathbf{p}_f - \mathbf{q}_1)\mathbf{x}_1} e^{-i(\mathbf{q}_1 - \mathbf{p}_i)\mathbf{x}_2} e^{-\frac{\mathbf{x}_2^2}{2\alpha}} e^{i(\mathbf{p}_f - \mathbf{q}_2)\mathbf{x}_3} e^{i(\mathbf{q}_2 - \mathbf{p}_i)\mathbf{x}_4} e^{-\frac{\mathbf{x}_4^2}{2\alpha}} \\
 & \quad \cdot \left[e^{-\frac{(\mathbf{x}_1 - \mathbf{x}_2)^2}{4r_C^2}} e^{-\frac{(\mathbf{x}_3 - \mathbf{x}_4)^2}{4r_C^2}} \cdot (1 - \vartheta(0))^2 + e^{-\frac{(\mathbf{x}_1 - \mathbf{x}_3)^2}{4r_C^2}} e^{-\frac{(\mathbf{x}_2 - \mathbf{x}_4)^2}{4r_C^2}} \cdot \frac{1}{2} \right] t^2 \\
 &= \delta_{\mu\nu} \frac{1}{(4\pi r_C^2)^d} \frac{\gamma^2 m_\mu^4}{m_0^4} \left((1 - \vartheta(0))^2 + \frac{1}{2} \right) \cdot t^2.
 \end{aligned}$$

where

$$\begin{aligned}
 U_1^{4,0}(t) + U_2^{4,0}(t) + U_3^{4,0}(t) &\equiv C_{4,0}^{(2)}(t), \\
 U_1^{3,1}(t) + U_2^{3,1}(t) + U_3^{3,1}(t) &\equiv C_{3,1}^{(2)}(t), \\
 U_1^{2,2}(t) + U_2^{2,2}(t) + U_3^{2,2}(t) &\equiv C_{2,2}^{(2)}(t)
 \end{aligned}$$

correspond to the integrals of the 4-point correlation functions of the noise field, which are calculated in Appendix C.

Consequently, the component of the transition probabilities, which corresponds to the second order by time t , equals to

$$\begin{aligned}
 P_{M_\mu \rightarrow M_\nu}^{(2)}(t) &= \delta_{\mu\nu} \frac{1}{(4\pi r_C^2)^d} \frac{\gamma^2 m_\mu^4}{m_0^4} \left(2\vartheta(0) \left(\vartheta(0) - 1 \right) + \frac{1}{2} \right) t^2 \quad (\text{B.9}) \\
 &= \delta_{\mu\nu} \frac{1}{2} \frac{1}{(4\pi r_C^2)^d} \frac{\gamma^2 m_\mu^4}{m_0^4} (1 - 2\vartheta(0))^2 t^2.
 \end{aligned}$$

Finally, collecting all the calculated terms (B.5)–(B.9), we obtain the transition probabilities for mass eigenstates

$$\begin{aligned}
 P_{M_\mu \rightarrow M_\nu}(t) &= \left[1 - \gamma \frac{m_\mu^2}{m_0^2} \frac{1}{(\sqrt{4\pi} r_C)^d} (1 - 2\vartheta(0)) t \right. \\
 &\quad \left. + \frac{\gamma^2 m_\mu^4}{2 m_0^4 (4\pi r_C^2)^d} (1 - 2\vartheta(0))^2 t^2 \right] \delta_{\mu\nu}.
 \end{aligned} \tag{B.10}$$

B.2 Transition probabilities for the flavor states

We perform the computations in the same manner as was done in Appendix A for the QMUPL model, and expand the probabilities for the flavor states for the mass-proportional CSL model in the following form

$$\begin{aligned}
 P_{M^0 \rightarrow M^0/\bar{M}^0}(t) &= \sum_{\mu, \mu'} \alpha_\mu \beta_\mu^* \alpha_{\mu'}^* \beta_{\mu'} P_{\mu\mu'}(t) \\
 &= \frac{1}{4} (P_{HH}(t) \pm P_{HL}(t) \pm P_{LH}(t) + P_{LL}(t)),
 \end{aligned} \tag{B.11}$$

where terms with same indexes P_{aa} and different ones P_{ab} are equal to

$$P_{aa}(t) = 1 - \frac{1}{(\sqrt{4\pi} r_C)^d} \frac{\gamma m_a^2}{m_0^2} (1 - 2\vartheta(0)) t + \frac{1}{2} \frac{1}{(4\pi r_C^2)^d} \frac{\gamma^2 m_a^4}{m_0^4} (1 - 2\vartheta(0))^2 t^2, \tag{B.12}$$

$$\begin{aligned}
 P_{ab}(t) &= e^{-i(m_a - m_b)t} \cdot \left\{ 1 - \frac{1}{(\sqrt{4\pi} r_C)^d} \frac{\gamma}{m_0^2} (m_a^2 + m_b^2) (1 - \vartheta(0)) - m_a m_b \right\} t \\
 &\quad + \frac{1}{(4\pi r_C^2)^d} \frac{\gamma^2}{m_0^4} \left[(m_a^4 + m_b^4) (1 - \vartheta(0))^2 - 2(m_a^3 m_b + m_a m_b^3) (1 - \vartheta(0)) \right. \\
 &\quad \left. + 2m_a^2 m_b^2 \left((1 - \vartheta(0))^2 + \frac{1}{2} \right) \right] t^2 \Big\}.
 \end{aligned} \tag{B.13}$$

Putting the terms together, we finally obtain the transition probability for the flavor states for the mass-proportional CSL model

$$\begin{aligned}
 P_{M^0 \rightarrow M^0/\bar{M}^0}(t) &= \frac{1}{2} \left\{ 1 - \frac{1}{2} \frac{1}{(\sqrt{4\pi} r_C)^d} \frac{\gamma(m_H^2 + m_L^2)}{m_0^2} (1 - 2\vartheta(0)) \cdot t \right. \\
 &\quad + \frac{1}{4} \frac{1}{(4\pi r_C^2)^d} \frac{\gamma^2(m_H^4 + m_L^4)}{m_0^4} (1 - 2\vartheta(0))^2 \cdot t^2 \\
 &\quad \pm \left[1 - \frac{1}{(\sqrt{4\pi} r_C)^d} \frac{\gamma}{m_0^2} (m_H^2 + m_L^2) (1 - \vartheta(0)) - m_H m_L \right] \cdot t \\
 &\quad + \frac{1}{2} \frac{1}{(4\pi r_C^2)^d} \frac{\gamma^2}{m_0^4} (m_H^4 + m_L^4) (1 - \vartheta(0))^2 - 2m_H m_L (m_H^2 + m_L^2) (1 - \vartheta(0)) \\
 &\quad \left. + 2m_H^2 m_L^2 \left((1 - \vartheta(0))^2 + \frac{1}{2} \right) \right] \cdot t^2 \cdot \cos[(m_H - m_L)t] \Big\}. \tag{B.14}
 \end{aligned}$$

Taking decay into account

$$\begin{aligned}
 P_{M^0 \rightarrow M^0/\bar{M}^0}(t) &= \frac{1}{4} \left\{ e^{-\Gamma_H t} + e^{-\Gamma_L t} \right. \\
 &\quad - \frac{1}{(\sqrt{4\pi} r_C)^d} \frac{\gamma}{m_0^2} (m_H^2 e^{-\Gamma_H t} + m_L^2 e^{-\Gamma_L t}) (1 - 2\vartheta(0)) \cdot t \\
 &\quad + \frac{1}{2} \frac{1}{(4\pi r_C^2)^d} \frac{\gamma^2}{m_0^4} (m_H^4 e^{-\Gamma_H t} + m_L^4 e^{-\Gamma_L t}) (1 - 2\vartheta(0))^2 \cdot t^2 \\
 &\quad \pm 2 \left[1 - \frac{1}{(\sqrt{4\pi} r_C)^d} \frac{\gamma}{m_0^2} (m_H^2 + m_L^2) (1 - \vartheta(0)) - m_H m_L \right] \cdot t \\
 &\quad + \frac{1}{2} \frac{1}{(4\pi r_C^2)^d} \frac{\gamma^2}{m_0^4} (m_H^4 + m_L^4) (1 - \vartheta(0))^2 \\
 &\quad - 2m_H m_L (m_H^2 + m_L^2) (1 - \vartheta(0)) + 2m_H^2 m_L^2 \left((1 - \vartheta(0))^2 + \frac{1}{2} \right) \Big] \cdot t^2 \\
 &\quad \left. \cdot \cos[(m_H - m_L)t] \cdot e^{-\frac{\Gamma_H + \Gamma_L}{2} t} \right\}. \tag{B.15}
 \end{aligned}$$

B.3 Transition probabilities with included effect of \mathcal{CP} violation

Since we seek to take into account the non-orthogonality of the mass eigenstates due to the violation of \mathcal{CP} symmetry in a neutral kaon system, $\langle K_L | K_S \rangle = \delta$, the functions (B.1)–(B.2), which form the components of the transition amplitude of different orders, should be modified. Using the coordinate representation and calculating the matrix

B.3. TRANSITION PROBABILITIES WITH INCLUDED EFFECT OF \mathcal{CP} VIOLATION

elements, we obtain components of the transition amplitudes in the following form

$$\begin{aligned}
K_{\mu\nu}^{(0)}(\mathbf{p}_f, \mathbf{p}_i, \alpha; t) &= M_{\mu\nu}^{(0)}(m_L, m_S) \cdot (2\sqrt{\alpha\pi})^{d/2} e^{-\frac{\alpha}{2}(\mathbf{p}_f - \mathbf{p}_i)^2}, \\
K_{\mu\nu}^{(1)}(\mathbf{p}_f, \mathbf{p}_i, \alpha; t) &= M_{\mu\nu}^{(1)}(m_L, m_S) \cdot \left[\left(\frac{1}{\sqrt{\alpha\pi}} \right)^{d/2} \int_0^t dt_1 \int d\mathbf{x}_1 w(t_1, \mathbf{x}_1) \cdot e^{-i(\mathbf{p}_f - \mathbf{p}_i)\mathbf{x}_1} e^{-\frac{\mathbf{x}_1^2}{2\alpha}} \right], \\
K_{\mu\nu}^{(2)}(\mathbf{p}_f, \mathbf{p}_i, \alpha; t) &= M_{\mu\nu}^{(2)}(m_L, m_S) \cdot \frac{1}{(2\pi)^d} \int d\mathbf{q}_1 \left[\left(\frac{1}{\sqrt{\alpha\pi}} \right)^{d/2} \int_0^t dt_1 \int_0^{t_1} dt_2 \iint d\mathbf{x}_1 d\mathbf{x}_2 \right. \\
&\quad \left. \cdot w(t_1, \mathbf{x}_1) w(t_2, \mathbf{x}_2) \cdot e^{-i(\mathbf{p}_f - \mathbf{q})\mathbf{x}_1} e^{-i(\mathbf{q} - \mathbf{p}_i)\mathbf{x}_2} e^{-\frac{\mathbf{x}_2^2}{2\alpha}} \right], \\
K_{\mu\nu}^{(3)}(\mathbf{p}_f, \mathbf{p}_i, \alpha; t) &= M_{\mu\nu}^{(3)}(m_L, m_S) \cdot \frac{1}{(2\pi)^{2d}} \iint d\mathbf{q}_1 d\mathbf{q}_2 \left[\left(\frac{1}{\sqrt{\alpha\pi}} \right)^{d/2} \int_0^t dt_1 \int_0^{t_1} dt_2 \int_0^{t_2} dt_3 \right. \\
&\quad \left. \cdot \iint d\mathbf{x}_1 d\mathbf{x}_2 d\mathbf{x}_3 w(t_1, \mathbf{x}_1) w(t_2, \mathbf{x}_2) w(t_3, \mathbf{x}_3) \cdot e^{-i(\mathbf{p}_f - \mathbf{q}_1)\mathbf{x}_1} e^{-i(\mathbf{q}_1 - \mathbf{q}_2)\mathbf{x}_2} e^{-i(\mathbf{q}_2 - \mathbf{p}_i)\mathbf{x}_3} e^{-\frac{\mathbf{x}_3^2}{2\alpha}} \right], \\
K_{\mu\nu}^{(4)}(\mathbf{p}_f, \mathbf{p}_i, \alpha; t) &= M_{\mu\nu}^{(4)}(m_L, m_S) \cdot \frac{1}{(2\pi)^{3d}} \iiint d\mathbf{q}_1 d\mathbf{q}_2 d\mathbf{q}_3 \\
&\quad \cdot \left[\left(\frac{1}{\sqrt{\alpha\pi}} \right)^{d/2} \int_0^t dt_1 \int_0^{t_1} dt_2 \int_0^{t_2} dt_3 \int_0^{t_3} dt_4 \iiint d\mathbf{x}_1 d\mathbf{x}_2 d\mathbf{x}_3 d\mathbf{x}_4 \right. \\
&\quad \left. \cdot w(t_1, \mathbf{x}_1) w(t_2, \mathbf{x}_2) w(t_3, \mathbf{x}_3) w(t_4, \mathbf{x}_4) \cdot e^{-i(\mathbf{p}_f - \mathbf{q}_1)\mathbf{x}_1} e^{-i(\mathbf{q}_1 - \mathbf{q}_2)\mathbf{x}_2} e^{-i(\mathbf{q}_2 - \mathbf{q}_3)\mathbf{x}_3} e^{-i(\mathbf{q}_3 - \mathbf{p}_i)\mathbf{x}_4} e^{-\frac{\mathbf{x}_4^2}{2\alpha}} \right],
\end{aligned}$$

where $M_{\mu\nu}^{(i)}(m_L, m_S)$ are the mass functions of i -th order defined below. The mass function of zeroth order is defined as following,

$$\begin{aligned}
M_{LL}^{(0)}(m_L, m_S) &= 1, \\
M_{LS}^{(0)}(m_L, m_S) &= \delta, \\
M_{SL}^{(0)}(m_L, m_S) &= \delta, \\
M_{SS}^{(0)}(m_L, m_S) &= 1.
\end{aligned}$$

The mass function of first order is defined as following,

$$\begin{aligned}
M_{LL}^{(1)}(m_L, m_S) &= \frac{m_L + \delta^2 m_S}{m_0}, \\
M_{LS}^{(1)}(m_L, m_S) &= \delta \cdot \frac{m_L + m_S}{m_0}, \\
M_{SL}^{(1)}(m_L, m_S) &= \delta \cdot \frac{m_L + m_S}{m_0}, \\
M_{SS}^{(1)}(m_L, m_S) &= \frac{\delta^2 m_L + m_S}{m_0}.
\end{aligned}$$

The mass function of second order is defined as following,

$$\begin{aligned}
 M_{LL}^{(2)}(m_L, m_S) &= \frac{m_L^2 + \delta^2(2m_L m_S + m_S^2)}{m_0^2}, \\
 M_{LS}^{(2)}(m_L, m_S) &= \delta \cdot \frac{m_L^2 + (1 + \delta^2)m_L m_S + m_S^2}{m_0^2}, \\
 M_{SL}^{(2)}(m_L, m_S) &= \delta \cdot \frac{m_L^2 + (1 + \delta^2)m_L m_S + m_S^2}{m_0^2}, \\
 M_{SS}^{(2)}(m_L, m_S) &= \frac{\delta^2(m_L^2 + 2m_L m_S) + m_S^2}{m_0^2}.
 \end{aligned}$$

The mass function of third order is defined as following,

$$\begin{aligned}
 M_{LL}^{(3)}(m_L, m_S) &= \frac{m_L^3 + \delta^2(3m_L^2 m_S + (2 + \delta^2)m_L m_S^2 + m_S^3)}{m_0^3}, \\
 M_{LS}^{(3)}(m_L, m_S) &= \delta \cdot \frac{m_L^2 + (1 + 2\delta^2)(m_L + m_S)m_L m_S + m_S^2}{m_0^3}, \\
 M_{SL}^{(3)}(m_L, m_S) &= \delta \cdot \frac{m_L^2 + (1 + 2\delta^2)(m_L + m_S)m_L m_S + m_S^2}{m_0^3}, \\
 M_{SS}^{(3)}(m_L, m_S) &= \frac{\delta^2(m_L^3 + (2 + \delta^2)m_L^2 m_S + 3m_L m_S^2) + m_S^3}{m_0^3}.
 \end{aligned}$$

The mass function of fourth order is defined as following,

$$\begin{aligned}
 M_{LL}^{(4)}(m_L, m_S) &= \frac{m_L^4 + \delta^2(4m_L^3 m_S + 3(1 + \delta^2)m_L^2 m_S^2 + 2(1 + \delta^2)m_L m_S^3 + m_S^4)}{m_0^4}, \\
 M_{LS}^{(4)}(m_L, m_S) &= \delta \cdot \frac{m_L^4 + (1 + 3\delta^2)m_L^3 m_S + (1 + 4\delta^2 + \delta^4)m_L^2 m_S^2 + (1 + 3\delta^2)m_L m_S^3 + m_S^4}{m_0^4}, \\
 M_{SL}^{(4)}(m_L, m_S) &= \delta \cdot \frac{m_L^4 + (1 + 3\delta^2)m_L^3 m_S + (1 + 4\delta^2 + \delta^4)m_L^2 m_S^2 + (1 + 3\delta^2)m_L m_S^3 + m_S^4}{m_0^4}, \\
 M_{SS}^{(4)}(m_L, m_S) &= \frac{\delta^2(m_L^4 + 2(1 + \delta^2)m_L^3 m_S + 3(1 + \delta^2)m_L^2 m_S^2 + 4m_L m_S^3) + m_S^4}{m_0^4}.
 \end{aligned}$$

As done in the previous subsections we start with transition probabilities for the mass eigenstates. Plugging in the modified transition amplitude we obtain the transition probabilities for the mass eigenstates which now reveal a more involved form for the

B.3. TRANSITION PROBABILITIES WITH INCLUDED EFFECT OF \mathcal{CP} VIOLATION

mass-proportional CSL model,

$$\begin{aligned}
 P_{K_L \rightarrow K_L}(t) = & e^{-\Gamma_L t} \left\{ 1 - \frac{1}{(\sqrt{4\pi} r_C)^d} \frac{\gamma}{m_0^2} \left(m_L^2 + \delta^2 (2m_L m_S + m_S^2) \right) (1 - 2\vartheta(0)) \cdot t \right. \\
 & + \frac{1}{2} \frac{1}{(4\pi r_C^2)^d} \frac{\gamma^2}{m_0^4} \left(m_L^2 + \delta^2 (2m_L m_S + m_S^2) \right)^2 (1 - 2\vartheta(0))^2 \cdot t^2 \\
 & - \delta^2 (1 - \delta^2) \frac{1}{(\sqrt{4\pi} r_C)^d} \frac{\gamma m_S^2}{m_0^2} \cdot t \\
 & \left. \cdot \left[1 - \frac{1}{(\sqrt{4\pi} r_C)^d} \frac{\gamma}{m_0^2} \frac{1 - \vartheta(0)}{2} \left((\Delta m)^2 + 4\delta^2 m_L m_S + 2(1 - 2\vartheta(0))(m_L^2 + m_S^2) \right) \cdot t \right] \right\},
 \end{aligned}$$

$$\begin{aligned}
 P_{K_S \rightarrow K_S}(t) = & e^{-\Gamma_S t} \left\{ 1 - \frac{1}{(\sqrt{4\pi} r_C)^d} \frac{\gamma}{m_0^2} \left(\delta^2 (m_L^2 + 2m_L m_S) + m_S^2 \right) (1 - 2\vartheta(0)) \cdot t \right. \\
 & + \frac{1}{2} \frac{1}{(4\pi r_C^2)^d} \frac{\gamma^2}{m_0^4} \left(\delta^2 (m_L^2 + 2m_L m_S) + m_S^2 \right)^2 (1 - 2\vartheta(0))^2 \cdot t^2 \\
 & - \delta^2 (1 - \delta^2) \frac{1}{(\sqrt{4\pi} r_C)^d} \frac{\gamma m_L^2}{m_0^2} \cdot t \\
 & \left. \cdot \left[1 - \frac{1}{(\sqrt{4\pi} r_C)^d} \frac{\gamma}{m_0^2} \frac{1 - \vartheta(0)}{2} \left((\Delta m)^2 + 4\delta^2 m_L m_S + 2(1 - 2\vartheta(0))(m_L^2 + m_S^2) \right) \cdot t \right] \right\},
 \end{aligned}$$

$$\begin{aligned}
 P_{K_L \leftrightarrow K_S}(t) = & \delta^2 e^{-\Gamma_{L/S} t} \left\{ 1 - \frac{1}{(\sqrt{4\pi} r_C)^d} \frac{\gamma}{m_0^2} \left(m_L^2 + (1 + \delta^2) m_L m_S + m_S^2 \right) (1 - 2\vartheta(0)) \cdot t \right. \\
 & + \frac{1}{2} \frac{1}{(4\pi r_C^2)^d} \frac{\gamma^2}{m_0^4} \left(m_L^2 + (1 + \delta^2) m_L m_S + m_S^2 \right)^2 (1 - 2\vartheta(0))^2 \cdot t^2 \\
 & + (1 - \delta^2) \frac{1}{(\sqrt{4\pi} r_C)^d} \frac{\gamma m_L m_S}{m_0^2} \cdot t \\
 & \left. \cdot \left[1 - \frac{1}{(\sqrt{4\pi} r_C)^d} \frac{\gamma}{m_0^2} \frac{1 - \vartheta(0)}{2} \left((\Delta m)^2 + 4\delta^2 m_L m_S + 2(1 - 2\vartheta(0))(m_L^2 + m_S^2) \right) \cdot t \right] \right\}.
 \end{aligned}$$

Then, collecting all the necessary transition probabilities for the mass eigenstates we obtain the transition probabilities for the flavor eigenstates,

$$\begin{aligned}
 P_{K^0 \rightarrow \bar{K}^0}(t) = & \frac{1}{4} \left\{ e^{-\Gamma_L t} \left(1 - \tilde{\Gamma}_L^{CSL} \cdot t + \frac{1}{2} (\tilde{\Gamma}_L^{CSL})^2 \cdot t^2 \right) + e^{-\Gamma_S t} \left(1 - \tilde{\Gamma}_S^{CSL} \cdot t + \frac{1}{2} (\tilde{\Gamma}_S^{CSL})^2 \cdot t^2 \right) \right. \\
 & - \delta(1-\delta) \frac{\gamma}{(\sqrt{4\pi} r_C)^d} \frac{\Delta m}{m_0^2} (m_L e^{-\Gamma_S t} - m_S e^{-\Gamma_L t}) \cdot t \\
 & \cdot \left[1 - \frac{\gamma}{(\sqrt{4\pi} r_C)^d} \frac{1 - \vartheta(0)}{2} \frac{(\Delta m)^2 + 4\delta^2 m_L m_S + (1 - 2\vartheta(0))(m_L + m_S)^2}{m_0^2} \cdot t \right] \\
 & + 2e^{-\frac{\Gamma_L + \Gamma_S}{2} t} \cos[t\Delta m] \left(1 - F(m_L, m_S) \cdot t + \frac{1}{2} F^2(m_L, m_S) \cdot t^2 \right. \\
 & \left. + \delta \frac{1-\delta}{8} \frac{\gamma^2}{(4\pi r_C^2)^d} \frac{(\Delta m)^2}{m_0^4} \left((\Delta m)^2 + 4\delta m_L m_S - (1 - 4\theta^2(0))(m_L + m_S)^2 \right) \cdot t^2 \right) \left. \right\},
 \end{aligned}$$

$$\begin{aligned}
 P_{K^0 \rightarrow K^0}(t) = & \frac{1}{4} \frac{1-\delta}{1+\delta} \left\{ e^{-\Gamma_L t} \left(1 - \tilde{\Gamma}_L^{CSL} \cdot t + \frac{1}{2} (\tilde{\Gamma}_L^{CSL})^2 \cdot t^2 \right) + e^{-\Gamma_S t} \left(1 - \tilde{\Gamma}_S^{CSL} \cdot t + \frac{1}{2} (\tilde{\Gamma}_S^{CSL})^2 \cdot t^2 \right) \right. \\
 & + \delta(1+\delta) \frac{\gamma}{(\sqrt{4\pi} r_C)^d} \frac{\Delta m}{m_0^2} (m_L e^{-\Gamma_S t} - m_S e^{-\Gamma_L t}) \cdot t \\
 & \cdot \left[1 - \frac{\gamma}{(\sqrt{4\pi} r_C)^d} \frac{1 - \vartheta(0)}{2} \frac{(\Delta m)^2 + 4\delta^2 m_L m_S + (1 - 2\vartheta(0))(m_L + m_S)^2}{m_0^2} \cdot t \right] \\
 & - 2e^{-\frac{\Gamma_L + \Gamma_S}{2} t} \cos[t\Delta m] \left(1 - F(m_L, m_S) \cdot t + \frac{1}{2} F^2(m_L, m_S) \cdot t^2 \right. \\
 & \left. - \delta \frac{1+\delta}{8} \frac{\gamma^2}{(4\pi r_C)^d} \frac{(\Delta m)^2}{m_0^4} \left((\Delta m)^2 - 4\delta m_L m_S - (1 - 4\theta^2(0))(m_L + m_S)^2 \right) \cdot t^2 \right) \left. \right\}
 \end{aligned}$$

with

$$\begin{aligned}
 F(m_L, m_S) &= \frac{1 \mp \delta}{2} \frac{\gamma}{(\sqrt{4\pi} r_C)^d} \frac{(\Delta m)^2}{m_0^2} + \frac{\tilde{\Gamma}_L^{CSL} + \tilde{\Gamma}_S^{CSL}}{2}, \\
 \tilde{\Gamma}_L^{CSL} &= (1 - 2\vartheta(0)) \frac{\gamma}{(\sqrt{4\pi} r_C)^d} \frac{m_L^2 \pm \delta(1 \pm \delta)m_L m_S \pm \delta m_S^2}{m_0^2}, \\
 \tilde{\Gamma}_S^{CSL} &= (1 - 2\vartheta(0)) \frac{\gamma}{(\sqrt{4\pi} r_C)^d} \frac{\pm \delta m_L^2 \pm \delta(1 \pm \delta)m_L m_S + m_S^2}{m_0^2},
 \end{aligned}$$

where the upper sign refers to the probability $P_{K^0 \rightarrow K^0}(t)$ and the lower sign refers to the probability $P_{K^0 \rightarrow \bar{K}^0}(t)$.



CORRELATION FUNCTIONS OF THE NOISE FIELD

C.1 Calculations with a 2-point correlation function

First-order components of the transition probabilities contain a 2-point correlation function of the noise. In the computations for the QMUPL model the noise is assumed to be a white one, i.e. any random process is uncorrelated to the random process at a later time point. Mathematically, one defines $\mathbb{E}[w(t_1)w(t_2)] = \frac{1}{2\pi} \int_{-\infty}^{\infty} d\omega e^{i\omega(t_1-t_2)} = \delta(t_1 - t_2)$. In our computations two different integrals have to be computed (corresponding to $T^{(0)*}T^{(2)}$ and $T^{(2)*}T^{(0)}$, respectively),

$$\begin{aligned} C_{2,0}^{(1)}(t) &= \int_0^t dt_1 \int_0^{t_1} dt_2 \delta(t_1 - t_2) \\ &= \int_0^t dt_1 (\vartheta(t_1) - \vartheta(0)) = (1 - \vartheta(0))t, \end{aligned} \quad (\text{C.1})$$

and the second one corresponds to the component $T^{(1)*}T^{(1)}$:

$$\begin{aligned} C_{1,1}^{(1)}(t) &= \int_0^t dt_1 \int_0^t dt_2 \delta(t_1 - t_2) \\ &= \int_0^t dt_1 (\vartheta(t_1) - \vartheta(t_1 - t)) = t. \end{aligned} \quad (\text{C.2})$$

In the d -dimensional case we define $\mathbb{E}[\mathbf{w}(t_1) \cdot \mathbf{w}(t_2)] = \delta(t_1 - t_2)$.

C.2 Calculations with a 4-point correlation function

Second-order components of the transition probabilities contain integrals of a 4-point correlation function of the noise field

$$\begin{aligned}
 C_{4,0}^{(2)}(t) &= \int_0^t dt_1 \int_0^{t_1} dt_2 \int_0^{t_2} dt_3 \int_0^{t_3} dt_4 \mathbb{E}[w(t_1)w(t_2)w(t_3)w(t_4)], \\
 C_{3,1}^{(2)}(t) &= \int_0^t dt_1 \int_0^{t_1} dt_2 \int_0^{t_2} dt_3 \int_0^t dt_4 \mathbb{E}[w(t_1)w(t_2)w(t_3)w(t_4)], \\
 C_{2,2}^{(2)}(t) &= \int_0^t dt_1 \int_0^{t_1} dt_2 \int_0^t dt_3 \int_0^{t_3} dt_4 \mathbb{E}[w(t_1)w(t_2)w(t_3)w(t_4)].
 \end{aligned}$$

Since the noise field is assumed to be a Gaussian white noise field, its 4th cumulant is equal to zero, $\kappa(w(t_1)w(t_2)w(t_3)w(t_4)) = 0$. On the other hand, odd moments of the Gaussian noise are equal to zero as well, therefore it is possible to reformulate its 4-point correlation function as a combination of 2-point correlation functions:

$$\begin{aligned}
 \mathbb{E}[w(t_1)w(t_2)w(t_3)w(t_4)] &= \mathbb{E}[w(t_1)w(t_2)]\mathbb{E}[w(t_3)w(t_4)] \\
 &+ \mathbb{E}[w(t_1)w(t_3)]\mathbb{E}[w(t_2)w(t_4)] \\
 &+ \mathbb{E}[w(t_1)w(t_4)]\mathbb{E}[w(t_2)w(t_3)].
 \end{aligned}$$

Accordingly, each second-order components of the transition probability contains three integrals of two 2-point correlation functions

$$\begin{aligned}
 C_{4,0}^{(2)}(t) &\equiv U_1^{4,0}(t) + U_2^{4,0}(t) + U_3^{4,0}(t), \\
 C_{3,1}^{(2)}(t) &\equiv U_1^{3,1}(t) + U_2^{3,1}(t) + U_3^{3,1}(t), \\
 C_{2,2}^{(2)}(t) &\equiv U_1^{2,2}(t) + U_2^{2,2}(t) + U_3^{2,2}(t).
 \end{aligned}$$

For the components $T^{(0)*}T^{(4)}$ and $T^{(4)*}T^{(0)}$ the first integral is equal to:

$$\begin{aligned}
 U_1^{4,0}(t) &= \int_0^t dt_1 \int_0^{t_1} dt_2 \int_0^{t_2} dt_3 \int_0^{t_3} dt_4 \delta(t_1 - t_2) \delta(t_3 - t_4) \\
 &= \int_0^t dt_1 \int_0^{t_1} dt_2 \int_0^{t_2} dt_3 (\vartheta(t_3) - \vartheta(0)) \delta(t_1 - t_2) \\
 &= \int_0^t dt_1 \int_0^{t_1} dt_2 t_2 (\vartheta(t_2) - \vartheta(0)) \delta(t_1 - t_2) \\
 &= \int_0^t dt_1 t_1 (\vartheta(t_1) - \vartheta(0))^2 = \frac{1}{2} (1 - \vartheta(0))^2 t^2.
 \end{aligned}$$

Second integral:

$$\begin{aligned}
 U_2^{4,0}(t) &= \int_0^t dt_1 \int_0^{t_1} dt_2 \int_0^{t_2} dt_3 \int_0^{t_3} dt_4 \delta(t_1 - t_3) \delta(t_2 - t_4) \\
 &= \int_0^t dt_1 \int_0^{t_1} dt_2 \int_0^{t_2} dt_3 (\vartheta(t_2) - \vartheta(t_2 - t_3)) \delta(t_1 - t_3) \\
 &= \int_0^t dt_1 \int_0^{t_1} dt_2 (\vartheta(t_2) - \vartheta(t_2 - t_1)) (\vartheta(t_1) - \vartheta(t_1 - t_2)) \\
 &= \int_0^t dt_1 t_1 (\vartheta^2(t_1) - \vartheta(t_1)) = 0.
 \end{aligned}$$

Third integral:

$$\begin{aligned}
 U_3^{4,0}(t) &= \int_0^t dt_1 \int_0^{t_1} dt_2 \int_0^{t_2} dt_3 \int_0^{t_3} dt_4 \delta(t_1 - t_4) \delta(t_2 - t_3) \\
 &= \int_0^t dt_1 \int_0^{t_1} dt_2 \int_0^{t_2} dt_3 (\vartheta(t_1) - \vartheta(t_1 - t_3)) \delta(t_2 - t_3) \\
 &= \int_0^t dt_1 \int_0^{t_1} dt_2 (\vartheta(t_1) - \vartheta(t_1 - t_2)) (\vartheta(t_2) - \vartheta(0)) \\
 &= \int_0^t dt_1 t_1 (\vartheta^2(t_1) - \vartheta(t_1)) = 0.
 \end{aligned}$$

For the components $T^{(1)*}T^{(3)}$ and $T^{(3)*}T^{(1)}$ the first integral is equal to:

$$\begin{aligned}
 U_1^{3,1}(t) &= \int_0^t dt_1 \int_0^{t_1} dt_2 \int_0^{t_2} dt_3 \int_0^t dt_4 \delta(t_1 - t_2) \delta(t_3 - t_4) \\
 &= \int_0^t dt_1 \int_0^{t_1} dt_2 \int_0^{t_2} dt_3 (\vartheta(t_3) - \vartheta(t_3 - t)) \delta(t_1 - t_2) \\
 &= \int_0^t dt_1 \int_0^{t_1} dt_2 (t_2 \vartheta(t_2) - (t_2 - t) \vartheta(t_2 - t)) \delta(t_1 - t_2) \\
 &= \int_0^t dt_1 (t_1 \vartheta(t_1) - (t_1 - t) \vartheta(t_1 - t)) (\vartheta(t_1) - \vartheta(0)) = \frac{1}{2} (1 - \vartheta(0)) t^2.
 \end{aligned}$$

Second integral:

$$\begin{aligned}
 U_2^{3,1}(t) &= \int_0^t dt_1 \int_0^{t_1} dt_2 \int_0^{t_2} dt_3 \int_0^t dt_4 \delta(t_1 - t_3) \delta(t_2 - t_4) \\
 &= \int_0^t dt_1 \int_0^{t_1} dt_2 \int_0^{t_2} dt_3 (\vartheta(t_2) - \vartheta(t_2 - t)) \delta(t_1 - t_3) \\
 &= \int_0^t dt_1 \int_0^{t_1} dt_2 (\vartheta(t_2) - \vartheta(t_2 - t)) (\vartheta(t_1) - \vartheta(t_1 - t_2)) \\
 &= \int_0^t dt_1 t_1 (\vartheta^2(t_1) - \vartheta(t_1)) = 0.
 \end{aligned}$$

Third integral:

$$\begin{aligned}
 U_3^{3,1}(t) &= \int_0^t dt_1 \int_0^{t_1} dt_2 \int_0^{t_2} dt_3 \int_0^t dt_4 \delta(t_1 - t_4) \delta(t_2 - t_3) \\
 &= \int_0^t dt_1 \int_0^{t_1} dt_2 \int_0^{t_2} dt_3 (\vartheta(t_1) - \vartheta(t_1 - t)) \delta(t_2 - t_3) \\
 &= \int_0^t dt_1 \int_0^{t_1} dt_2 (\vartheta(t_1) - \vartheta(t_1 - t)) (\vartheta(t_2) - \vartheta(0)) \\
 &= \int_0^t dt_1 t_1 (\vartheta(t_1) - \vartheta(t_1 - t)) (\vartheta(t_1) - \vartheta(0)) = \frac{1}{2} (1 - \vartheta(0)) t^2.
 \end{aligned}$$

For the component $T^{(2)*}T^{(2)}$ the first integral is equal to:

$$\begin{aligned}
 U_1^{2,2}(t) &= \int_0^t dt_1 \int_0^{t_1} dt_2 \int_0^t dt_3 \int_0^{t_3} dt_4 \delta(t_1 - t_2) \delta(t_3 - t_4) \\
 &= \int_0^t dt_1 \int_0^{t_1} dt_2 \int_0^t dt_3 \delta(t_1 - t_2) (\vartheta(t_3) - \vartheta(0)) \\
 &= (1 - \vartheta(0)) t \int_0^t dt_1 \int_0^{t_1} dt_2 \delta(t_1 - t_2) \\
 &= (1 - \vartheta(0)) t \int_0^t dt_1 (\vartheta(t_1) - \vartheta(0)) = (1 - \vartheta(0))^2 t^2.
 \end{aligned}$$

Second integral:

$$\begin{aligned}
 U_2^{2,2}(t) &= \int_0^t dt_1 \int_0^{t_1} dt_2 \int_0^t dt_3 \int_0^{t_3} dt_4 \delta(t_1 - t_3) \delta(t_2 - t_4) \\
 &= \int_0^t dt_1 \int_0^{t_1} dt_2 \int_0^t dt_3 (\vartheta(t_2) - \vartheta(t_2 - t_3)) \delta(t_1 - t_3) \\
 &= \int_0^t dt_1 \int_0^{t_1} dt_2 (\vartheta(t_2) - \vartheta(t_2 - t_1)) (\vartheta(t_1) - \vartheta(t_1 - t)) \\
 &= \int_0^t dt_1 t_1 (\vartheta(t_1) - \vartheta(-t_1)) (\vartheta(t_1) - \vartheta(t_1 - t)) = \frac{1}{2} t^2.
 \end{aligned}$$

Third integral:

$$\begin{aligned}
 U_3^{2,2}(t) &= \int_0^t dt_1 \int_0^{t_1} dt_2 \int_0^t dt_3 \int_0^{t_3} dt_4 \delta(t_1 - t_4) \delta(t_2 - t_3) \\
 &= \int_0^t dt_1 \int_0^{t_1} dt_2 \int_0^t dt_3 (\vartheta(t_1) - \vartheta(t_1 - t_3)) \delta(t_2 - t_3) \\
 &= \int_0^t dt_1 \int_0^{t_1} dt_2 (\vartheta(t_1) - \vartheta(t_1 - t_2)) (\vartheta(t_2) - \vartheta(t_2 - t)) \\
 &= \int_0^t dt_1 t_1 (\vartheta^2(t_1) - \vartheta(t_1)) = 0,
 \end{aligned}$$

where we assumed $\vartheta(t) = 1$ for all the integrals since $t > 0$.

In the d -dimensional case second-order components of the transition probability form the following combination of 4-point correlation functions:

$$\begin{aligned}
 & \mathbb{E} \left[\left(\mathbf{w}(t_1) \cdot \mathbf{w}(t_2) \right) \left(\mathbf{w}(t_3) \cdot \mathbf{w}(t_4) \right) + \left(\mathbf{w}(t_1) \cdot \mathbf{w}(t_3) \right) \left(\mathbf{w}(t_2) \cdot \mathbf{w}(t_4) \right) \right. \\
 & \quad \left. + \left(\mathbf{w}(t_1) \cdot \mathbf{w}(t_4) \right) \left(\mathbf{w}(t_2) \cdot \mathbf{w}(t_3) \right) \right] \\
 & = 3 \cdot \left\{ \mathbb{E}[\mathbf{w}(t_1) \cdot \mathbf{w}(t_2)] \mathbb{E}[\mathbf{w}(t_3) \cdot \mathbf{w}(t_4)] + \mathbb{E}[\mathbf{w}(t_1) \cdot \mathbf{w}(t_3)] \mathbb{E}[\mathbf{w}(t_2) \cdot \mathbf{w}(t_4)] \right. \\
 & \quad \left. + \mathbb{E}[\mathbf{w}(t_1) \cdot \mathbf{w}(t_4)] \mathbb{E}[\mathbf{w}(t_2) \cdot \mathbf{w}(t_3)] \right\}. \tag{C.3}
 \end{aligned}$$

2-point correlation functions are equal to ones for 1-dimensional case, therefore the corresponding integrals can be calculated in the same manner as done above.



COMPUTATIONS OF THE DECAY RATES

Here we will stick to the scenario which considers spontaneous collapse as a sole source of the decay of mass eigenstates (that is $\Gamma_\mu^{exp} = \Gamma_\mu^{CSL}$) and discuss the method to compute the values of the respective decay rates $\frac{\Gamma_L^{CSL} - \Gamma_H^{CSL}}{\Gamma_L^{CSL} + \Gamma_H^{CSL}}$ highlighted in (5.23). We seek to obtain the decay rates for four types of mesons (\mathbf{K} , \mathbf{D} , \mathbf{B}_d , \mathbf{B}_s), but the corresponding procedures vary for different mesons due to available data in [84]. We start with \mathbf{D} and \mathbf{B}_d mesons which lead to an easier procedure. The authors of Ref. [84] provide experimental values of the quantity $\Delta\Gamma/\Gamma$, namely

$$\frac{\Delta\Gamma}{\Gamma} = \begin{cases} \text{D-mesons: } \left(1.29 \begin{cases} +0.14 \\ -0.18 \end{cases}\right) \cdot 10^{-2}, \\ \text{B}_d\text{-mesons: } (0.1 \pm 1.0) \cdot 10^{-2}, \end{cases} \quad (\text{D.1})$$

where $\Delta\Gamma = \Gamma_L^{exp} - \Gamma_H^{exp}$ and $\Gamma = \frac{1}{2}(\Gamma_L^{exp} + \Gamma_H^{exp})$. Therefore, we can easily obtain required decay rates for \mathbf{D} and \mathbf{B}_d mesons by dividing the quantity $\Delta\Gamma/\Gamma$ by 2

$$\left(\frac{\Gamma_L^{CSL} - \Gamma_H^{CSL}}{\Gamma_L^{CSL} + \Gamma_H^{CSL}}\right)_{\mathbf{D}, \mathbf{B}_d} = \frac{1}{2} \frac{\Delta\Gamma}{\Gamma} = \begin{cases} \text{D-mesons: } 0.00645 \begin{cases} +0.0007 \\ -0.0009 \end{cases} \\ \text{B}_d\text{-mesons: } 0.0005 \pm 0.005 \end{cases} \quad (\text{D.2})$$

Then we take into account mean lifetime of a meson $\tau = \frac{1}{\Gamma} = \frac{2}{\Gamma_L^{exp} + \Gamma_H^{exp}}$ and recover the decay constants for the light and heavy mass eigenstates of D and B_d mesons

$$\Gamma_L^{D,B_d} = \frac{1}{2\tau} \left(2 + \frac{\Delta\Gamma}{\Gamma} \right) = \begin{cases} \text{D-mesons: } \left(2.4542 \begin{cases} +0.006782 \\ -0.007270 \end{cases} \right) \cdot 10^{12} \text{ s}^{-1}, \\ \text{B}_d\text{-mesons: } (0.6582 \pm 0.001557) \cdot 10^{12} \text{ s}^{-1}, \end{cases}$$

$$\Gamma_H^{D,B_d} = \frac{1}{2\tau} \left(2 - \frac{\Delta\Gamma}{\Gamma} \right) = \begin{cases} \text{D-mesons: } \left(2.4227 \begin{cases} +0.011056 \\ -0.010568 \end{cases} \right) \cdot 10^{12} \text{ s}^{-1}, \\ \text{B}_d\text{-mesons: } (0.6576 \pm 0.005020) \cdot 10^{12} \text{ s}^{-1}, \end{cases}$$

where the errors are calculated up to the first order of Taylor series.

For K and B_s mesons the authors of Ref. [84] provide the values of mean lifetimes of the corresponding mass eigenstates, τ_L for the light one (short-lived state as in the case of K-mesons) and τ_H for the heavy one (long-lived state as in the case of K-mesons)

$$\tau_L = \begin{cases} \text{K-mesons: } (0.8954 \pm 0.0004) \cdot 10^{-10} \text{ s}, \\ \text{B}_s\text{-mesons: } (1.414 \pm 0.010) \cdot 10^{-12} \text{ s}, \end{cases} \quad (\text{D.3})$$

$$\tau_H = \begin{cases} \text{K-mesons: } (5.116 \pm 0.021) \cdot 10^{-8} \text{ s}, \\ \text{B}_s\text{-mesons: } (1.624 \pm 0.014) \cdot 10^{-12} \text{ s}. \end{cases} \quad (\text{D.4})$$

Using the definition of the decay constant of the mass eigenstate $\Gamma_\mu = \frac{1}{\tau_\mu}$ we obtain the following decay rates

$$\left(\frac{\Gamma_L^{CSL} - \Gamma_H^{CSL}}{\Gamma_L^{CSL} + \Gamma_H^{CSL}} \right)_{\text{K}, \text{B}_s} = \frac{\frac{1}{\tau_L} - \frac{1}{\tau_H}}{\frac{1}{\tau_L} + \frac{1}{\tau_H}} = \begin{cases} \text{K-mesons: } 0.996506 \pm (1.2760 \cdot 10^{-5}), \\ \text{B}_s\text{-mesons: } 0.069124 \pm (7.7058 \cdot 10^{-4}), \end{cases} \quad (\text{D.5})$$

where the errors are calculated up to the first order of Taylor series. The decay constants for the mass eigenstates can be recovered by inverting the mean lifetimes

$$\Gamma_L^{K,B_s} = \begin{cases} \text{K-mesons: } (1.1168 \pm 0.0005) \cdot 10^{10} \text{ s}^{-1}, \\ \text{B}_s\text{-mesons: } (7.0721 \pm 0.010) \cdot 10^{11} \text{ s}^{-1}, \end{cases}$$

$$\Gamma_H^{K,B_s} = \begin{cases} \text{K-mesons: } (1.9547 \pm 0.0500) \cdot 10^7 \text{ s}^{-1}, \\ \text{B}_s\text{-mesons: } (6.1576 \pm 0.0531) \cdot 10^{11} \text{ s}^{-1}, \end{cases}$$

where the errors are calculated up to the first order of Taylor series.

BIBLIOGRAPHY

- [1] A. Einstein, B. Podolsky and N. Rosen, *Phys. Rev.* **47**, 777 (1935).
- [2] J. S. Bell, *Physics* **1**, 195 (1966).
- [3] E. Specker, *Dialectica* **14**, 239 (1960).
- [4] S. Kochen and E. Specker, *J. Math. Mech.* **17**, 59 (1967).
- [5] A. Bassi and G. C. Ghirardi, *Phys. Rep.* **379**, 257 (2003).
- [6] A. Bassi et al., *Rev. Mod. Phys.* **85**, 471 (2013).
- [7] A. Bassi and D. Dürr, *J. Phys. A* **42**, 485302 (2009).
- [8] A. Bassi and S. Donadi, *Phys. Lett. A* **378**, 761 (2014).
- [9] C. Curceanu, B. C. Hiesmayr and K. Piscicchia, *J. Adv. Phys.* **4**, 263 (2015).
- [10] C. Curceanu, S. Bartalucci, A. Bassi, M. Bazzi, S. Bertolucci, C. Berucci, A. M. Bragadireanu, M. Cargnelli, A. Clozza, L. De Paolis, S. Di Matteo, S. Donadi, A. D’Uffizi, J.-P. Egger, C. Guaraldo, M. Iliescu, T. Ishiwatari, M. Laubenstein, J. Marton, E. Milotti, A. Pichler, D. Pietreanu, K. Piscicchia, T. Ponta, E. Sbardella, A. Scordo, H. Shi, D. L. Sirghi, F. Sirghi, L. Sperandio, O. Vazquez Doce and J. Zmeskal, *Found. Phys.* **46**, 263 (2016).
- [11] K. Piscicchia, C. Curceanu, S. Bartalucci, A. Bassi, S. Bertolucci, C. Berucci, A. M. Bragadireanu, M. Cargnelli, A. Clozza, L. De Paolis, S. Di Matteo, S. Donadi, A. D’Uffizi, J.-P. Egger, C. Guaraldo, M. Iliescu, T. Ishiwatari, M. Laubenstein, J. Marton, E. Milotti, D. Pietreanu, T. Ponta, E. Sbardella, A. Scordo, H. Shi, D. L. Sirghi, F. Sirghi, L. Sperandio, O. Vazquez Doce and J. Zmeskal, *Acta Phys. Pol. B* **46**, 147 (2015).
- [12] O. Romero-Isart, *Phys. Rev. A* **84**, 052121 (2011).

BIBLIOGRAPHY

- [13] J. van Wezel and T. H. Oosterkamp, Proc. R. Soc. A **468**, 35 (2011).
- [14] T. Juffmann, H. Ulbricht and M. Arndt, Rep. Prog. Phys. **76**, 086402 (2013).
- [15] M. Arndt and K. Hornberger, Nat. Phys. **10**, 271 (2013).
- [16] S. Belli, R. Bonsignori, G. D’Auria, L. Fant, M. Martini, S. Peirone, S. Donadi and A. Bassi, Phys. Rev. A **94**, 012108 (2016).
- [17] D. Goldwater, M. Paternostro and P. F. Barker, Phys. Rev. A **94**, 010104(R) (2016).
- [18] S. McMillen, M. Brunelli, M. Carlesso, A. Bassi, H. Ulbricht, M. G. A. Paris and M. Paternostro, Phys. Rev. A **95**, 012132 (2017).
- [19] J. Zhang, T. Zhang and J. Li, Phys. Rev. A **95**, 012141 (2017).
- [20] M. Bahrami, M. Paternostro, A. Bassi and H. Ulbricht, Phys. Rev. Lett. **112**, 210404 (2014).
- [21] S. Nimmrichter, K. Hornberger and K. Hammerer, Phys. Rev. Lett. **113**, 020405 (2014).
- [22] L. Diósi, Phys. Rev. Lett. **114**, 050403 (2015).
- [23] S. Donadi, A. Bassi, C. Curceanu, A. Di Domenico and B. C. Hiesmayr, Found. Phys. **43**, 813 (2013).
- [24] M. Bahrami, S. Donadi, L. Ferialdi, A. Bassi, C. Curceanu, A. Di Domenico and B. C. Hiesmayr, Sci. Rep. **3**, 1952 (2013).
- [25] K. Simonov and B. C. Hiesmayr, Phys. Lett. A **380**, 1253 (2016).
- [26] F. Ambrosino et al. (KLOE collaboration), Phys. Lett. B **642**, 315 (2006).
- [27] A. Di Domenico et al. (KLOE Collaboration), J. Phys.: Conf. Ser. **171**, 012008 (2008).
- [28] A. Di Domenico et al. (KLOE Collaboration), Found. Phys. **40**, 852 (2010).
- [29] A. Go et al. (Belle Collaboration), Phys. Rev. Lett. **99**, 131802 (2007).
- [30] G. Richter, “*Stability of Nonlocal Quantum Correlations in Neutral B-Meson Systems*” (PhD thesis, Technische Universität Wien, 2008).

-
- [31] B. D. Yabsley, “*Quantum entanglement at the $\psi(3770)$ and $\Upsilon(4S)$ ” (Flavor Physics & CP Violation Conference, Taipei, 2008).*
- [32] M. Bilardello, S. Donadi, A. Vinante and A. Bassi, Phys. A **462**, 764 (2016).
- [33] T. Josset, A. Perez and D. Sudarsky, Phys. Rev. Lett. **118**, 021102 (2017).
- [34] B. C. Hiesmayr, Found. Phys. Lett. **14**, 231 (2001).
- [35] R. A. Bertlmann and B. C. Hiesmayr, Phys. Rev. A **63**, 062112 (2001).
- [36] R. A. Bertlmann, W. Grimus and B. C. Hiesmayr, Phys. Lett. A **289**, 21 (2001).
- [37] A. Di Domenico, A. Gabriel, B. C. Hiesmayr, F. Hipp, M. Huber, G. Krizek, K. Mühlbacher, S. Radic, C. Spengler and L. Theussl, Found. Phys. **42**, 778 (2012).
- [38] B. C. Hiesmayr and J.-Å. Larsson, Phys. Rev. A **93**, 020106(R) (2016).
- [39] G. C. Ghirardi, A. Rimini and T. Weber, Phys. Rev. D **34**, 470 (1986).
- [40] L. Diósi, Phys. Rev. A **40**, 1165 (1989).
- [41] P. Pearle, Phys. Rev. A **39**, 2277 (1989).
- [42] G. C. Ghirardi, P. Pearle and A. Rimini, Phys. Rev. A **42**, 78 (1990).
- [43] G. C. Ghirardi, R. Grassi and F. Benatti, Found. Phys. **25**, 5 (1995).
- [44] S. L. Adler, J. Phys. A: Math. Theor. **40**, 2935 (2007).
- [45] A. Bassi and H. Ulbricht, J. Phys. Conf. Ser. **504**, 012203 (2014).
- [46] A. Bassi, D. Dürr and G. Hinrichs, Phys. Rev. Lett. **111**, 210401 (2011).
- [47] S. L. Adler and A. Bassi, J. Phys. A **40**, 15083 (2007).
- [48] S. Donadi, “*Electromagnetic Radiation Emission and Flavour Oscillations in Collapse Models*” (PhD thesis, Università degli studi di Trieste, 2012).
- [49] C. W. Gardiner, “*Handbook of Stochastic Methods for Physics, Chemistry and the Natural Sciences*”, Springer-Verlag (1985).
- [50] L. Arnold, “*Stochastic Differential Equations: Theory and Applications*”, Wiley-Interscience (1974).

- [51] B. Øksendal, “*Stochastic Differential Equations: An Introduction with Applications*”, Springer-Verlag (2003).
- [52] A. Bassi, E. Ippoliti and B. Vacchini, *J. Phys. A* **38**, 8017 (2005).
- [53] A. Bassi and L. Ferialdi, *Phys. Rev. A* **80**, 012116 (2009); A. Bassi and L. Ferialdi, *Phys. Rev. Lett.* **103**, 050403 (2009).
- [54] L. Ferialdi and A. Bassi, *Phys. Rev. A* **86**, 022108 (2012).
- [55] G. Jaeger, “*Quantum Information: An Overview*”, Springer-Verlag (2007).
- [56] J. F. Clauser, M. A. Horne, A. Shimony and R. A. Holt, *Phys. Rev. Lett.* **23**, 880 (1969).
- [57] C. Budroni, “*Temporal quantum correlations and hidden variable models*” (PhD thesis, Universität Siegen, 2014).
- [58] T. D. Lee and C. S. Wu, *Rev. Nucl. Sci.* **16**, 511 (1966).
- [59] H. J. Lipkin, *Phys. Rev.* **176**, 1715 (1968).
- [60] M. Gell-Mann and A. Pais, *Phys. Rev.* **97**, 1387 (1955).
- [61] V. Weisskopf and E. P. Wigner, *Z. Phys.* **63**, 54 (1930).
- [62] O. Nachtmann, “*Phänomene und Konzepte der Elementarteilchenphysik*”, Vieweg (1986).
- [63] R. A. Bertlmann, W. Grimus and B. C. Hiesmayr, *Phys. Rev. A* **73**, 054101 (2006).
- [64] V. Gorini, A. Kossakowski and E. C. G. Sudarshan, *J. Math. Phys.* **17**, 821 (1976).
- [65] G. Lindblad, *Commun. Math. Phys.* **48**, 119 (1976);
- [66] P. A. M. Dirac, *Proc. Roy. Soc. A* **117**, 610 (1928).
- [67] C. D. Anderson, *Phys. Rev.* **43**, 491 (1933).
- [68] A. D. Sakharov, *JETP Lett.* **5**, 24 (1967).
- [69] J. H. Christenson, J. W. Cronin, V. L. Fitch and R. Turlay, *Phys. Rev. Lett.* **13**, 138 (1964).

- [70] E. Abouzaid et al., Phys. Rev. D **83**, 092001 (2011).
- [71] V. Fanti et al., [NA48 Collab.], Phys. Lett. B **465**, 335 (1999).
- [72] A. Alavi-Harati et al., [KTeV Collab.], Phys. Rev. Lett. **83**, 22 (1999).
- [73] J. G. Muga, R. Sala Mayato and I. L. Egusquiza (eds.), *“Time in Quantum Mechanics”* (Springer, Berlin, 2002).
- [74] M. Courbage, T. Durt and S. M. Saberi Fathi, *“A wave-function model for the CP-violation in mesons”*, arXiv:0903.4143 (2009).
- [75] T. Durt, *“Crucial tests of the existence of a Time Operator”*, arXiv:1003.2781 (2010).
- [76] T. Durt, Int. J. Mod. Phys. B, **27**, 1345015 (2013).
- [77] M. Courbage, T. Durt and S. M. Saberi Fathi, J. Phys. G: Nucl. Part. Phys. **39**, 045008 (2012).
- [78] J. A. Vaccaro, Found. Phys. **45**, 691 (2015).
- [79] T. Durt, A. Di Domenico and B. C. Hiesmayr, *“Falsification of a Time Operator Model based on Charge-Conjugation-Parity violation of neutral K-mesons”*, arXiv:1512.08437 (2015).
- [80] K. Simonov and B. C. Hiesmayr, Phys. Rev. A **94**, 052128 (2016).
- [81] K. Simonov, B. C. Hiesmayr, *“Can a spontaneous collapse in flavour oscillations be tested at KLOE?”*, arXiv:1705.00913 (2017).
- [82] W. Feldmann and R. Tumulka, J. Phys. A: Math. Theor. **45**, 065304 (2012).
- [83] P. Pearle and E. Squires, Phys. Rev. Lett. **73**, 1 (1994).
- [84] K. A. Olive et al. (Particle Data Group), Chin. Phys. C **38**, 090001 (2014).
- [85] D. G. Hill, M. Sakitt, O. Skjeggstad, J. Canter, Y. Cho, A. Dralle, A. Engler, H. Fisk, R. Kraemer, C. Meltzer, T. Kikuchi, D. K. Robinson and C. Tilger, Phys. Rev. D **4**, 7 (1971).
- [86] W. A. W. Mehlhop, S. S. Murty, P. Bowles, T. H. Burnett, R. H. Good, C. H. Holland, O. Piccioni and R. A. Swanson, Phys. Rev. **172**, 1613 (1968).

BIBLIOGRAPHY

- [87] A. Vinante, M. Bahrami, A. Bassi, O. Usenko, G. Wijts and T. H. Oosterkamp, Phys. Rev. Lett. **116**, 090402 (2016).
- [88] M. Toroš and A. Bassi, “*Bounds on Collapse Models from Matter-Wave Interferometry: Computational details*”, arXiv:1601.02931 (2016).
- [89] M. Carlesso, A. Bassi, P. Falferi and A. Vinante, Phys. Rev. D **94**, 124306 (2016).
- [90] J. Bernabéu, N. E. Mavromatos and P. Villanueva-Pérez, Phys. Lett. B **724**, 269 (2013).
- [91] K. A. Smolinski, Phys. Rev. A **92**, 032128 (2015).
- [92] L. Diósi, Phys. Lett. A **105**, 199 (1984).
- [93] R. Penrose, Gen. Relat. Gravit. **28**, 581 (1996).
- [94] R. Penrose, Phil. Trans. Roy. Soc. Lond. **356**, 1927 (1998).
- [95] R. Penrose, Found. Phys. **44**, 557 (2014).
- [96] S. Carlip, Class. Quantum Grav. **25**, 154010, (2008).
- [97] M. Bahrami, A. Großardt, S. Donadi and A. Bassi, New. J. Phys. **16**, 115007 (2014).
- [98] A. Großardt and B. C. Hiesmayr, Phys. Rev. D **91** 064056, (2015).
- [99] H. D. Zeh, Found. Phys. **1**, 69 (1970).
- [100] W. H. Zurek, Phys. Rev. D **24**, 1516 (1981).
- [101] W. H. Zurek, Phys. Rev. D **26**, 1862 (1982).
- [102] E. Joos and H. D. Zeh, Z. Phys. B **59**, 223 (1985).
- [103] W. H. Zurek, Phys. Today **44**, 36 (1991).
- [104] W. H. Zurek, Rev. Mod. Phys. **75**, 715 (2003).
- [105] M. Schlosshauer, Rev. Mod. Phys. **76**, 1267 (2004).